University of Alberta

The Expression of Transmembrane AMPA Receptor Regulatory Proteins (TARPs) in Developing Zebrafish (*Danio rerio*)

by

Marcus Edwin Cunningham

A thesis submitted to the Faculty of Graduate Studies and Research
in partial fulfillment of the requirements for the degree of

Master of Science

in

Physiology, Cell & Developmental Biology

Biological Sciences

Fall 2013
Edmonton, Alberta

This thesis is dedicated to my ego: 1986-2012, R.I.P.

You had a good run.

Abstract

In embryonic vertebrates, newly-formed synapses are quiet until they are unsilenced through a process that resembles synaptic plasticity but remains mechanistically unclear. I used gene expression to determine if Transmembrane AMPA Receptor Regulatory Proteins (TARPs), AMPA receptor auxiliary subunits critical for synaptic plasticity in adults, could be involved in creating the excitability of neurons during development. The sequenced genome of zebrafish makes measuring and manipulating their genetic expression relatively simple, and their quick development into free-swimming larva makes behavioural studies after antisense gene knockdown possible. The duplicated TARP genes of zebrafish are orthologous to those of mice, and were found to be expressed in two waves starting at 12-36hpf or 48hpf. The developmentally important γ2 and γ4 isoforms are expressed ubiquitously at 12hpf, but are exclusive to the nervous tissue of the head by 48hpf. Antisense knockdown experiments failed to show a phenotype distinguishable from that of off-target effects.

Acknowledgements

I would like to thank Declan for his support and advice over the years – the experience of working in the lab has taught me a lot about both science and myself, and I will always value the personal growth I've experienced as a result of undertaking the massive challenge that has been graduate studies. I'd also like to thank James Stafford and John Greer for their excellent mentorship as members of my committee – I chose you both because I respect your work and knew that you would challenge me and keep me on my toes, and you have never let me down. Thank you to Debbie McKenzie for agreeing to be my external examiner – I hope I can convince you of my competence! I'd like to thank Andrew Waskiewicz and particularly Laura Pillay for their patient assistance with all things *in situ,* and Jocelyn Hall for an excellent crash course in phylogenetics. I'd like to thank all of the current and former members of the Ali lab, especially those who have helped me with advice or experiments along the way: Chris Coutts, Kessen Patten, Dinesh Witharana, Dan Brewster, Bipu Roy, Taylor Bucyk, Kazi Ahmed, Alexandra Seal, Lindsey Bergevin, Punit Virk and Savanna Boutin. A big thanks goes out to the friends I've made over the years as a result of my involvement with science – too many to name, but generally speaking anyone from: Goss lab, Stafford lab, Waskiewicz lab, Chang lab and Belosevic lab. Special shoutouts for my J's (James, Josh, Jordan, Jeremy), the Shafongs, Ben & Jill, Vantensity & Joey Totempole, Dave G, Tay, El Tigre, Dave B, Dr. Pash, Scott, Leon & Candace, Patrik, Karlijn, Jacky, Joe, Aga, Sal, Bendy, Sam, Alex, Herman, Chris and Kessen – you have all made the ups and downs that much sweeter. Michelle, I think I would have gone crazy if not for you… or maybe I already have and you've made me feel ok about it; thank you for being my friend and sounding board and biggest fan – I can't wait to be able to return the favour. Finally, thanks to my parents, my siblings and my extended family for their unconditional love and support – it has always been an enormous source of confidence for me to know that you have my back no matter what!

Table of Contents

List of Figures

1. Introduction

The central nervous system (CNS) is the sensor, integrator and effector of all our experiences; incredibly complex in adult organisms, it, along with the rest of our bodies, must arise from a single zygotic cell. As development proceeds, nerve cells (neurons) develop branches that grow from the cell body and creep along invisible pathways that lead them to their neighbours. Though initially silent, the communication points (synapses) between each nerve cell slowly awaken and begin to communicate as the nervous system develops (Durand et al., 1996), a change that has been associated with an increased number of neurotransmitter receptors at the synapse (Isaac et al., 1995, Liao et al., 1995). The vast majority of vertebrate neurons use chemical messages called neurotransmitters that must be exquisitely matched across the gulf of the synapse to the correct neurotransmitter receptor, or nothing happens and communication breaks down. Neurotransmitters are the currency of neuronal activity – these small molecules diffuse across the synapse, and it is the balance of inputs from excitatory and inhibitory neurotransmitters on the neurotransmitter receptors of the post-synaptic membrane that determines whether the next neuron in line will be activated or inhibited. It is the job of the neurotransmitter receptor to transduce the binary signal of neurotransmitter binding into a cellular response, and it is the neurotransmitter receptors that provide the most granular mechanisms of controlling that response. Therefore, the study of neurotransmitter receptors is critical to our basic understanding of the function of our nervous system.

1.1 Neurotransmitter Receptors

The activity of all of a neuron's neurotransmitter receptors is the basis for the electrical impulse that determines whether that neuron will fire an action potential or not; therefore, the study of the population and activity of these neurotransmitter receptors reveals a critical component of neuronal function. The most common neurotransmitter in the brain is glutamate, an amino acid, which acts on a variety of excitatory neurotransmitter receptors. These excitatory glutamate receptors can be either *ionotropic* or *metabotropic*: metabotropic receptors connect to the cell's second messenger system which may or may not connect to ion channels, while ionotropic receptors contain a built-in ion channel and can pass ions in or out of the cell. There are several classes of ionotropic glutamate receptors in the CNS (all of which are named after receptor specific agonists discovered experimentally): N-Methyl-D-Aspartate (NMDA) receptors (NMDARs) (Watkins, 1981), Kainate receptors (Bettler et al., 1990, Boulter et al., 1990) and 2-amino-3-(3-hydroxy-5-methyl-isoxazol-4-yl)propanoic acid (AMPA) receptors (AMPARs) (Honore et al., 1982). All of these glutamate receptors are excitatory, but their pharmacology and physiology are slightly different. We are interested in the AMPAR subtype, because it is the most abundant excitatory neurotransmitter receptor in the CNS and because it forms a ligand-gated ion channel that is heavily regulated *in vivo* in order to modulate its function – both in adult organisms and during development.

1.1.1 *AMPAR Subunit Composition and Trafficking*

AMPA receptors consist of four different subunits, termed GluA1-4 (Bettler et al., 1990, Boulter et al., 1990, Collingridge et al., 2009), with each subunit consisting of a large extracellular N-terminal domain (NTD), two ligand-binding domains (LBDs: S1 and S2) separated in the primary structure by four transmembrane domains (TMDs: M1-M4), and a small intracellular C-terminal domain (CTD) (Hollmann et al., 1994). During their synthesis and processing, LBDs and NTDs of single GluA subunits interact with each other to form dimers, which then dimerize with another dimer to create a "dimer of dimers" tetramer, which results in the variety of different homo- and hetero-tetramers we observe in nature (Armstrong et al., 1998, Armstrong and Gouaux, 2000, Ayalon and Stern-Bach, 2001, Mansour et al., 2001, Greger et al., 2007).

Post-transcriptional modifications such as alternative splicing and RNA editing further increase the functional variety AMPARs formed by these GluA subunits. Alternative splicing of introns and exons in the pre-mRNA yields "flip" and "flop" isoforms of each of the GluA subunits, which results in different AMPAR channel properties (Sommer et al., 1990, Mosbacher et al., 1994). The expression of these flip and flop isoforms changes developmentally, with the flip isoform being expressed during early development, while the flop isoform comes to predominate in mature AMPARs (Monyer et al., 1991). The GluA subunits also undergo a variety of RNA editing events, which alter mRNA codons and introduce non-genomically encoded amino acids in the mature protein. One codon just prior to the flip/flop splice site on the pre-mRNA transcripts for the

GluA2-4 subunits is modified to replace the genomic positively charged arginine (R) with a neutral glycine (G) (Sommer et al., 1991). Another modification specific to GluA2 has proven to be very important for the physiology of AMPARs: by exchanging a glutamine (Q) with a positively-charged arginine (R) at a site within the M2 transmembrane loop, which forms the pore of the channel, RNA editing causes AMPARs containing mature GluA2 subunits to be Ca^{2+}-impermeable (Higuchi et al., 1993, Hollmann et al., 1994, Lomeli et al., 1994). In zebrafish, the genes encoding AMPAR subunits undergo post-transcriptional modifications just as mammals do, but they also have a second copy of GluA2 that genomically encodes the R form of the subunit, which creates interesting opportunities for researchers who use zebrafish (Kung et al., 2001, Lin et al., 2006). The Q/R editing site in GluA2 also regulates the subunit's exit from the ER, with immature Q-containing GluA2 subunits being forward-trafficked easily as tetramers from the ER, while much of the mature R-containing GluA2 is stably stored in the ER as individual subunits (Greger et al., 2002, Greger et al., 2003). The subunits dimerize, form tetramers and associate with auxiliary subunits in the ER (Bedoukian et al., 2006) before moving on to the Golgi apparatus where their glycosylation matures. AMPAR subunits preferentially form heterodimers, and then these dimers join with each other to form heterotetramers with a 2:2 stoichiometry; homomers are possible, but unfavourable and unlikely *in vivo* due to the presence of other subunit types (Mansour et al., 2001, Brorson et al., 2004). This preference for heteromers over homomers is so strong that it even extends to similar subunits with different flip-flop splice status (Brorson et al., 2004). As

they associate with each other, the subunits arrange themselves so that similar monomers do not touch, which results in an alternating pattern of the two subunits that constitute a given heterotetramer around the pore (Mansour et al., 2001). Fully-formed AMPARs exit the Golgi apparatus in vesicles and fuse with the membrane by the same v-SNARE/t-SNARE-dependent mechanism that allows neurotransmitter vesicle fusion at the pre-synaptic membrane (Luscher et al., 1999). The storage of R-containing GluA2 subunits in the ER ensures that they are always available to form AMPARs and be exported, which is important for normal physiology because most endogenous AMPARs contain GluA2 and are cycled in and out of the membrane depending on the activity of the synapse (Wenthold et al., 1996, Shi et al., 2001). Finally, Kessen Patten's previous research in our lab demonstrated that the subunit composition of the AMPARs at the synapse changes developmentally, through a process that requires PKCγ (Patten and Ali, 2007, Patten et al., 2010). Aside from the involvement of PKCγ, this developmental switch in AMPAR composition and function is poorly understood from a mechanistic standpoint, and surely requires the involvement of other enzymes and proteins in order to occur.

1.1.2 *AMPAR Function*

Once at the synapse, AMPARs act as ligand-gated ion channels; however, the receptors must first travel to and be anchored at the post-synaptic density (PSD) from the extrasynaptic sites they are delivered to (Shi et al., 1999). Different subunit compositions of AMPARs are used by neurons to colonize different types of synapses: GluA1-containing receptors are used to colonize new

synapses without other AMPARs and GluA3-containing receptors are continuously cycled in and out of established synapses (Shi et al., 2001).

AMPARs can bind up to four glutamate molecules – one on each subunit – to reach their maximum channel conductance, but they must bind only two in order to open (Rosenmund et al., 1998). Once open, AMPARs can pass cations such as Na^+, K^+, and sometimes Ca^{2+} down their electrochemical gradients, though most AMPARs contain the charge-selective GluA2 subunit and will therefore exclude Ca^{2+}. The less charge-selective NMDA receptor can pass Na^+, K^+, and Ca^{2+}, but its pore is blocked at resting membrane potential by a Mg^{2+} ion that sits on the extracellular side of the channel (Mayer et al., 1984, Nowak et al., 1984). In synapses containing AMPARs and NMDARs, the AMPARs will open first and create an initial depolarization that drives the Mg^{2+} block from the pore of the NMDAR and allows the channel to pass current. It is the immediate functionality of AMPARs as compared to NMDARs in synapses that underlies key aspects of the process we call synaptic plasticity.

1.2 Synaptic Plasticity

The adult human brain contains approximately 80 billion neurons (Azevedo et al., 2009), each of which may have as many as hundreds or even thousands of synaptic contacts. These synaptic contacts are the result of years of careful pruning and enhancement in response to the amount of use they see, and synaptic plasticity describes the spectrum of mechanisms behind this process. Most mechanisms of synaptic plasticity alter the strength of the synapse by changing

the postsynaptic response (Kerchner and Nicoll, 2008), though some mechanisms can alter presynaptic properties in order to have similar short-term effects (Byrne and Kandel, 1996). The Canadian neuropsychologist, Donald Hebb, described the concept of synaptic strengthening as such:

"When an axon of cell A is near enough to excite cell B and repeatedly or persistently takes part in firing it, some growth process or metabolic change takes place in one or both cells such that A's efficiency, as one of the cells firing B, is increased."(Hebb, 1949)

This statement, which has become known as Hebb's postulate, aptly describes the general process we now know as long-term potentiation (LTP); however, figuring out the details of the "growth process or metabolic change" that takes place has been a much more complicated task than Dr. Hebb may have anticipated.

LTP is an experimentally induced set of processes that modify the properties of a synapse in order to increase the fidelity of events between the pre- and post-synaptic neurons. The most extensively studied form of LTP requires NMDAR activity (Harris et al., 1984, Reymann et al., 1989) – specifically Ca^{2+} influx at the postsynaptic surface (Lynch et al., 1983, Malenka et al., 1988) – and works by increasing the number and responsiveness of AMPARs on postsynaptic surfaces (Kauer et al., 1988, Muller et al., 1988, Barria et al., 1997a, Barria et al., 1997b, Lee et al., 2000). Somewhat paradoxically, NMDARs require a coincident depolarization in addition to ligand binding in order to pass current as a result of

their Mg^{2+} block at resting membrane potential (Mayer et al., 1984, Nowak et al., 1984). This means that excitatory synapses in the CNS that contain NMDARs but lack AMPARs are "silent" synapses because they cannot respond to presynaptic activity at resting membrane potential (Isaac et al., 1995). Synaptic unsilencing is an activity-dependent process that occurs *in vivo* which is experimentally indistinguishable from NMDA-dependent LTP; therefore the molecular mechanisms of LTP are a good starting point in examining the molecular mechanisms of synaptic unsilencing (Kerchner and Nicoll, 2008).

Importantly, there is further evidence to suggest that synaptic unsilencing is a developmentally regulated process, which opens up the possibility that the mechanisms of LTP may also be used developmentally in the pruning and enhancement of early synapses (Durand et al., 1996, Hsia et al., 1998). Synaptogenesis seems to occur through many of the same mechanisms by which synapses are strengthened in adults: NMDARs begin to colonize the PSDs, and the AMPAR-containing synapses that are receiving presynaptic input are strengthened by further addition of AMPARs (Isaac et al., 1997, Petralia et al., 1999). Other potential sites of developmental regulation are the auxiliary subunits and scaffolding proteins that complex with AMPARs at the synapse and are known to alter trafficking and kinetic properties of AMPARs in adults – though any developmental role remains unclear.

1.3 The Post-Synaptic Density (PSD)

The population of membrane-associated proteins associated with pre- and postsynaptic surfaces helps keep synaptic membranes distinct from other regions of cell membrane. Integral proteins that interact on their extracellular domains link pre- and postsynaptic membranes in order to maintain the synaptic cleft (Biederer et al., 2002, Verpelli et al., 2012). The membrane of postsynaptic terminals is extensively populated with scaffolding protein complexes that anchor proteins to synaptic sites, organize activity and ensure modulators are close enough to their substrates to work effectively. These collections of proteins are known as the postsynaptic density (PSD). PSD proteins are necessary for synaptic plasticity: NMDAR-dependent LTP would be impossible if AMPARs could not be reliably anchored to the PSD, not to mention the specific functions of PSD proteins in other types of synaptic plasticity (Sun and Turrigiano, 2011) and the interactions of PSD proteins with AMPAR auxiliary subunits (Bedoukian et al., 2008). AMPARs interact with the PSD through C-terminal **P**SD-95/**D**iscs large/**Z**ona occludens (PDZ)-binding domains, which bind to scaffolding proteins with matching PDZ domains and anchor the AMPAR at the synapse. The main PDZ domain-containing proteins of the PSD are the **M**embrane **A**ssociated **Gu**anylate Kinases (MAGUKs), a family of proteins that can be found anywhere that cells contact each other. MAGUKs of particular importance for synaptic function are PSD-93, PSD-95, **S**ynapse **A**ssociated **P**rotein (SAP) 97 and SAP 102 (Verpelli et al., 2012). Rather than acting as **G**uanylate **K**inases (GKs) as their name might suggest, MAGUKs contain a catalytically inactive GK domain

(Olsen and Bredt, 2003), and instead function by taking advantage of several protein-protein interaction domains, including PDZ domains. The specific PDZ domain bound by each subunit is different - GluA1 interacts with SAP97's type I PDZ domain (Leonard et al., 1998), while GluA2 interacts with PICK1 (Xia et al., 1999) and GRIP/ABP (Dong et al., 1997, Srivastava et al., 1998, Dong et al., 1999, Srivastava and Ziff, 1999, Wyszynski et al., 1999) through a multi-PDZ domain – these differential interactions allow for certain types of AMPARs to be preferentially anchored with certain other proteins and enzymes (Colledge et al., 2000). These close connections between AMPARs and the proteins that modulate them allows for much more rapid catalytic activity than if the proteins were relying on simple diffusion.

1.4 Transmembrane AMPAR Regulatory Proteins

Transmembrane **A**MPAR **R**egulatory **P**roteins (TARPs) are auxiliary subunits of AMPARs (Vandenberghe et al., 2005b), belonging to the voltage-gated Ca^{2+} channel gamma subunit gene family (*Cacng*). They are four-pass transmembrane proteins with an intracellular N-terminus and an intracellular C-terminus of variable length (Figure 1A). For phylogenetic purposes, the *Cacng* family's nearest relative is the Claudin superfamily: proteins involved in regulation of paracellular permeability through tight junctions (Morita et al., 1999, Price et al., 2005). The *Cacng* family share some sequence similarity and their overall transmembrane topology with the Claudins and possess a highly conserved Claudin motif in their first extracellular loops (-GWL$[X]_2$C$[X]_{8-10}$C-) (Price et al., 2005, Li et al., 2013). The *Cacng* gene family can be divided into

three functional groups: actual calcium channel gamma subunits, Type I (typical) TARPs, and Type II (atypical) TARPs. Of the eight members of the family (Burgess et al., 1999, Klugbauer et al., 2000, Burgess et al., 2001, Chu et al., 2001), two are Ca^{2+} channel gamma subunits (*Cacng1*/γ1 protein, *Cacng6*/γ6 protein) (Glossmann et al., 1987, Jay et al., 1990, Lee et al., 2010), four are Type I TARPs (*Cacng2*/γ2 protein/Stargazin, *Cacng3*/γ3 protein, *Cacng4*/γ4 protein, *Cacng8*/γ8 protein) (Tomita et al., 2003), and two are Type II TARPs (*Cacng5*/γ5 protein, *Cacng7*/γ7 protein) (Kato et al., 2007, Kato et al., 2008). These 8 mammalian genes arose from a common ancestor through several duplication events, making *Cacng2/3*, *Cacng4/8*, *Cacng5/7* and *Cacng1/6* paralogs to each other (Burgess et al., 2001, Chu et al., 2001). In zebrafish, an additional teleost genome duplication event (Jaillon et al., 2004) has resulted in 16 *Cacng* genes, of which 12 are likely to encode TARP proteins orthologous to γ2, γ3, γ4, γ5, γ7 and γ8.

Type I TARPs have been the most extensively studied and have the best characterized physiological role, while the physiological role of Type II TARPs remains somewhat unclear. Type I TARPs contain a C-terminal PDZ-binding motif that allows them to interact with PSD-95 (Chen et al., 2000), a **N**euronal isoform of **P**rotein **I**nteracting **S**pecifically with **T**C10 (nPIST) domain that influences TARPed AMPAR trafficking to the membrane (Cuadra et al., 2004), as well as several C-terminal serine, threonine and tyrosine residues that can be substrates for phosphorylation (Chetkovich et al., 2002, Choi et al., 2002, Tomita et al., 2005b). The extracellular loop between transmembrane domains 1 and 2

(ECL1) of the Type I TARPs interacts with the pore domain of the GluA subunit (Figure 1B, C) (Nakagawa et al., 2005, Nakagawa et al., 2006, Payne, 2008) and the interaction between TARPs and GluA subunits is thought to help bring the AMPAR to the Golgi for glycosylation (Tomita et al., 2003, Ives et al., 2004). The first extracellular loop of the Type II TARPs does not have the same functionality as the Type I TARPs – in fact, the critical differences between the two subfamilies are associated with their C-termini and their first extracellular loops (Tomita et al., 2004). Once in the Golgi, AMPAR trafficking to the synapse occurs in two steps: first, the AMPAR is exported to the membrane from the Golgi; then, the AMPAR diffuses to the PSD and is anchored there by direct and indirect (TARP-mediated) (Chen et al., 2000, Cuadra et al., 2004) attachment to scaffolding proteins. The mRNA transcripts of Type I TARPs are differentially expressed in both space and developmental time in the mammalian brain: *Cacng2* is expressed mainly in the cerebellum and is important throughout both development and adulthood; *Cacng3* is expressed in the cortex; *Cacng4* is expressed in the caudate putamen, glial cells, habenula, and is robustly expressed early in postnatal development, becoming less important in the adult; and *Cacng8* is expressed mainly in the hippocampus and is also important throughout development (Klugbauer et al., 2000, Tomita et al., 2003, Menuz et al., 2009). TARPs begin their association with AMPARs while both proteins are still in the ER and TARP/AMPAR complexes assemble with 0-4 TARPs per AMPAR depending on the expression level of the TARP protein (Shi et al., 2009, Kim et al., 2010). The stoichiometry of TARPs with AMPAR subunits is one area where

the precise rules remain unclear. Using GluA1 homomers expressed in *Xaenopus laevis* oocytes, Lu Chen's group recently examined the differential stoichiometry of the "classical" (Type I) TARPs, and found that AMPARs containing γ2 or γ3 could contain between 0 and 4 TARPs, but that most AMPARs contained 2-3 (Hastie et al., 2013). Conversely, the maximum number of TARPs found associated with γ4 or γ8 was 2, suggesting a significant functional difference between the interactions of γ2/3 and γ4/8 with AMPARs (Hastie et al., 2013). These results have yet to be confirmed *in vivo*, or with a more physiologically relevant AMPAR heteromer; however they suggest a possible explanation for the functional differences between AMPARs associated with γ2/3 or γ4/8. Though TARPs act as important chaperones in the trafficking process, they are not irrevocably attached to AMPARs – one important mechanism of cycling AMPARs out of the synapse involves dissociating them from their TARP auxiliary subunits (Tomita et al., 2004). In this experiment, researchers monitored surface expression of γ2 and γ3 in primary cortical neuron cultures while inducing endocytosis of AMPARs, and found that the TARP proteins remain on the surface even as AMPARs are being cycled back into the endosomal system (Tomita et al., 2004). The different TARPs also have differential effects on AMPAR kinetics, and are differentially affected by pharmacological agents.

γ2 is the prototypical TARP – also known as Stargazin in honour of the phenotype its knockout confers on mice. The *Stargazer* knockout mouse is prone to absence epilepsy and cerebellar ataxia (Letts et al., 1998) - deficits that are a result of impaired AMPAR trafficking (Chen et al., 2000). γ2 associates with

AMPAR subunits in the ER as a part of normal biosynthesis, and is important for trafficking to the PSD (Tomita et al., 2003, Vandenberghe et al., 2005a, Shi et al., 2009); however the injection of any of the other Type I TARPs is sufficient to rescue AMPAR currents in *Stargazer* mice (Tomita et al., 2003), suggesting a functional redundancy among the Type I TARPs. Indeed, the only Type I TARP gene for which a single knockout is sufficient to produce a behavioural phenotype in mice is γ2: other Type I TARPs require double or even triple knockouts to produce an obvious phenotype (Letts et al., 2005, Menuz et al., 2008). TARPs are also targets of a number of enzymes involved in synaptic plasticity, and activation or deactivation of TARPs by these enzymes is used throughout the lifetime of an AMPAR to anchor it to or remove it from the post-synaptic density in response to activity (Choi et al., 2002, Tomita et al., 2004, Tomita et al., 2005b). A threonine residue within the PDZ-binding motif of Stargazin (γ2) has been demonstrated to be a substrate for Protein Kinase A (PKA) phosphorylation, which causes the PDZ-binding motif to dissociate from PSD-95 and thereby loosens or severs the connection of the TARP-AMPAR complex to the PSD (Choi et al., 2002). Conversely, several serine and threonine residues elsewhere in the C-terminus have been shown to be phosphorylated by Calcium Calmodulin Kinase II (CaMKII) and Protein Kinase C (PKC) in order to enhance their association with the PSD (Tomita et al., 2005b). Aside from their role in AMPAR trafficking and plasticity, TARPs also have differential and modulatory effects on AMPAR current kinetics, suggesting an involvement deeper than that of a pure chaperone.

The association of Type I TARPs with AMPARs has been shown not only to promote and facilitate trafficking, but also to alter the physiological properties of the AMPARs themselves in a TARP isoform-specific manner (Kott et al., 2007, Milstein et al., 2007, Kott et al., 2009, Jackson et al., 2011). Stargazin (γ2) is known to alter the properties of AMPARs by increasing sensitivity to glutamate, slowing the time course of channel deactivation and binding site desensitization, and increasing the rate of channel opening (Priel et al., 2005, Tomita et al., 2005a). In Ca^{2+}-permeable GluA1 homomers, γ3 has also been shown to slow deactivation and desensitization very similarly to γ2; while γ4 and γ8 slow deactivation and desensitization more dramatically, and also slow the opening kinetics of the AMPAR (Milstein et al., 2007). In a more physiologically relevant system that examined GluA2/4 heteromers with TARPs, the different TARP isoforms were shown to differentially alter AMPAR conductance in the following manner: GluA2/4 < GluA2/4+γ2 ≅ GluA2/4+γ3 ≤ GluA2/4+γ4 < GluA2/4+γ8 (Jackson et al., 2011). All of the Type I TARPs except γ8 have also been shown to dramatically enhance the steady-state opening of the AMPAR (Jackson et al., 2011). These differential effects on AMPAR kinetics and conductance were shown to be mediated by the first extracellular loop of the TARP proteins (Milstein et al., 2007). All of these differential effects of TARP proteins on AMPAR function also depend on the AMPAR subunit composition, including the level of post-transcriptional modification of the AMPAR subunits (Kott et al., 2007); which in sum, sets the stage for exquisite levels of physiological tuning of

the post-synaptic responses of this one neurotransmitter receptor type from cell to cell.

TARPs have also been found to alter the pharmacological reactivity of AMPARs, which has made some pharmacological agents less useful in certain systems, but also provided a number of creative assays for different TARP/AMPAR combinations. The association of TARPs with AMPARs increases the AMPAR's affinity to the partial agonist Kainate (Turetsky et al., 2005, Kott et al., 2007, Milstein et al., 2007), which provides an electrophysiological mechanism to detect TARPs. CNQX is a competitive AMPAR antagonist that has been very widely used to block AMPAR activity; however it has also been found to cause depolarization in certain populations of interneurons, suggesting a more complex effect than that of a simple competitive antagonist (Maccaferri and Dingledine, 2002). More recently this effect has been elaborated on, and CNQX has been shown to work as a partial *agonist* of AMPARs that are associated with TARPs, when expressed in heterologous HEK293T cells (Menuz et al., 2007). Endogenous polyamines such as spermine, which normally work by blocking the pore of the GluA2-lacking AMPAR channel from the intracellular side, resulting in rectification at depolarized membrane potentials (Bowie and Mayer, 1995, Kamboj et al., 1995, Koh et al., 1995), block the pore incompletely when the AMPAR is associated with a TARP, and therefore exhibit only partial rectification (Turetsky et al., 2005, Cho et al., 2007, Soto et al., 2007). Polyamine toxins purified from the venom of certain wasps and spiders are capable of blocking the pore of ionotropic glutamate

receptors from the extracellular side, and have historically been powerful but non-selective tools to examine the activity of ionotropic receptors; however recent careful modifications of the basic structures of these toxins have yielded more selective isoforms (Stromgaard et al., 2005). Philanthotoxin-7,4 (PhTx-74), a polyamine toxin that blocks GluA2-containing AMPARs at high concentrations has also been developed (Kromann et al., 2002, Nilsen and England, 2007). Of particular interest to TARP researchers, the action of PhTx-74 changes depending on the TARP associated with the AMPAR – PhTx-74 preferentially blocks AMPARs associated with γ4/ γ8 rather than γ2/ γ3 (Jackson et al., 2011).

Given the variety of functional roles for TARPs described previously, it may not be surprising to know that the TARPs differentially affect AMPARs based also on their subunit composition (Cho et al., 2007, Kott et al., 2007), meaning that altering the subunit composition of native AMPARs could vary the effects of TARPs in vivo.

1.4.1 *TARPs in Synaptic Plasticity*

TARPs can be modulated as part of both long-term potentiation (LTP) and long-term depression (LTD). Their role as a chaperone during the trafficking of AMPARs makes them a critical determinant of whether the post-synaptic response will be strengthened or weakened in response to different levels of activity (Tomita et al., 2005b). A considerable body of research has suggested that multiple TARPs are capable of being expressed in a given cell type (Menuz et al., 2008, Menuz et al., 2009); while other studies have shown that AMPAR

composition varies by cell type (Greger et al., 2007). Phosphorylation of a conserved threonine residue within the PDZ domain of γ2's C-terminus disrupts its interaction with PSD-95 and allows the AMPAR to float free of the PSD (Choi et al., 2002). NMDAR currents can activate Protein Kinase C (PKC), Ca^{2+}-dependent Calmodulin Kinase II (CaMKII), and Protein Phosphatase 1 (PP1), which can in turn phosphorylate and dephosphorylate γ2 at a number of conserved serine residues: phosphorylation of γ2 results in increased AMPAR current, while dephosphorylation results in a decrease in AMPAR current (Tomita et al., 2005b). The conservation of these residues among the Type I TARPs of zebrafish suggests that all of the TARP proteins are capable of being regulated in a similar fashion.

1.5 Nervous System Development

As neural development proceeds, neurons in each segment begin to send out processes known as growth cones, which grope upwards along chemical gradients in order to find their desired targets. The small processes of these axonal growth cones, called filopodia, reach out towards the dendritic filopodia of their target cells, and somehow communicate with each other in order to form organized synapses. Once filopodia from either the axon (Washbourne et al., 2002, Meyer and Smith, 2006) or the dendrite (Sabo et al., 2006) find their desired target cells, the precise location of the synapse depends on the coordination of a large number of molecules in both the pre- and post-synaptic neurons that are somehow involved in synaptogenesis. These locations for synaptogenesis seem predetermined somehow, as presynaptic synaptogenic vesicles will pause and cycle with the membrane at future synaptic locations before there is any direct

neuronal or glial interaction (Sabo et al., 2006). Stable accumulation of post-synaptic scaffolding proteins has also been shown to be sufficient for synaptic localization (Gerrow et al., 2006); therefore the "predetermination" of synaptic sites is likely the result of a complex interplay between pre- and post-synaptic factors. Once the synaptic site has been chosen, NMDARs are recruited to the synapse almost immediately – with a very similar time course to the recruitment of pre-synaptic components – whereas AMPARs are recruited to the synapse later, usually after an hour (Washbourne et al., 2002). This finding suggests that synapses, at least in cultured neurons, are not kept silent for very long; however further studies have suggested that other factors, including the presence of NMDARs, can help keep synapses silenced *in vivo* (Adesnik et al., 2008). Clearly the developmental unsilencing of *in vivo* synapses must be regulated carefully, and the variety of mechanisms underlying that process remains unclear.

1.6 Zebrafish as a Model System for Studies of Neurodevelopment

Zebrafish (*Danio rerio*) are a freshwater teleost fish of the family Cyprinidae, native to the Himalayas of South Asia. They are small fish, rarely exceeding 4cm, which makes them simple and inexpensive to keep in captivity, and they can be bred frequently (every 14 days) without any negative long-term consequences. This fecundity makes zebrafish particularly popular for developmental studies, as they develop quickly and in great enough numbers for high throughput experiments (1000 embryos per tank every 14 days is not unheard of). Newly laid zebrafish embryos are small (~1mm in diameter) with a clear and colourless shell (the chorion). Zebrafish embryos develop into free-

swimming larva in 48 hours, and exhibit stereotypical escape response behaviours as early as 27 hours.

Even the simplest movements and behaviours in an adult are incredibly complex at the cellular level, requiring precisely tuned communication between many neurons and other tissues at many levels of the nervous system; therefore, a common tool of neurophysiologists is to examine an easily evoked movement-behaviour that requires very few synaptic connections. In our lab, we use the C-turn escape response of zebrafish as our model system. This model is ideal for our studies because it relies on a simple reflex arc that is present as early as 27 hours post-fertilization (hpf) (Saint-Amant and Drapeau, 1998); consisting of sensory neurons associated with sensing sound and pressure, a large interneuron called a Mauthner cell, motor neurons and muscle cells. The stereotypical escape response causes the fish to turn 90° away from a stimulus at either the tail or the otic vesicle (in doing so, forming the eponymous "C" shape) and swim rapidly away. The Mauthner neuron that mediates this response can be identified by its large cell body in a consistent region of the hindbrain (Kimmel et al., 1995) and have its electrical activity recorded as early as 24 hpf, allowing researchers to examine the populations of neurotransmitter receptors that underlie Mauthner cell activity. Alterations to neuronal function in this pathway are often accompanied by perturbations to the time course and efficiency of the escape response (Low et al., 2012), which can provide a good foundation for further functional studies. Importantly, former members of our lab have extensively examined the developmental changes to the AMPAR currents in Mauthner cells (Patten and Ali,

2007, 2009, Patten et al., 2010), and my examination of the expression of TARPs during development and their functional role in the escape response sets a foundation for future studies examining TARP and AMPAR relationships in the developing zebrafish.

One group has examined the conservation of γ2-like proteins in an invertebrate system (Walker et al., 2006); however no studies have examined TARP expression or activity in non-mammalian vertebrates. Moreover, the paralogous genes for the GluA2 AMPAR subunit in zebrafish have been shown to be functionally different, genomically encoding both Ca^{2+}-permeable and Ca^{2+}-impermeable versions (Kung et al., 2001), suggesting that the paralogs that have been retained in zebrafish are not necessarily identical copies of each other. Given that all of the *Cacng* genes have preserved paralogs, I am interested in investigating the possible differences in expression and function between the Type I TARPs.

1.7 Project Aims and Hypotheses

TARPs have been extensively studied in mammals, and more recently in *C. elegans*; however no studies have examined TARPs in a non-mammalian vertebrate such as zebrafish. Zebrafish present an interesting system to study TARPs in because of their more recently duplicated genome, which has resulted in the preservation of additional apparent paralogs for each TARP gene. *My first objective* was to confirm the identity of these genes as TARP paralogs, through an examination of the phylogenetic relationships of the TARP family in zebrafish

and other vertebrates. I hypothesized that in spite of the additional paralogous genes, the TARPs of zebrafish would display the same intra-familial relationships as their vertebrate orthologs.

It has been suggested in the mammalian literature that the main TARPs expressed during development are *Cacng2* and *Cacng4*; however, since no literature exists to describe the pattern of expression in a non-mammalian system, *My second objective* was to thoroughly examine the expression pattern of all the available TARP genes during the development of the nervous system in zebrafish, from 12hpf until 96hpf – when the larva is a fully independent organism – using RT-PCR. I hypothesized that the TARPs would be expressed as early as 12 hpf and that their expression levels would increase over developmental time.

The mammalian literature shows clear differential spatial expression patterns for the Type I TARP genes in the CNS, and demonstrates that these expression patterns change developmentally. The zebrafish genome contains twice as many TARP genes as the mammalian genome; moreover, zebrafish and mice are separated by significant evolutionary distance. *My third objective* was to determine the spatial expression pattern of selected TARPs in zebrafish during development using *in situ* hybridization. I hypothesized that the expression patterns of the zebrafish TARPs would be the same as their murine cousins.

Finally, Stargazin was initially identified in a murine model system designed to mimic absence epilepsy and cerebellar ataxia – functional aberrations in neuronal activity that can easily be assayed because of the movement deficits

they result in. *My final objective* was to determine the effect of single TARP gene knockdowns on zebrafish escape and swimming behaviour. Single knockouts of other murine TARPs did not result in an obvious phenotype because of broad functional redundancy among TARPs. In zebrafish, where paralogous genes may make TARPs twice as redundant as they are in mice, the effect of the knockdown of single genes corresponding to Stargazin and γ4 is simply not yet known. I hypothesized that the single gene knockdowns would be unlikely to have a noticeable effect due to the considerable redundancy of zebrafish TARPs.

The relevance of this project is its potential to provide important data on the developmental expression of TARP genes in a non-mammalian vertebrate, and suggest a possible functional role for TARPs during the escape response. This project lays the groundwork for our lab to continue its characterization of changes to AMPAR activity during development in zebrafish.

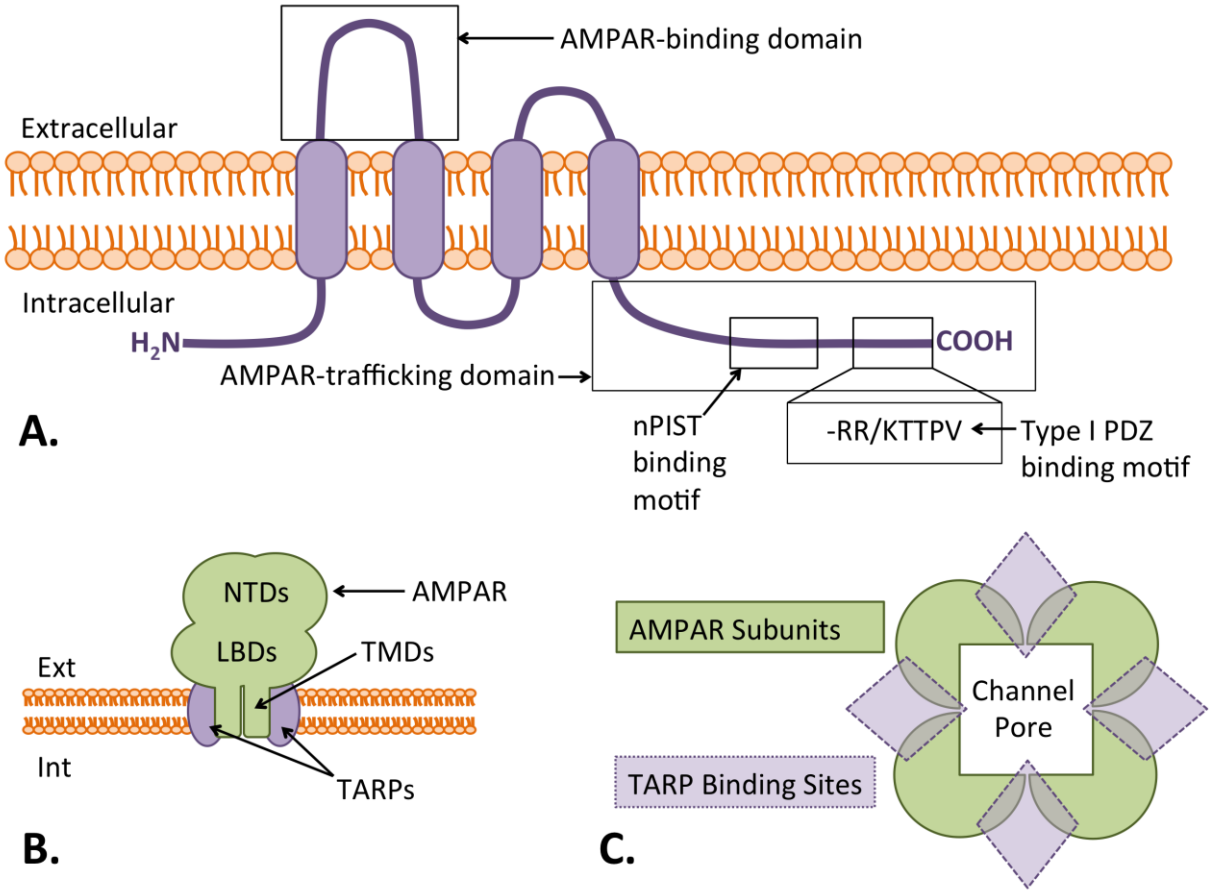

Figure 1 Schematic of Transmembrane AMPAR Regulatory Protein (TARP) structure and interaction with AMPARs. A) Topology of a generic TARP, highlighting the first extracellular loop (responsible for binding to AMPARs and altering the properties of the AMPAR channel and ligand-binding domains [LBDs]) and the C-terminus (responsible for AMPAR trafficking and anchoring to the post-synaptic density [PSD]). B) Schematic showing AMPAR/TARP interaction. TARPs interact with the transmembrane domains (TMDs) and LBDs of the AMPAR, but not the N-terminal domains (NTDs). C) Hypothetical model of TARP/AMPAR binding and stoichiometry. AMPARs can bind up to four TARPs, depending on the subunit composition of the AMPAR and the identity of the TARP isoform. Hashed diamonds represent potential TARP binding sites.

2. Materials & Methods

2.1 Animal Care

Zebrafish from the Oregon AB wild-type line were obtained from the University of Oregon and stored in the aquatics facility in the Department of Biological Sciences at the University of Alberta according to established protocols (Westerfield, 2007). Zebrafish embryos were obtained by placing males and females in mesh-bottomed mating tanks overnight and harvesting the fertilized eggs the following morning. Embryos were stored at 28.5°C in Egg Water (60µg/mL "Instant Ocean" [United Pet Group]) or Embryo Medium (mM: 13.7 NaCl; 0.54 KCl; 0.025 Na_2HPO_4; 0.044 KH_2PO_4; 1.3 $CaCl_2$; 1.0 $MgSO_4$; 0.42 $NaHCO_3$; pH=7.2) containing Methylene Blue (Sigma; 0.003%) and PenStrep (Sigma; 10mL/L) until being taken out for use in experiments.

2.2 Phylogenetic Analysis

No previous studies have examined TARPs in zebrafish, so I wanted to begin by examining differences between zebrafish and mouse TARPs at the level of their genetic sequence. Sequences for the *Cacng* genes and their associated amino acid (AA) sequences were taken from the Ensembl (http:// uswest.ensembl.org) genome databases for zebrafish (*Danio rerio*), mouse (*Mus musculus*), frog (*Xenopus sp.*), chicken (*Gallus gallus*) and human (*Homo sapiens*) by searching for members of the *Cacng* gene family. Two zebrafish transcripts were present for

each transcript in the other species, and were designated as *CacngXa* or *CacngXb.* All of the *Cacng* AA sequences for mice were compared with those of zebrafish using pBLAST (http://blast.ncbi.nlm.nih.gov/) (a **b**asic **l**ocal **a**lignment **s**earch **t**ool specific for **p**rotein sequence) against the zebrafish genome in order to determine the overall level of AA sequence identity between the *Cacng* sequences of mice and zebrafish (Altschul et al., 1997, Altschul et al., 2005). The full-length AA sequences of all the *Cacng* genes in mice and zebrafish were then fed one by one into TMpred (http://www.ch.embnet.org/software/TMPRED_form.html), a server that predicts the number and orientation of transmembrane domains for a given AA sequence (Hofmann, 1993). The sequences were then collated and aligned using the TM-Coffee web server (http://tcoffee.crg.cat/tmcoffee), which aligns AA sequences and predicts transmembrane domains (Chang et al., 2012) in order to confirm the results of the TMpred process. Once identified, sections of sequence in the zebrafish TARPs that have been shown to be functionally important in the mammalian TARPs – the first extracellular loop and the C-terminus – were examined so as to determine the level of sequence identity between the two species in these functionally important regions. In order to further clarify the evolutionary history of the TARP gene family, I constructed phylogenetic trees.

2.2.1 Tree Construction

Cacng isoforms were examined at the amino acid level in order to produce better alignments and avoid issues associated with frameshifts from mRNA alignment-imposed sequence gaps. Claudin-1 (*Cldn1*) was arbitrarily chosen as

the member of the Claudin superfamily to use as the outgroup for the trees. Amino acid sequences for the *Cacng* family in zebrafish, mouse, and zebrafish + other vertebrates were aligned using the T-Coffee web server (http://tcoffee.crg.cat/apps/tcoffee/index.html) using the T-Coffee, M-Coffee, TM-Coffee, and Expresso multiple sequence alignment algorithms. T-Coffee provides a basic iterative alignment algorithm that combines both pair-wise and family-wide alignments to generate the final consensus alignment (Notredame et al., 2000). M-Coffee builds upon the foundation of T-Coffee but adds robustness by meta-analysis of multiple individual methods (Wallace et al., 2006, Moretti et al., 2007). TM-Coffee is a T-Coffee variant that specializes in alignments of transmembrane proteins (Chang et al., 2012), and Expresso uses predicted 3D protein structure information to assist the alignment process (Armougom et al., 2006). Each of these four alignment algorithms optimizes based on a slightly different set of variables, so the outputs of each alignment method were themselves aligned using the Combine feature of the T-Coffee webserver, providing what I believe is the most robust possible alignment for each group of sequences, and allowed me to control for possible errors in any individual alignment method. The combined alignment for a given sequence group was fed into the RaxML BlackBox (http://phylobench.vital-it.ch/raxml-bb/) or MEGA 5.2.2 and maximum-likelihood (ML) trees were generated for each alignment using the Gamma model of rate heterogeneity (Stamatakis et al., 2008). As the trees were constructed, 100 or 500 random positions along the amino acid primary structure were resampled and analyzed in a statistical process known as

bootstrapping. Bootstrap values indicate the number of trees (out of the 100 bootstraps) where a given branch existed as shown. Generally speaking, bootstrap values of 70 or above are considered strong support for a particular branch, while a bootstrap value lower than 70 suggests that the branch is not well supported and cannot be assumed to represent the true relationship between its arms.

2.3 **Semi-Quantitative RT-PCR**

Previous work has demonstrated that AMPAR genes in zebrafish are developmentally upregulated between 12 and 72hpf (Lin et al., 2006), as the cells of the nervous system begin to develop, differentiate and connect with each other (Kimmel et al., 1995). Research on TARPs in mice has suggested that *Cacng2* and *Cacng4* may be more important during development than *Cacng3* and *Cacng8* (Tomita et al., 2003, Menuz et al., 2009); therefore I set out to do the first comprehensive study of TARP gene expression during zebrafish neurodevelopment using **R**everse **T**ranscriptase **P**olymerase **C**hain **R**eaction (RT-PCR).

2.3.1 Primer Design

Primers for the *Cacng* genes were designed using a variety of methodologies: by hand according to ClustalW2 alignments; using NCBI's Primer-BLAST; using DNAStar's Lasergene PrimerSelect program; and using IDT's PrimerQuest tool. All methodologies were found to produce equally functional primers at a similar rate (data not shown). Primers were designed to amplify a fragment of approximately 1000bp for each gene.

Table 1. Primers used to assay *Cacng* gene expression through RT-PCR.

Gene Name	Ensembl Gene ID	Forward 5'-3' Sequence	Reverse 5'-3' Sequence	Product Size (bp)
Cacng1a	ENSDARG00000008772	CAGATCTCTGTTTCATATATAAAAA	CACTCTTCATATTGCATTTTAGAG	1058
Cacng2a	ENSDARG00000032565	TTTTTAAATTTGGTTTGGTCCCGT	GTAGGTGGCGGTGGGGGTGCCGTG	918
Cacng2b	ENSDARG00000009621	CCGTCGCTCGTGCTCGTGTTT	CAGACGCCGCGCGAGTACAG	834
Cacng3a	ENSDARG00000058460	CGACAACGACACAAACCGCAAGAA	TTATGAAAGTGTGCGAAGCCGTGG	741
Cacng3b	ENSDARG00000076401	TGGAGCATGGAGTCCGCGCACCAG	TCGGAGTTAAGCAAGGCACCCATT	954
Cacng4a	ENSDARG00000074669	TGGCTTGGTGTGATCGCAGAG	CTGAAGTTGTGGTGCTGAAGATCA	916
Cacng4b	ENSDARG00000039238	ATCGGGACCGATTACTGGCTGTAT	TATCCGTGCCTGATTTGAGAGGGT	787
Cacng5a	ENSDARG00000003326	ACCGAAATCCGCATGTCTCTA	AATTCAGAGTTTTAAGAAAAGGCA	948
Cacng6a	ENSDARG00000036457	GACGCAAGCGAAGACACAGAACAC	CTTATTTGGGTTAAATATACATAT	1136
Cacng7b	ENSDARG00000070624	GAGTATTTCACAGAGCCAGAGA	CTCTAAAGTGTACGTCTACATAAA	1070
Cacng8a	ENSDARG00000020450	CTTCATCTGCAACAGCACTGCCAA	GACTGTGCCATACATTGGTGGCTT	865
Cacng8b	ENSDARG00000070626	CAAGAGGACCCCCATAATAAGGA	CCAGTTTGGGGTCACGGGAGA	697

2.3.2 RNA Extraction and cDNA Synthesis

In order to compile the necessary cDNA samples to examine the developmental expression of the *Cacng* genes, particularly those with demonstrated Type I TARP function (*Cacng2, 3, 4* and *8*), I first had to isolate RNA from organisms at the appropriate time points. After numerous false starts with a variety of different developmental ranges, I eventually settled on 12, 18, 24, 36, 48, 72, and 96hpf as my developmental range, with an adult brain isolate as my positive developmental control. Three cohorts of 4 adult fish (n=3) were anaesthetized in 0.02% Tricaine Methanesulfonate (MS-222; Sigma), sacrificed, and had their brains dissected out in order to provide the necessary mass of tissue (50-100mg) for TRIzol (Invitrogen/Life Technologies) RNA extraction. RNA was extracted from cohorts of 30-60 whole embryos at a particular age from a single parental tank, and was repeated three times using different parental tanks to produce an *n* of 3. RNA extraction was carried out according to the manufacturer's protocol.

Briefly, tissues were homogenized on ice in 1mL TRIzol reagent, which contains phenol and the denaturing agent guanidinium isothiocyanate in order to protect the integrity of the RNA. Chloroform was added and the solution was mixed and centrifuged to allow the protein and DNA to separate from the RNA, which stays in the uppermost aqueous layer. The RNA-containing aqueous layer was then treated with isopropyl alcohol in order to cause the RNA to precipitate

out of the solution. An RNA pellet was harvested by centrifugation, and washed in 75% ethanol in order to remove any residual salts. The clean RNA pellet was resuspended in a small amount of molecular biology grade (RNAse-free) water and the concentration and purity of the RNA was determined by NanoDrop spectrophotometry (Thermo Scientific). A 260/280nm ratio of 1.90 and a 260/230nm ratio of 2.30 was considered pure. RNA stocks were stored at -80°C when not in use.

1μg of each RNA stock was used as the starting material for first-strand cDNA synthesis using a Maxima First Strand cDNA Synthesis kit (Thermo Scientific). This kit converts all RNA present in the sample into cDNA using Oligo $dT_{(18)}$ and random hexamer primers for maximum cDNA yield. cDNA synthesis was carried out according to the manufacturer's protocol.

2.3.3 RT-PCR and Product Sequencing

In order to examine the timeline of *Cacng* expression in zebrafish – particularly the expression of the genes encoding orthologs of the Type I TARPs in mice (*Cacng2a/b*, *Cacng3a/b*, *Cacng4a/b*, *Cacng8a/b*) – RT-PCR was carried out using Phusion High Fidelity DNA polymerase (New England BioLabs), with the reactions being set up according to the manufacturer's guidelines. Final concentrations of each component were as follows: 1X HF buffer, 200μM dNTPs, 0.5μM forward and reverse primers, 1 unit/50μL reaction volume Phusion DNA polymerase, and <250ng of template cDNA. The reactions were run in an Eppendorf Mastercycler Gradient thermocycler under the following conditions:

initial denaturation 98°C 40s; and then 30 cycles of 98°C 15s, 60°C 20s, 72°C 30s; followed by a final elongation step of 72°C for 7min. Experimental reactions using *Cacng* primers were run on agarose gels side-by-side with a set of positive control reactions using primers for Elongation Factor 1α (EF1α) – a developmental housekeeping gene (McCurley and Callard, 2008) (Forward 5'-GGC CAC GTC GAC TCC GGA AAG TCC-3'; Reverse 5'-TCA AAA CGA GCC TGG CTG TAA GG-3'). Products were visualized under ultraviolet (UV) light after bathing the gels in 0.5μg/mL ethidium bromide (Sigma) solution and destaining in dH_2O.

PCR products were cut out of the gel using a clean razorblade and extracted from the gel using a QIAQuick Gel Extraction Kit (QIAGEN). Isolated products were then ligated into the pJET1.2 vector using a CloneJet PCR Cloning Kit (Thermo Scientific) and the blunt-end cloning protocol. 25μL aliquots of competent *E. coli* cells from the NEB10β line (New England BioLabs) were then transformed with a small volume (1-2μL) of ligation product, according to the manufacturer's High Efficiency Transformation protocol. The transformation mixture was then plated out on Lysogeny Broth (LB) (g/L: 10 NaCl, 10 Bacto-tryptone, 5 Bacto-yeast extract, 20 Agar for LB Agar – excluded for broth) agar plates containing 100μg/mL ampicillin (Amp_{100}) and incubated overnight at 37°C. Resultant colonies were screened for the presence of the appropriate insert by colony PCR using Taq polymerase (Fermentas) and the pJET primers included in the CloneJet PCR Cloning Kit. Upon visualization with ethidium bromide, bands at the appropriate product size indicated the presence of the insert in that colony,

and several positive colonies were selected to be grown up in LB+Amp_{100} media at 37°C overnight. Each culture of transformed *E. coli* cells was centrifuged at 3500rpm for 5 minutes at room temperature to pellet out the cells, and the pellet was processed according to the QIAPrep Spin Miniprep Kit (QIAGEN). Purified plasmids were resuspended in molecular biology-grade water, analyzed for concentration and purity using NanoDrop spectrophotometry as previously described, and stored at -20°C when not in use.

Plasmids were sequenced using BigDye Terminator v3.1 (Applied BioSystems). Sequence PCR was set up using 400ng of plasmid as the template, 1X BigDye Terminator 3.1 buffer, and 3.2pmol of pJET forward primer. Sequence PCR reactions were run in an Eppendorf Mastercycler Personal thermocycler for 25 cycles under the following protocol: 96°C 30s, 50°C 15s, 60°C 2min. Sequence PCR products were then precipitated using NaOAc EDTA/Ethanol. Briefly, NaOAc-EDTA and 95% ethanol were added to each sample such that the final concentrations of each were 2.6mM EDTA, 62.5mM NaOAc, and 67-71% ethanol. The solutions were mixed thoroughly, incubated on ice for 15 minutes to precipitate the sequencing product and then spun in a 4°C centrifuge at 13000rpm for 15 minutes to pellet out the product. The supernatant was aspirated away, the pellet was washed with 75% ethanol, and the pellet was spun down again in a 4°C centrifuge at 13000rpm for 5 minutes. The remaining supernatant was aspirated away and the pellet was allowed to air dry, before being submitted to the department's Molecular Biology Service Unit (MBSU) for analysis on their 3730 DNA Analyzer (Applied Biosystems). The identities of

sequenced products were confirmed by comparing the obtained sequences with zebrafish genomic databases through BLAST searches.

2.3.4 Semi-Quantitative Analysis

Photographs of gels were analyzed using ImageJ (NIH)(Schneider et al., 2012). The darkness of the bands was quantified and *Cacng* bands at a given developmental age were compared as a fraction of *EF1α* bands at the same age, from the same gel. Standard errors are given in order to help show the range of band densities observed; however no statistics were performed on the resulting data, as regular RT-PCR cannot really be used to make judgements about *levels* of expression.

2.4 *In Situ* Hybridization

In situ hybridization (ISH) is used to qualitatively examine the topographical expression of a particular gene (or genes) in an organism. Like RT-PCR, ISH is used to track the expression of mRNA transcripts; however ISH has the capacity to provide a more granular output, showing where particular transcripts are expressed. ISH can also be used in a developmental context, to show how mRNA expression patterns change during development.

2.4.1 Probe Synthesis

Anti-sense (AS) ISH probes of ~1000bp were created from the PCR products for the TARP genes most associated with development in mammals – *Cacng2a/b* and *Cacng4a/b*. Purified plasmids containing the correctly oriented sequenced products for each gene of interest were used to transform competent *E.*

coli cells as previously described, and the resultant cultures were plated onto LB+Amp_{100} agar and incubated at 37°C overnight. One colony from each plate was grown up as a 5mL starter culture in LB+Amp_{100} broth for 8-10 hours at 37°C in a shaking incubator. 800µL of each starter culture was mixed with 200µL of 100% glycerol in a screw-cap tube, snap frozen with dry ice, and stored at -80°C. 1mL of each starter culture was then added to 200mL of LB+Amp_{100} and incubated overnight at 37°C in a shaking incubator. These 200mL *E. coli* cultures were subsequently processed using a Plasmid *Plus* Maxi Kit (QIAGEN) in order to harvest the high-concentration plasmids for each of the genes of interest. Maxipreps were performed according to manufacturer's instructions, eluted in molecular biology grade (DNAse/RNAse free) water, and products were NanoDropped to confirm concentration and purity before being stored at -20°C.

10µg of the maxiprepped pJET1.2 plasmids for *Cacng2a*, *Cacng2b*, *Cacng4a*, and *Cacng4b* were linearized in 1X Tango Buffer (Thermo Scientific) with 25u of the restriction enzyme XBaI (Thermo Scientific) in a 40µL reaction volume at 37°C for 2 hours. Linearized plasmid was separated from the other reaction components through a phenol/chloroform extraction. Briefly, 160µL of RNAse free (DEPC-treated) water was added to each sample for a total volume of 200µL, then 200µL of Phenol/Chloroform/Isoamyl Alchohol (Fisher Scientific) was added and the sample was vortexed and centrifuged at maximum speed for 5 minutes. After centrifugation, the uppermost layer was transferred to a new tube and 200µL of chloroform was added. The tube was vortexed and centrifuged at maximum speed for 5 minutes, and the uppermost layer was transferred to a new

tube. The isolated linearized DNA was then precipitated out using the NaOAc-EDTA/Ethanol method previously described and resuspended in RNAse-free H_2O. The concentration and purity of this linearized DNA solution was determined using NanoDrop spectrophotometry (described previously) and the solution was stored at -20°C when not in use.

2µg of linearized DNA solution was used as the template material for probe synthesis, which included 1X DIG-Labeling Mix (Roche), 1X Transcription Buffer (Roche), 20u of T7 RNA Polymerase (Roche) and 40u of RNAse OUT (Invitrogen) in a 20µL total reaction volume. This probe synthesis reaction and the ISH protocol that follows is based closely on the procedure used by the Thisse group (Thisse and Thisse, 2008) for their high throughput *in situ* hybridization experiments, which are the gold standard in whole mount zebrafish ISH. Pure RNA probe stocks were stored at -80°C. RNA probe for use was diluted 1/200 in hybridization medium (HM)(50% formamide, 5X SSC buffer [20X stock: 3M NaCl, 300mM trisodium citrate, pH 7.0], 50µg/mL heparin [Sigma], 500µg/mL Type II-C Ribonucleic acid from torula yeast core [tRNA replacement; Sigma], 0.1% Tween-20 [Fisher Scientific], 0.092M Citric acid) and stored at -20°C.

2.4.2 In Situ *Hybridization Protocol*

Embryos intended for use in ISH were set aside between 12 and 24hpf and placed in 0.003% 1-phenyl 2-thiourea (PTU) (Sigma) in Embryo Medium in order to inhibit pigment formation. Embryos and larvae were removed from this solution for ISH at 12, 24, 48 and 72hpf, and placed in 4% paraformaldehyde

(PFA) fixative for 2 hours at room temperature or overnight at 4°C. Fixed embryos were washed immediately with 1X Phosphate Buffered Saline with Tween (PBS-T) (10X PBS-T stock, g/L: 10.8 Na_2HPO_4, 65 NaH_2PO_4, 80 NaCl, 2 KCl, pH 5.5; 0.1% Tween-20), 5x5min. Embryos that remained unhatched at this point were dechorionated manually during the PBS-T washes. **NB: At this point, future studies should consider a 1 hr RNAse-free DNAse treatment (50 U/ml in DNAse buffer) at 37°C in order to eliminate the genomic DNA and ensure probe specificity.** Embryos were permeablized with Proteinase K (10 μg/mL in PBS-T; Sigma) for varying times, depending on the developmental stage of the embryo: 1min for 12 hpf, 5 min for 24 hpf, 25 min for 48 hpf and 60min for 72 hpf. Permeablized embryos were refixed in 4% PFA for 20min, rinsed with PBS-T 5x5min and then pre-hybridized in 500μL HM for at least 60min at 65°C. *In situ* probes in HM (HM + probe) were pre-warmed during this time, and when the pre-hybridization solution was removed, it was replaced with HM + probe. Attaining sufficient staining for the *Cacng* genes was found to be quite challenging, and required a 40hr hybridization period at 65°C. After hybridization, the HM + probe solution was retained and stored at -20°C for future reuse.

Following the hybridization period, embryos underwent several washes at 65°C in order to wash them out of HM and into sequentially higher proportions of 2X SSC, and then from 2X SSC down to 0.2X SSC + 0.01% Tween and eventually down to 0.1X SSC + 0.01% Tween. These latter SSC + Tween washes are stringency washes that help to prevent nonspecific binding of the probe. At this point, the embryos were removed from the 65°C bath and placed at room

temperature, and the solutions were now progressively washed into higher proportions of PBS-T. Once in 100% PBS-T, the embryos were placed in a blocking solution (2% sheep serum [Sigma], 2mg/mL bovine serum albumin [Sigma] in PBS-T) and shaken for 1hr at room temperature. Anti-DIG antibody (Roche) solution was prepared by diluting the antibody 1/5000 in blocking solution, and embryos were placed on a shaker in this anti-DIG antibody solution for 2hr at room temperature or overnight at 4°C. After the antibody incubation, embryos were washed 5-7x15min depending on the length of the incubation.

Embryos were given two to three quick washes in molecular grade H_2O and then the colouration reaction was started by incubating the embryos in 1mL each of BM Purple (Roche) at room temperature in the dark. Again, staining the *Cacng* genes proved to be challenging, requiring colouration times of 2.5-3.5hr for sufficiently dark staining, depending on the gene. The colouration reaction was stopped by washing the embryos twice in 100% Methanol + 0.01% Tween, and the embryos that were not processed immediately were stored in the dark at 4°C on a shaker in this stop solution. Embryos were processed for mounting by washing them progressively into PBS-T. Once in PBS-T, embryos were sunk in progressively higher concentrations of glycerol, culminating at ~90% glycerol. At this point, embryos 24hpf and older were de-yolked, had their tails removed, and frontal sections were cut from a few of the heads in the 48 and 72 hpf groups. Whole 12hpf embryos were imaged in glycerol in porcelain viewing dishes using a dissecting microscope; while older embryos and larvae were mounted in glycerol on microscope slides and imaged using bright field (BF) and differential

interference contrast (DIC) optics on an Axio Imager compound light microscope (Carl Zeiss International), with its Axio Cam camera and Axio Vision software (Carl Zeiss International).

2.5 **Morpholino Oligonucleotide Knockdowns**

In order to begin to determine the functional role of TARPs in zebrafish, specific splice-blocking Morpholino Oligonucleotides (MOs) targeted to *Cacng2a, Cacng2b, Cacng4a* and *Cacng4b* were ordered from Gene-Tools LLC. The types of MO generally used to knock down genes are characterized as either translation-blocking or splice-blocking: translation-blocking MOs bind to the start codon of the mRNA and sterically block the translation of the message; splice-blocking MOs bind to exon/intron splice sites in the pre-mRNA, blocking the assembly of the spliceosome and causing the intron to be included. Splice-blocking MOs usually knock down their targets by inducing a frameshift, resulting in a premature stop codon; however, depending on the location of the splice site along the length of the mRNA sequence, this method does not necessarily result in complete knock down of the protein, as the shortened mRNA may still be translated and form a partially or completely functional protein. The splice-blocking type of MO was chosen over the alternative translation-blocking MOs because knockdown of splice-blocking MOs can theoretically be assayed using simple RT-PCR rather than requiring specific antibodies (antibodies that do not exist for zebrafish TARPs).

2.5.1 MO Design and Injection

Specific splice-blocking MOs were designed on our behalf by staff at Gene-Tools LLC. MO stocks were created by resuspending the MO in molecular-grade H_2O at a concentration of 1mM. The sequences of our MOs were as follows:

Cacng2a e1i1 – GGCATAACAGTCGCCTTACCTTCCA

Cacng2b e4i4 – AGGAACACACGGAGCCGCTCACCT

Cacng4a e2i2 – AAGGCAGTCACTCACGTAAGAGATA

Cacng4b e1i1 – ACATGCATCCGTTTACCTTCGATAC

MOs were prepared and injected according to the guidelines set out by Stephen Ekker's lab (Bill et al., 2009). In brief, the effective dosage was determined by testing three different concentrations – 1, 2 and 4ng/nL – and the highest dosage without significant mortality or MO-induced toxicity was chosen for each MO. In all four cases, that dosage was 4ng/nL. The injection solutions consisted of 4ng/nl MO and 0.05% Phenol Red in 1X Danieau solution (mM: 58 NaCl, 0.7 KCl, 0.4 MgSO4, 0.6 $Ca(NO_3)_2$, 5.0 HEPES, pH 7.6). Borosilicate glass capillary tubes BF-120-94-10 (Sutter Instrument Co.) were pulled into micro-injection needles using a P-97 pipette puller (Sutter Instrument Co.)(Box filament; Heat 475, Pull 30, Velocity 50, Time 220, Pressure 200), and the tips of these needles were broken back under a dissecting microscope using #5 forceps (Dumont). Micro-injection needles were backfilled with injection solution using Microloader pipette tips (Eppendorf) and mounted on the micromanipulator. A

Picospritzer III Microinjection System (Parker) was calibrated to reliably eject 1nL boluses of solution from each micro-injection needle using a foot pedal control. 30-50 embryos at the 1-4 cell stage were injected at a time, and then returned to Embryo Medium + MB + Penstrep to continue development. Injected embryos intended for use in ISH experiments were placed in 0.003% PTU between 12 and 24hpf and then fixed at 48hpf. Injected embryos used for cDNA synthesis (RT-PCR) or for behavioural assays were raised in Embryo Medium + MB + Penstrep until 48hpf.

2.5.2 Knockdown Assessment

In order to assess the extent of the knockdown, RT-PCR was performed. MOs were injected at all three concentrations, and injected 48hpf fish were used for RNA Extraction and cDNA Synthesis as previously described. cDNA was also synthesized from mock-injected 48hpf control embryos and uninjected 48hpf embryos. These five cDNA groups were tested for their expression of the relevant *Cacng* gene in comparison to their expression of *EF1α* in order to confirm the specificity of the knockdown and the quality of the cDNA. The RT-PCR protocol was identical to the protocol used for the Semi-quantitative RT-PCR experiments described previously. New primers had to be designed for *Cacng2b, Cacng4a* and *Cacng4b*.

The extent of MO knockdown was also assayed using ISH as described previously. Side-by-side ISH experiments using 4ng injected and uninjected

48hpf embryos were performed in order to confirm both the presence of knockdown and the specificity of our ISH probes.

Gene Name	Forward Primer 5'-3' Sequence	Reverse Primer 5'-3' Sequence	Product Size (bp)
Cacng2b	CGTTTCTGCAGCAGGTCTGAG	ATAATCTGCTCCTCGCACTCG	238
Cacng4a	GCTGCCAAAGAAAACTCGGG	CTGCCAACACAGCAATGGTC	449
Cacng4b	CCACCGTTGGAGCTTTTGTG	CCAGCAACAGCAGGATGGGA	327

Table 2 Primers used to assay MO knockdown by RT-PCR in 48 hpf zebrafish embryos.

2.5.3 Behavioural Assays

The escape behaviour of free-swimming fish was used to determine if single knockdowns of *Cacng* mRNA transcripts would result in a noticeable deficit in the swimming ability of the fish. Microinjection needles were pulled and broken back as previously described, and backfilled with an Ejection Marker solution (0.05% Phenol Red in Embryo Medium). The Picospritzer was set to deliver a 20ms pulse at 50psi, and injected 48hpf fish were placed in 1mL bubbles of Embryo Medium. An S-PRI*plus* high-speed camera (AOS Technologies AG) was

mounted to the headstage of the dissecting microscope and connected to a consumer PC running AOS Imaging Studio (AOS Technologies AG). The camera was set to capture images at a framerate of 1000 frames/s. The microinjection needle was carefully adjusted so that the tip was as close to the skin of the tail as possible without disturbing the fish, and the pulse of solution and camera shutter were triggered simultaneously using the footpedal for the microinjection system and the hand trigger for the camera. Collected videos were analyzed for the morphology of the fish tested and the latency of the escape response using AOS Imaging Studio (AOS Technologies AG), and data were statistically analyzed using student's t-tests ($p<0.05$)

3. Results

3.1 Phylogenetic Analysis

Ours is the first study of the *Cacng* family in a non-mammalian vertebrate; therefore I first examined the known sequence data in order to confirm the identities of the zebrafish *Cacng* family members, as well as to probe their similarity to their hypothetical orthologs in mice. Previous research has identified two regions of the TARP protein that are particularly important for its function: the first extracellular loop (Milstein et al., 2007), which mediates the interaction of the TARP with the pore of the AMPA receptor; and the C-terminus (Tomita et al., 2005a, Tomita et al., 2005b), which meditates the trafficking and anchoring of the TARP-AMPAR complex to the post-synaptic density.

3.1.1 Conservation of TARP C-Terminal Domains

The C-termini of the aligned TARP sequences were isolated using TMpred, and analyzed by eye to determine the levels of sequence identity between orthologs, as well as the level of conservation of phosphorylatable residues (serine [S], threonine [T], tyrosine [Y]). Considerable research in mammals has already established certain residues of the C-terminus as being phosphorylatable (Choi et al., 2002, Tomita et al., 2005b) and/or involved in trafficking (Cuadra et al., 2004); my objective here was to determine the extent to which these previously identified residues are conserved in zebrafish.

I began my examination by BLASTing all of the mouse and zebrafish *Cacng* AA sequences to determine their level of *overall* identity between species – this was used as a benchmark when comparing specific regions of AA sequence. The level of sequence identity between each mouse gene and its zebrafish counterparts was averaged in order to account for varying levels of identity between the zebrafish paralogs. AA sequence identities between mice and zebrafish are as follows: γ1 - 62.5%; γ2 - 86.5%; γ3 - 71.5%; γ4 - 65%; γ5 - 89.5%; γ6 - 43.5%; γ7 - 81.5%; γ8 - 67%. The highest identity is found in γ5, a Type II TARP, and the lowest identity is found in γ6, which functions as a calcium channel γ subunit, not a TARP. Of the Type I TARPs, γ2 and γ3 are most similar between mice and zebrafish at 86.5% and 71.5%, respectively, while γ4 and γ8 are less conserved (65% and 67%). Interestingly, both of the Type II TARPs show very strong sequence identity (>80%), while the four Type I TARPs show a greater range of sequence identities (65-86.5%).

In examining the C-Termini of the TARP proteins (Figure 2), one notices almost immediately that the level of homology is quite a bit less than what one might expect from the overall sequence homologies reported above. Where the overall AA homologies of the Type I TARPs range from 65-86.5%, the homologies of the C-Termini of those same molecules range from 24.5-64.6%, with an average much closer to 24.5% - a statistically significant decrease at the 95% confidence level (unpaired t-test). Figure 2 highlights the **n**euronal isoform of **p**rotein **i**nteracting **s**pecifically with **T**C10 (nPIST) domain and the PDZ domain, which are involved in trafficking the TARP/AMPAR complex from the golgi apparatus (Cuadra et al., 2004) and anchoring said complex to the PSD, respectively. nPIST domains are still relatively poorly described, so the large purple block represents a conservative guess at the general area that acts as an nPIST domain. I took note of the conserved phosphorylatable residues within the nPIST domain between mice and zebrafish for each of the Type I TARPs, but most of them occur at the beginning of the nPIST domain, and coincide with several previously characterized sites of phosphorylation that occur just prior to the nPIST domain (Payne, 2008). Ultimately, examining the C-termini of the Type I TARPs gives us two pieces of important information: 1) the C-termini are not generally well conserved, but 2) the phosphorylated residues (that we know of) seem to be quite well conserved. This interesting finding led me to further examine another fragment of sequence that is important for TARP function: the first extracellular loop.

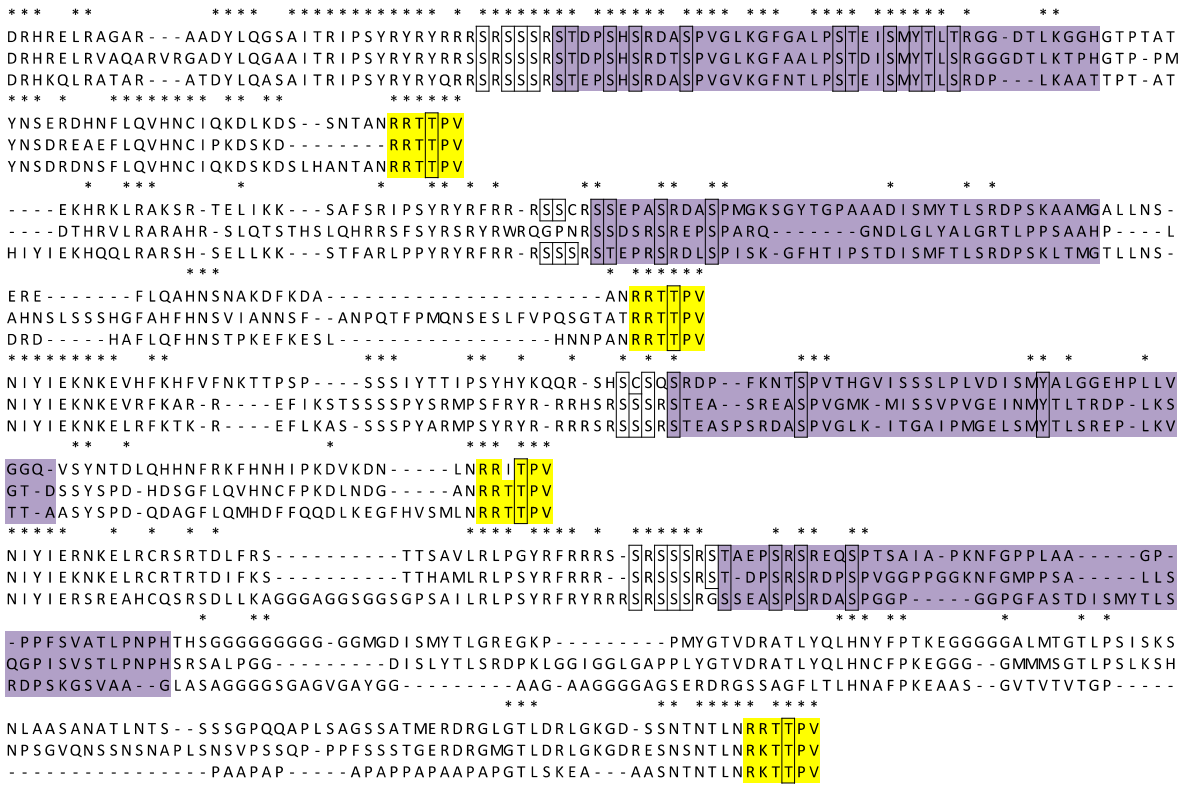

	γ2	γ3	γ4	γ8	Average	t-Test (p<0.05)
Overall Identity (%)	86.5	71.5	65	67	72.5	-
C-Term Identity (%)	64.6	24.5	31.3	25.4	36.5	0.004*
nPIST Identity (%)	67.2	21.1	20.5	11.8	30.1	0.002*

Figure 2 The sequence of the C-Terminus of the TARP protein differs significantly between zebrafish and mice. The overall sequence identity (using the full-length AA sequence for each set of orthologs), the sequence identity specific to the C-terminus, and the sequence identity specific to the nPIST domains are shown. The C-Termini are significantly less well-conserved than the rest of the AA sequences (two-tailed t-test, $p<0.05$). The nPIST domains are also significantly more poorly conserved relative to the overall identity of the protein (t-test, $p<0.05$; but not significantly worse than the rest of the C-terminus, $p=0.08$). In spite of these widespread changes, the terminal PDZ binding domains and the phosphorylated serine residues prior to the nPIST are well-conserved. TARP amino acid sequences were fed into TMPred and TM-Coffee in order to determine the location of the C-terminus. C-terminal sequences for all the zebrafish and mouse TARPs were then aligned with T-Coffee and each set of orthologs was manually inspected for sequence identities (*). The neuronal isoform of protein-interacting specifically with TC10 (nPIST) domains from mice are highlighted in purple, the type I PDZ-binding domain is highlighted in yellow, boxes surround conserved phosphorylatable residues (S, T, Y) within the nPIST domain, as well as the serine residues outside the nPIST domain that have been shown to be phosphorylated. The percentage of sequence identity between the different species for each TARP isoform is shown in the table.

3.1.2 Conservation of TARP Extracellular Loop 1

The first extracellular loops (ECL1) of the TARP proteins interact with the pore of the AMPAR complex (Figure 1) and modulates the pharmacology, gating, and kinetic properties of the AMPAR. ECL1s were isolated using TMpred and TM-Coffee by the same method as was used for the C-Termini and sequence identities were determined by eye. Surprisingly, no studies have examined the specific residues responsible for the interaction between TARPs and AMPARs. I began by quantifying the level of sequence identity specific to the ECL1 for each TARP isoform (Figure 3). The best-conserved first extracellular loop belongs to γ3 with 84% identity, while the least-conserved is γ4 with 59% ECL1 identity. The average sequence identity of ECL1 of the TARPs is 75% - statistically almost identical to the average overall sequence identity of the same genes (76.8%) (unpaired t-test, $p=0.75$). From these data there is nothing to suggest that ECL1 is especially well conserved compared to the rest of the protein sequence for a given TARP: however ECL1 *is* significantly better conserved than the C-termini in a given protein (unpaired t-test, $p<0.05$). Importantly, the cysteine residues implicated in forming the pore of Claudin proteins are conserved in all of the *Cacng* genes surveyed here across mice and zebrafish. I also determined the level of conservation of the charged residues of ECL1, in order to determine the potential role of charge in modulation of the properties of AMPARs. The positive (R, H, K) and negative (D, E) amino acid residues of ECL1 are extremely well-conserved – ranging from 75% (γ4) to 100% (γ3 and γ5) identity, with an average of 91.2% identity between the mouse and zebrafish orthologs. This was found to

be a significant increase relative to the level of overall sequence identity for a given set of orthologs (unpaired t-test, $p<0.05$), suggesting that these charged residues are highly selected for. Finally, by tallying the number of positive and negative residues, I determined that ECL1 of all of the TARPs carries a net negative charge of either -1 or -2.

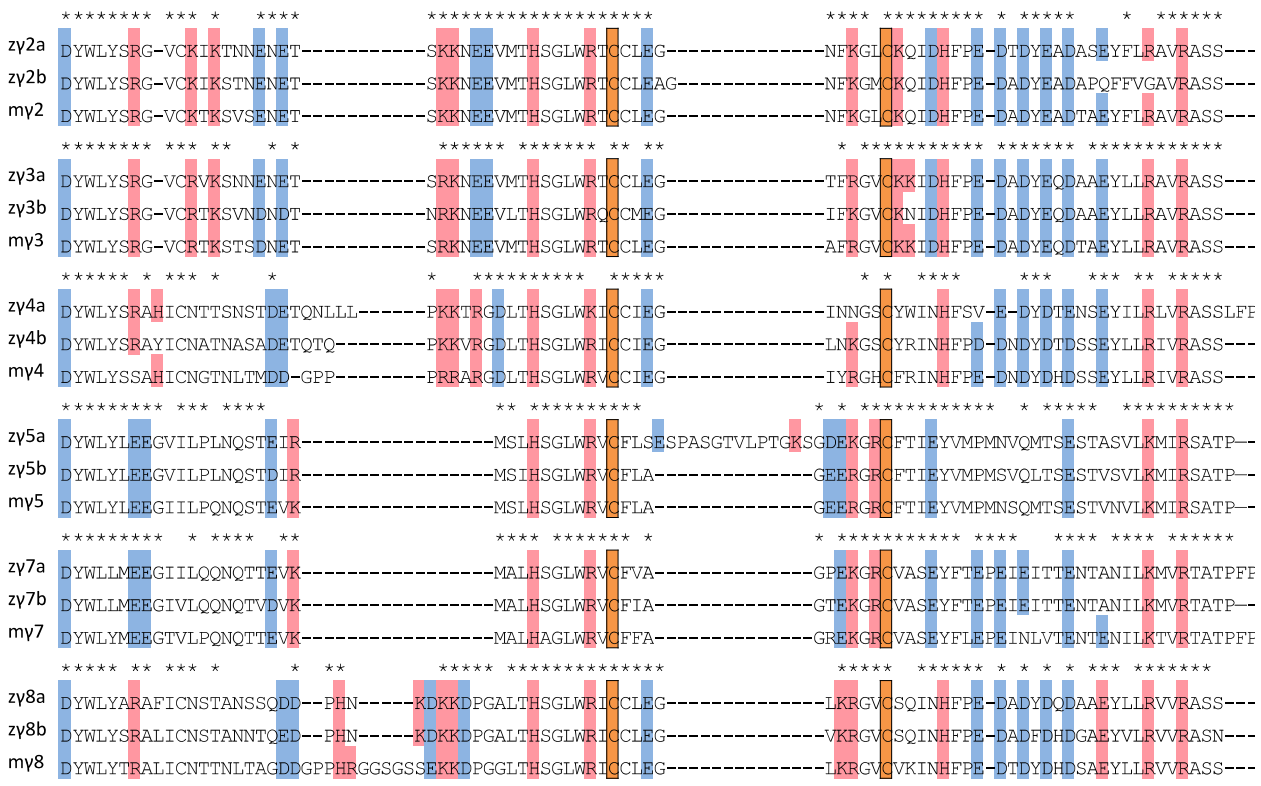

	γ2	γ3	γ4	γ5	γ7	γ8	Average	t-Test (p<0.05)
Ex Loop 1 Identity (%)	82	84	59	76	79	70	75	0.75
Overall Identity (%)	86.5	71.5	65	89.5	81.5	67	76.8	-
Charged Residue Identity (%)	92	100	75	100	88.2	92	91.2	0.03*

Figure 3 The charged amino acids of the first extracellular loop are significantly better conserved than the rest of the protein. TARP amino acid sequences for mouse (mγX) and zebrafish (zγXa/b) were fed into TMPred and TM-Coffee in order to determine the location of the first extracellular loop. Loop sequences for each TARP were then aligned with T-Coffee and manually inspected for sequence identities (*). The sequence was also manually inspected for positively charged (red) and negatively charged (blue) conserved residues, the total of which was quantified relative to the total number of charged residues (including nonconserved residues). The pore-forming Claudin-related cysteine residues are highlighted in orange and boxed. Sequence identities for the first extracellular loop and its charged AA residues between mouse and zebrafish are quantified in the bottom table, and shown compared to the overall identity between the complete sequence in each species for each protein. Significance was determined using an unpaired two-tailed t-test ($p<0.05$)

3.1.3 Phylogenetic Analysis of Mouse and Zebrafish TARP AA Sequences

After my sequence analysis of the potential functional regions of the zebrafish TARP proteins, I wanted to learn what I could about the evolutionary history of the TARP proteins in zebrafish as compared to mice: in particular, I wanted to confirm the status of the additional zebrafish *Cacng* genes as paralogs to each other and orthologs to the appropriate murine *Cacng* genes. I began with an alignment of all the TARPs in mice, and created a maximum-likelihood (ML) tree in order to examine some of the basic relationships between the proteins (Figure 4A). Based on the sequences given, the tree suggests that the Type I TARPs (*Cacng2, Cacng3, Cacng4, Cacng8*) are the most derived members of the TARP family, followed by the Type II TARPs (*Cacng5* and *Cacng7*); the basal members of the family, according to this tree, are the voltage-gated calcium channel gamma subunits: *Cacng1* and *Cacng6*.

Another ML tree was produced using all of the zebrafish TARP amino acid sequences; however this tree suggests different evolutionary relationships between the *Cacng* genes (Figure 4B). In particular, *Cacng1* and *Cacng6* are the most derived members of the family, while the Type I TARPs are now basal. Notably, the bootstrap support values for the placement of the Type I TARPs on this tree are low (≤70), with the only strong values being those that link the paralogs of *Cacng3* and *Cacng8*.

In order to improve the accuracy of the predictions of my phylogenetic tree, I created a ML gene tree containing all of the *Cacng* AA sequences of mice,

zebrafish, humans, chickens and frogs. This tree had similar architecture to the tree for the zebrafish sequences, but had the advantage of stronger bootstrap support values and clear grouping relationships between the different genes (Figure 5). All of the predicted orthologs formed monophyletic groups with each other. Based on this tree, we can confidently conclude that the duplicated TARP genes we find in zebrafish are indeed paralogous and are the appropriate orthologs to their murine and vertebrate counterparts.

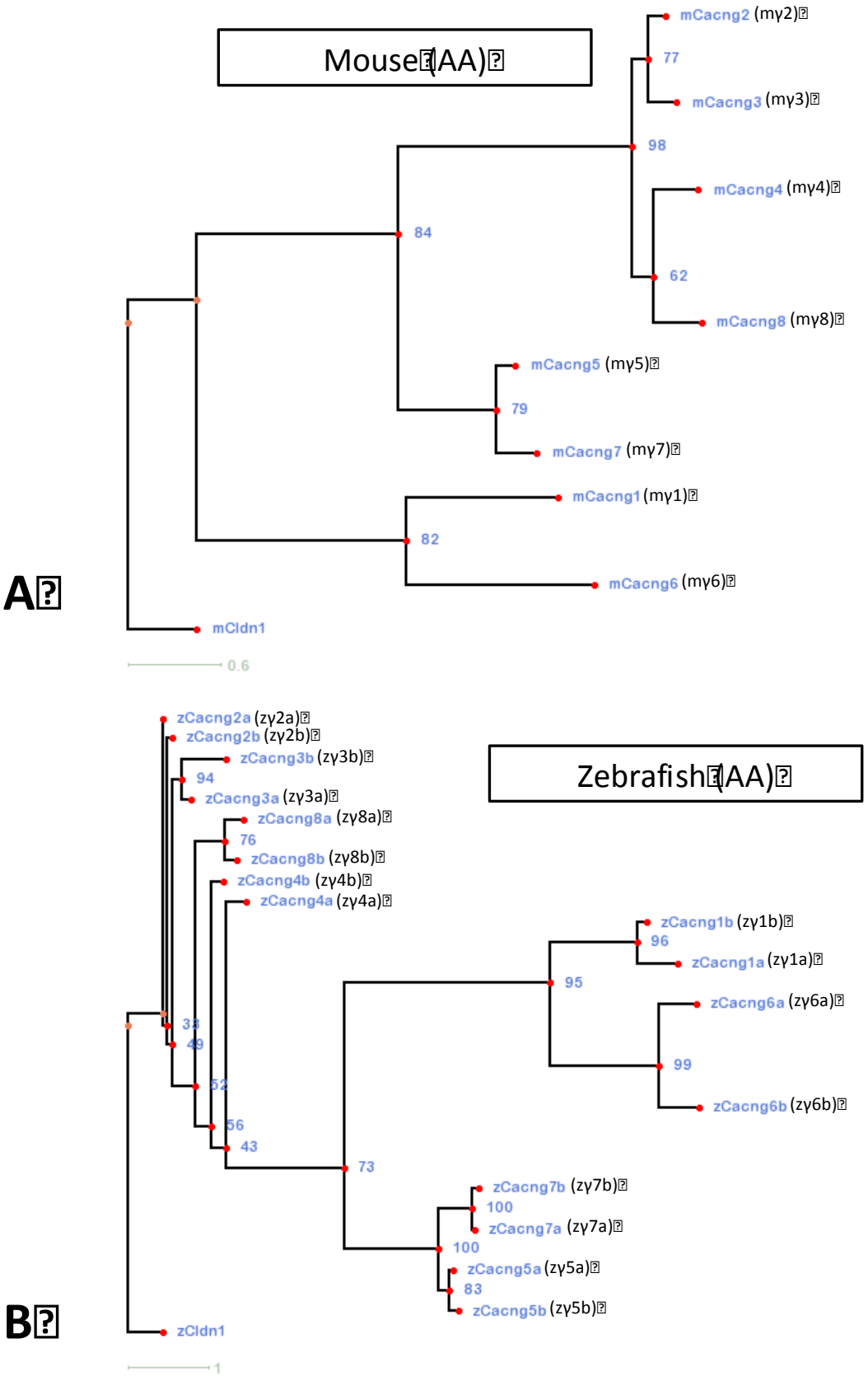
Mouse (AA)
mCacng2 (mγ2)
77
mCacng3 (mγ3)
98
mCacng4 (mγ4)
84
62
mCacng8 (mγ8)
mCacng5 (mγ5)
79
mCacng7 (mγ7)
mCacng1 (mγ1)
82
mCacng6 (mγ6)
mCldn1
0.6
A
Zebrafish (AA)
zCacng2a (zγ2a)
zCacng2b (zγ2b)
zCacng3b (zγ3b)
94
zCacng3a (zγ3a)
zCacng8a (zγ8a)
76
zCacng8b (zγ8b)
zCacng4b (zγ4b)
zCacng4a (zγ4a)
zCacng1b (zγ1b)
96
zCacng1a (zγ1a)
95
zCacng6a (zγ6a)
38
49
99
52
zCacng6b (zγ6b)
56
43
73
zCacng7b (zγ7b)
100
zCacng7a (zγ7a)
100
zCacng5a (zγ5a)
83
zCacng5b (zγ5b)
zCldn1
1
B

Figure 4 The phylogenetic relationships of the *Cacng* genes in mice (A) and zebrafish (B) are not clearly the same. Amino acid sequences for each *Cacng* gene were taken from the Ensembl genome database and fed through several T-Coffee multiple sequence alignments (T-Coffee, TM-Coffee, M-Coffee, Expresso) before being collated using T-Coffee Combine to create a master alignment for the gene family in each species. Master alignments were analyzed using RAxML BlackBox, using the Gamma model of rate heterogeneity and accounting for the proportion of invariant sites, in order to produce the maximum-likelihood trees shown here. The best supported nodes in each species support previous work grouping the different members of the family together (Type I/II TARPs, calcium channel *gamma* subunits), as well as grouping (most of) the paralogous genes in zebrafish together. Claudin-1 (*Cldn1*) was chosen as the outgroup for both species. Bootstrap support at each node is indicated, with values greater than 70 indicating strong bootstrap support for a given node. The scale below each tree is relative, indicating the relative number of differences in the sequences with longer horizontal branch lengths.

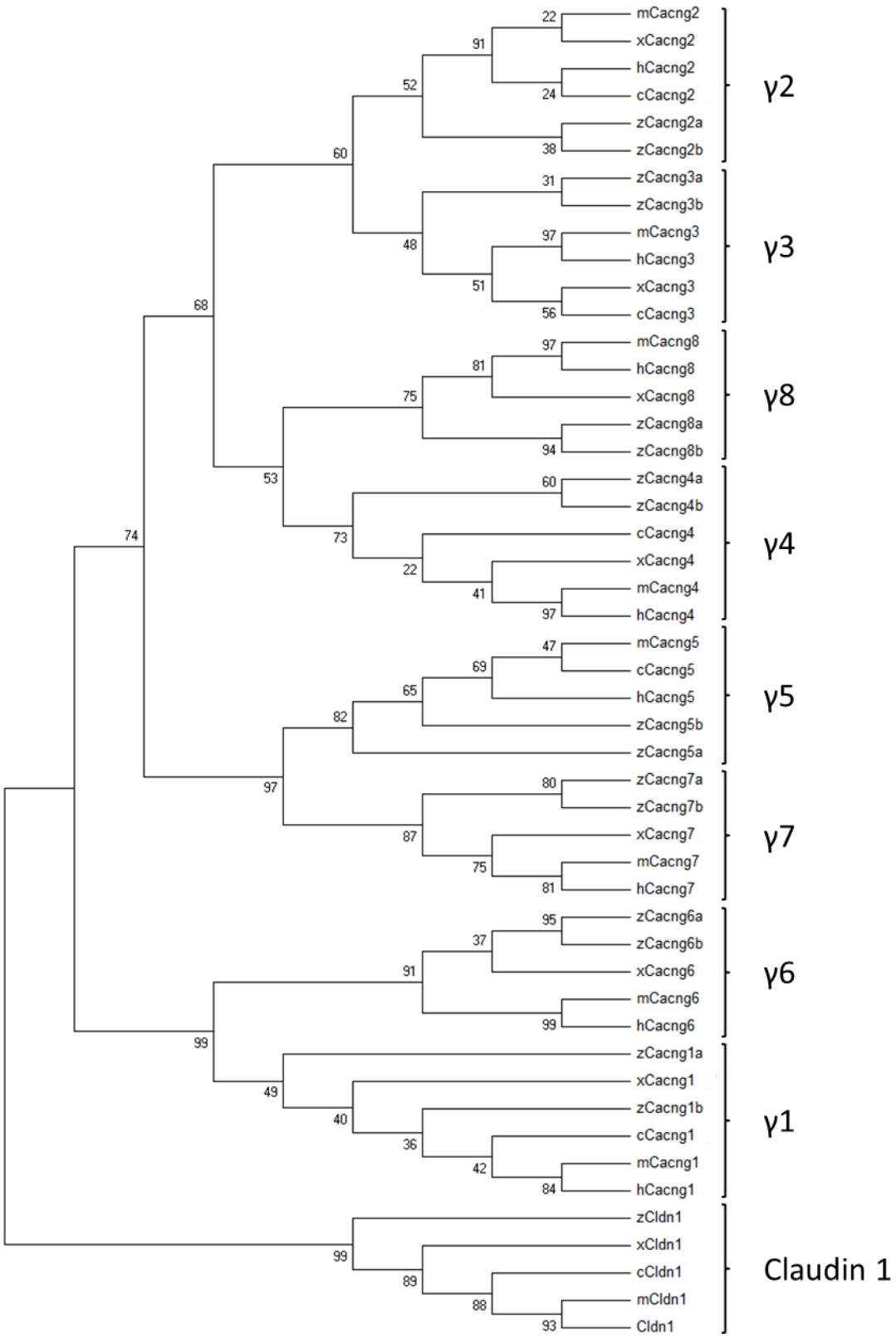
mCacng2
xCacng2
hCacng2
cCacng2
zCacng2a
zCacng2b
γ2
zCacng3a
zCacng3b
mCacng3
hCacng3
xCacng3
cCacng3
γ3
mCacng8
hCacng8
xCacng8
zCacng8a
zCacng8b
γ8
zCacng4a
zCacng4b
cCacng4
xCacng4
mCacng4
hCacng4
γ4
mCacng5
cCacng5
hCacng5
zCacng5b
zCacng5a
γ5
zCacng7a
zCacng7b
xCacng7
mCacng7
hCacng7
γ7
zCacng6a
zCacng6b
xCacng6
mCacng6
hCacng6
γ6
zCacng1a
xCacng1
zCacng1b
cCacng1
mCacng1
hCacng1
γ1
zCldn1
xCldn1
cCldn1
mCldn1
Cldn1
Claudin 1

Figure 5 The *Cacng* genes of vertebrates are orthologous to each other. The evolutionary history was inferred using the Maximum Likelihood method using the JTT with frequency model. Amino acid sequences for the *Cacng* genes (and *Cldn1* as the outgroup) of several vertebrates were taken from the Ensembl genome database and fed through several T-Coffee multiple sequence alignments (T-Coffee, TM-Coffee, M-Coffee, Expresso) before being collated using T-Coffee Combine to create a master alignment for the gene family that included all species. The phylogenetic relationships between the *Cacng* AA sequences in zebrafish (*zCacng*), mice (*mCacng*), humans (*hCacng*), chickens (*cCacng*) and frogs (*xCacng*) are shown; the grouping together of the *Cacng* subtypes regardless of species is a strong indicator of homology between the genes. The tree with the highest log likelihood (-3887.5261) is shown. The initial tree for the heuristic search was obtained by applying the Neighbor-Joining method to a matrix of pairwise distances estimated using a JTT model. A discrete Gamma distribution was used to model evolutionary rate differences among sites (5 categories (+G, parameter = 6.0805)). The rate variation model allowed for some sites to be evolutionarily invariable ([+I], 0.0000% sites). The bootstrap analysis involved 49 amino acid sequences. All positions containing gaps and missing data were eliminated. There were a total of 105 positions in the final dataset. Evolutionary analyses were conducted in MEGA5.

3.2 RT-PCR

After examining the conservation of the TARP genes at the amino acid sequence level, I wanted to determine what their general patterns of mRNA expression were during the development of the nervous system and locomotion (12-96 hpf). Expression of the Type I and II TARPs in developing zebrafish was assayed using RT-PCR, and band intensities at each developmental time point were measured and compared with expression of a housekeeping gene at the same developmental time point. This non-quantitative method means that I cannot make claims about the expression level of a particular gene at a particular time point – I can only say whether a gene is "on" or "off". The general trend for all of the TARPs is that they turn on at some point between 12 and 96 hpf. The figures for PCR have been arranged to reflect the phylogenetic relationships within the *Cacng* family, with each side of the Type I TARP fork – containing *Cacng2/3* and *Cacng4/8* respectively – presented on its own, and the Type II TARPs – *Cacng5* and *Cacng7* – presented on their own.

3.2.1 Developmental Expression of Cacng2 and Cacng3

Figure 6 shows the expression pattern of *Cacng2a/b* and *Cacng3a/b* from 12-96 hpf whole-animal preparations and in the brain isolate of adult fish. Expression of *Cacng2a* turns on between 12 and 48 hpf; a similar expression pattern is seen with *Cacng2b*, turns on between 12 and 24 hpf, and plateaus slightly earlier - at 36 hpf. *Cacng3a* is not appreciably expressed until 48 hpf and then jumps to a plateau from 72 hpf onwards. The expression of *Cacng3b* differs from its paralog as its expression turns on more gradually, between 24 and 72 hpf.

3.2.2 Developmental Expression of Cacng4 and Cacng8

The expression of the genes that make up the other half of the Type I TARP fork, *Cacng4* and *Cacng8,* is shown in Figure 7. *Cacng4a* is barely expressed at 12 hpf, but just six hours later at 18 hpf it has reached its expression plateau. On the other hand, *Cacng4b* expression appears to be present throughout the 12-96 hpf developmental time period I used. The expression of *Cacng8a* turns on between 24 and 72 hpf, where it reaches a plateau. The expression of *Cacng8b* is reminiscent of the expression of *Cacng4a,* as it appears to also be barely expressed at a low level at 12 hpf, and then turn on by 18 hpf.

3.2.3 Developmental Expression of Cacng5 and Cacng7

I decided very early on to focus my efforts on examining the expression and function of a selection of Type I TARPs, so when I discovered that all of the TARP genes had duplicates, I made the decision not to run PCR on the paralogs of the Type II TARPs. As such, I can only provide preliminary data on the expression of Type II TARPs during zebrafish development, with *Cacng5a* and *Cacng7b* (Figure 8). *Cacng5a* and *Cacng7b* share a similar expression pattern to *Cacng3a*, with expression not turning on until 72 hpf.

3.2.4 Summary of Expression of Type I TARPs and Adult TARP expression

Half of the Type I TARP genes are turned on between 48 and 72 hpf: *Cacng2a, Cacng3a, Cacng3b, Cacng8a.* The other half of the Type I TARP genes reach their plateau levels of expression earlier, sometime between 12 and 36 hpf:

Cacng2b, Cacng4a, Cacng4b, Cacng8b. Based on what is known about TARP gene expression in mice (Tomita et al., 2003), I did not expect to see a significant amount of *Cacng4* expression in our adult brain isolates; however all of the TARP genes we examined, including *Cacng4a* and *Cacng4b*, were robustly expressed in our adult brain cDNA.

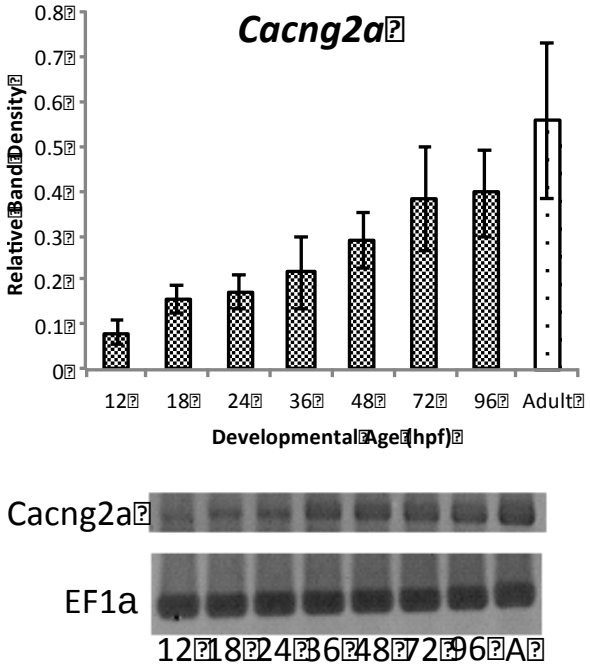
Cacng2a
Relative Band Density
0.8
0.7
0.6
0.5
0.4
0.3
0.2
0.1
0
12 18 24 36 48 72 96 Adult
Developmental Age (hpf)
Cacng2a
EF1a
12 18 24 36 48 72 96 A

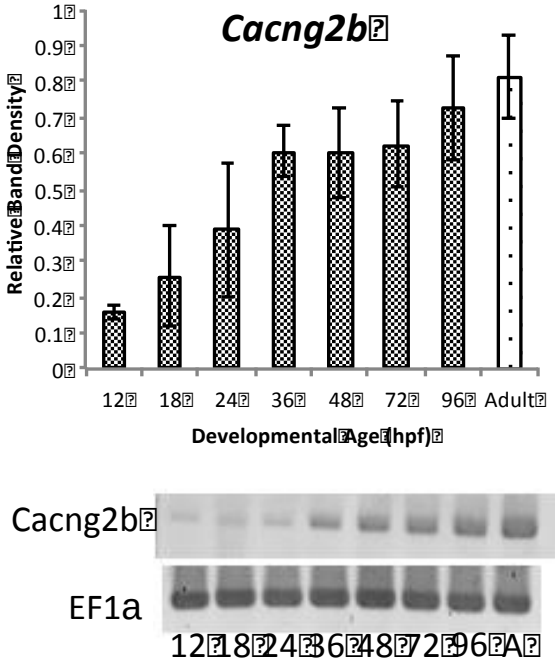
Cacng2b
Relative Band Density
1
0.9
0.8
0.7
0.6
0.5
0.4
0.3
0.2
0.1
0
12 18 24 36 48 72 96 Adult
Developmental Age (hpf)
Cacng2b
EF1a
12 18 24 36 48 72 96 A

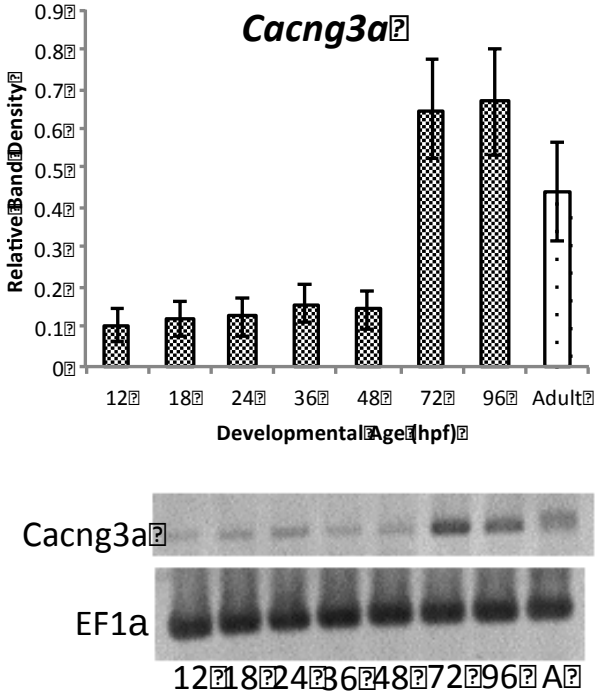
Cacng3a
Relative Band Density
0.9
0.8
0.7
0.6
0.5
0.4
0.3
0.2
0.1
0
12 18 24 36 48 72 96 Adult
Developmental Age (hpf)
Cacng3a
EF1a
12 18 24 36 48 72 96 A

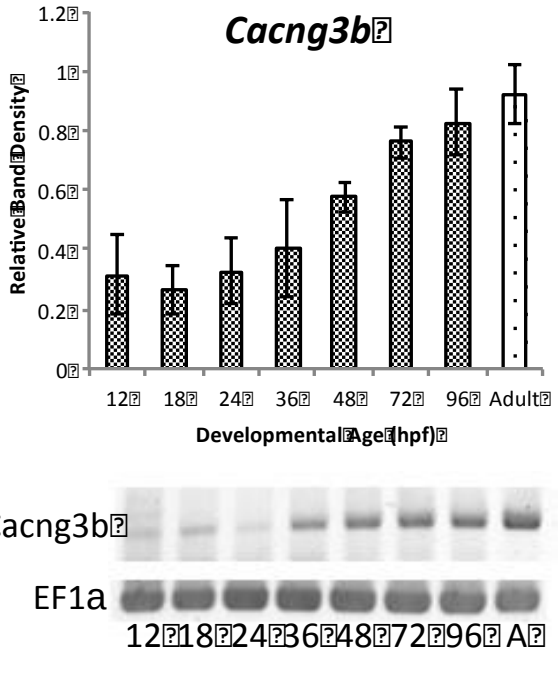
Cacng3b
Relative Band Density
1.2
1
0.8
0.6
0.4
0.2
0
12 18 24 36 48 72 96 Adult
Developmental Age (hpf)
Cacng3b
EF1a
12 18 24 36 48 72 96 A

Figure 6 *Cacng2* and *Cacng3* transcripts are differentially expressed during zebrafish development. Expression of TARP genes (*Cacng*) was assayed using RT-PCR on a set of developmental cDNA samples harvested from whole zebrafish embryos. *Cacng2b* reaches its expression plateau at a younger age (36 hpf) than the other TARPs shown here. Band densities for the TARP genes and EF1α were calculated using ImageJ (NIH). Data are expressed as a ratio of density of TARP to the density of EF1α housekeeping gene ± SEM for a given developmental age (n=3).

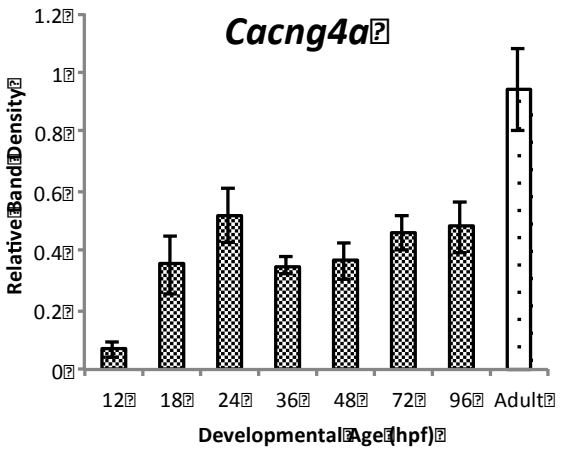
Cacng4a
Relative Band Density
1.2
1
0.8
0.6
0.4
0.2
0
12 18 24 36 48 72 96 Adult
Developmental Age (hpf)

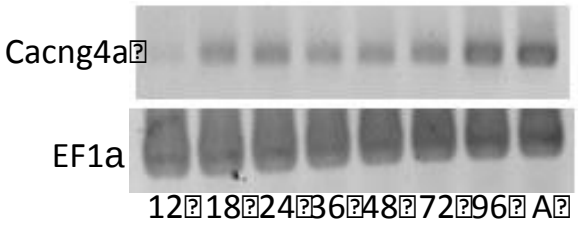
Cacng4a
EF1a
12 18 24 36 48 72 96 A

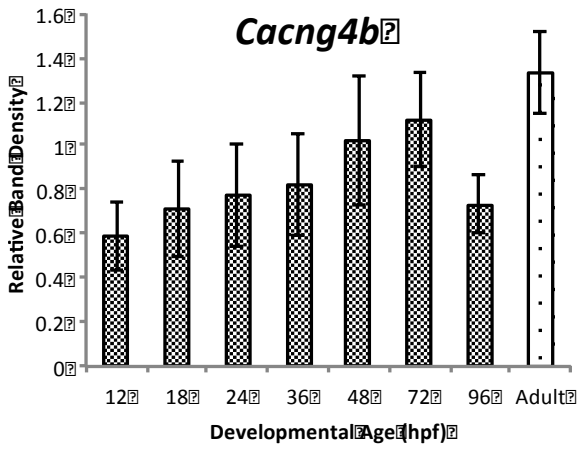
Cacng4b
Relative Band Density
1.6
1.4
1.2
1
0.8
0.6
0.4
0.2
0
12 18 24 36 48 72 96 Adult
Developmental Age (hpf)

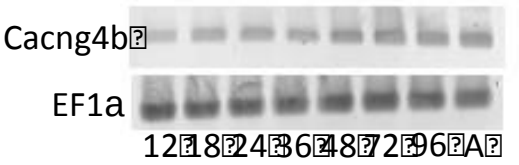
Cacng4b
EF1a
12 18 24 36 48 72 96 A

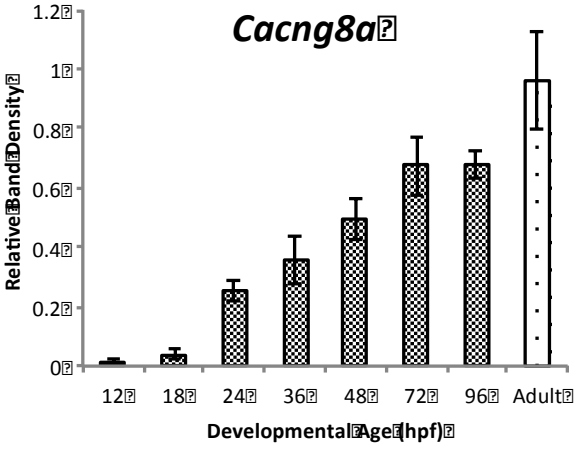
Cacng8a
Relative Band Density
1.2
1
0.8
0.6
0.4
0.2
0
12 18 24 36 48 72 96 Adult
Developmental Age (hpf)

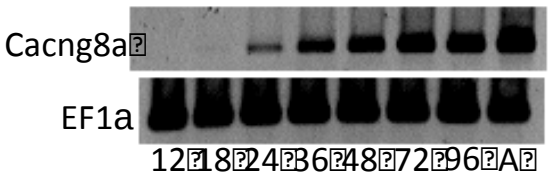
Cacng8a
EF1a
12 18 24 36 48 72 96 A

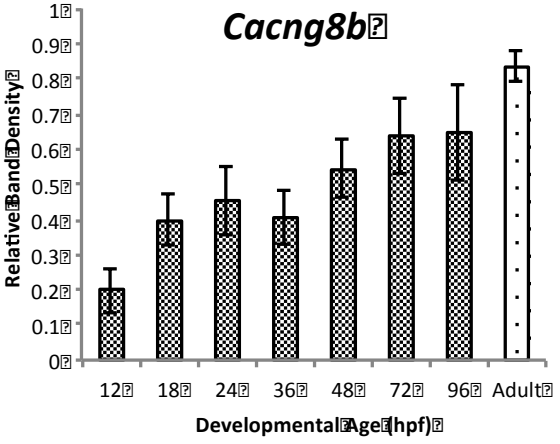
Cacng8b
Relative Band Density
1
0.9
0.8
0.7
0.6
0.5
0.4
0.3
0.2
0.1
0
12 18 24 36 48 72 96 Adult
Developmental Age (hpf)

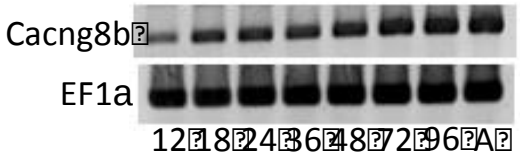
Cacng8b
EF1a
12 18 24 36 48 72 96 A

Figure 7 *Cacng4* and *Cacng8* transcripts are differentially expressed during zebrafish development. Expression of TARP genes (*Cacng*) was assayed using RT-PCR on a set of developmental cDNA samples harvested from whole zebrafish embryos. *Cacng8a* reaches its expression plateau at an older age (72 hpf) than the other TARPs shown here. Band densities for the TARP genes and EF1α were calculated using ImageJ (NIH). Data are expressed as a ratio of density of TARP to the density of EF1α housekeeping gene ± SEM for a given developmental age (n=3).

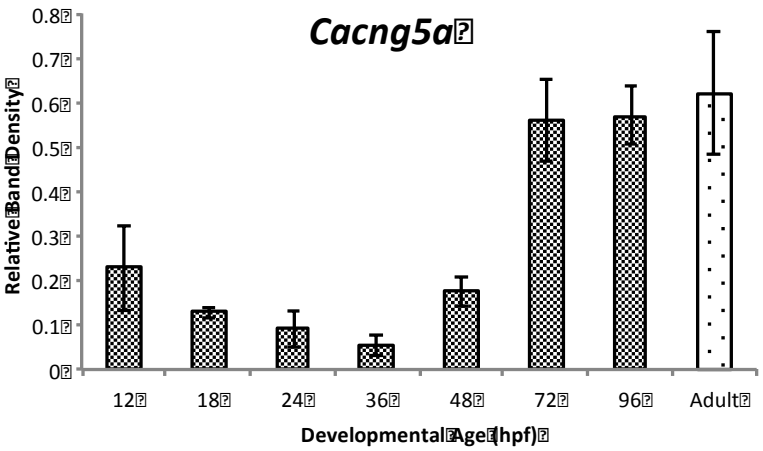
Cacng5a
Relative Band Density
0.8
0.7
0.6
0.5
0.4
0.3
0.2
0.1
0
12
18
24
36
48
72
96
Adult
Developmental Age (hpf)

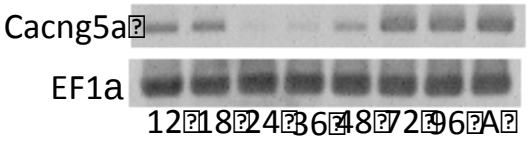
Cacng5a
EF1a
12 18 24 36 48 72 96 A

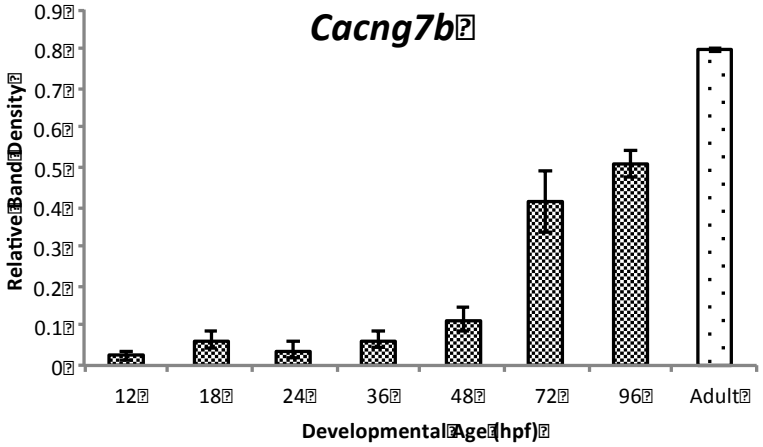
Cacng7b
Relative Band Density
0.9
0.8
0.7
0.6
0.5
0.4
0.3
0.2
0.1
0
12
18
24
36
48
72
96
Adult
Developmental Age (hpf)

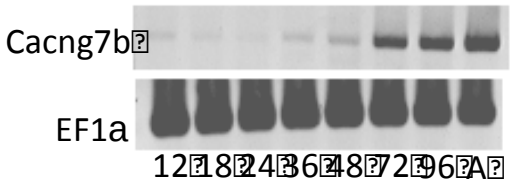
Cacng7b
EF1a
12 18 24 36 48 72 96 A

Figure 8 Expression of Type II TARP transcripts increases during zebrafish development. Expression of TARP genes (*Cacng*) was assayed using RT-PCR on a set of developmental cDNA samples harvested from whole zebrafish embryos. *Cacng5a* and *Cacng7b* both reach their expression plateau at around 72 hpf. Band densities for the TARP genes and EF1α were calculated using ImageJ (NIH). Data are expressed as a ratio of density of TARP to the density of EF1α housekeeping gene ± SEM for a given developmental age (n=3).

3.3 *In Situ* Hybridization

Having determined the overall pattern of expression during development for the Type I TARPs, I wanted to see if there was any differential expression of those genes in different areas of the CNS. Given the robust early expression (between 18-36 hpf) of certain TARP genes in my own PCR experiments, including *Cacng2b* and *Cacng4a/b*, and given the previous literature that has shown *Cacng4* (but not *Cacng2*) to be broadly expressed during embryonic and postnatal development in rats (Tomita et al., 2003), I chose to focus on *Cacng2a/b* and *Cacng4/b* for my *In Situ* Hybridization (*IS*H) experiments. *IS*H experiments were performed at four time points, chosen because of their relevance to the development of locomotory behaviour in zebrafish: 12 hpf, 24 hpf, 48 hpf and 72 hpf. Roughly speaking, between 12 and 24 hpf, the basic architecture of the nervous system is forming and connecting; locomotion develops from 24 to 48 hpf, starting as spontaneous coiling contractions and culminating in the larva hatching from the chorion. By 72 hpf, the larvae are fully independent organisms, reliant upon their locomotory abilities to avoid predators and feed themselves – much like adult fish. My *in situ* experiments were run with a basic no probe control and limited positive controls, but without the necessary controls (sense probe, nonsense probe, consistent positive control) to be treated as anything more than preliminary results. Further properly-controlled experiments must be performed to determine the validity of my results.

3.3.1 Developmental Expression of Cacng2

Cacng2a (Figure 9) and *Cacng2b* (Figure 10) share virtually identical developmental expression patterns, when assayed via *IS*H. There is strong diffuse staining throughout the body at 12 hpf, with dark patches corresponding to the eye and otic vesicle. By 24 hpf, this staining has clarified somewhat and become isolated to within the nervous system. In Figures 9D and 10D, we can see very clearly the formation of the fore-, mid- and hind-brain thanks to strong specific staining in the neural tube, particularly on the medial sides, which continues down the length of the spinal cord (not shown). At this stage we can also begin to see the structures of the eye, with strong staining in the lens, what appears to be the ganglion cell layer and more diffuse staining throughout. By 48 hpf, the nervous system is well-developed, and we can see staining for *Cacng2a* and *Cacng2b* throughout the brain and eyes (Figures 9 and 10, E and F). By 48 hpf the staining in the spinal cord has begun to weaken, and is eliminated by 72 hpf. By 72 hpf, the expression pattern has sharpened, with little/no staining persisting past the hindbrain and into the tail, but still strong staining in the forebrain, midbrain, and eyes. (Figs 9 and 10, G and H).

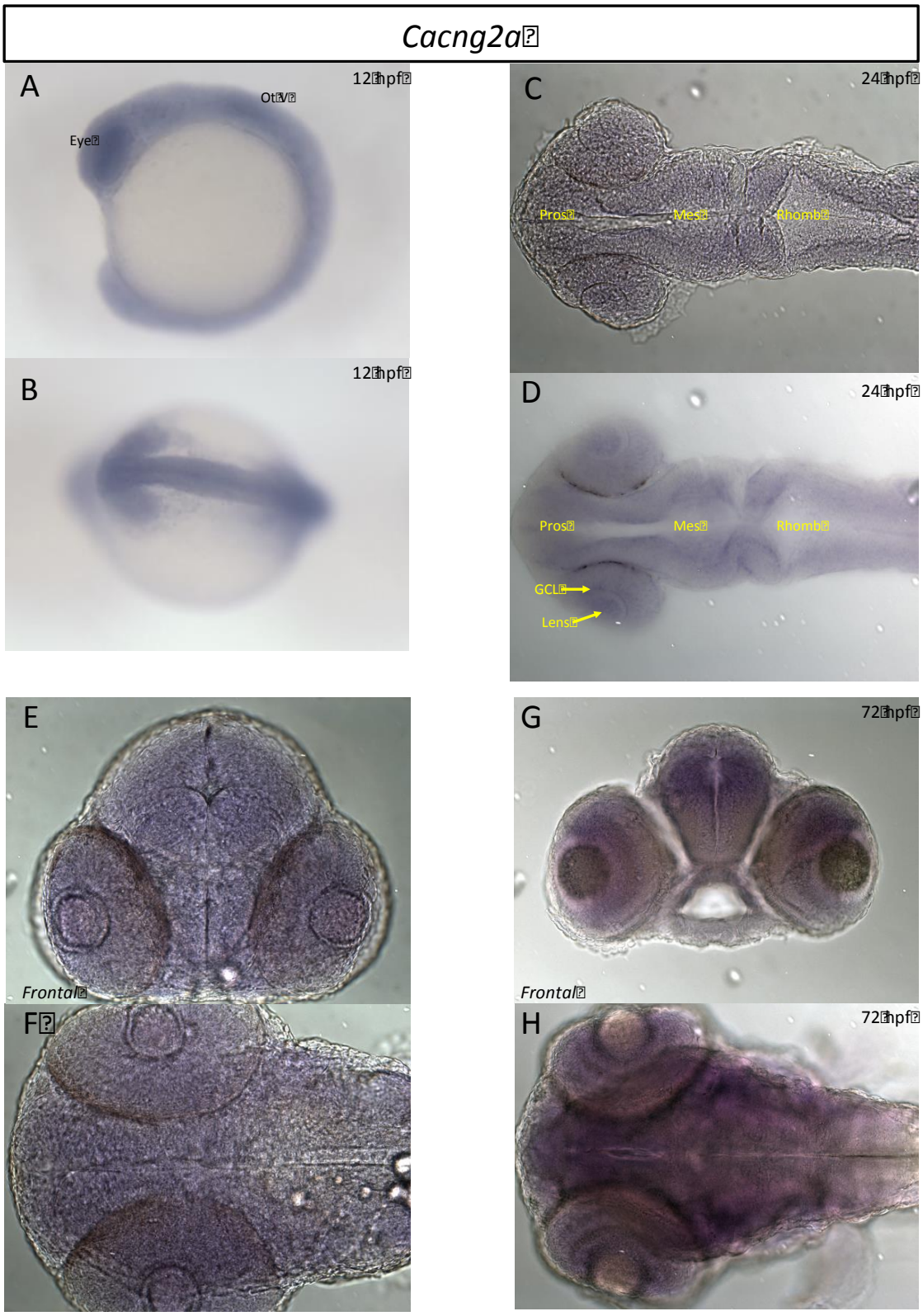
Cacng2a
A
12 hpf
Otv
Eye
B
12 hpf
C
24 hpf
Pros
Mes
Rhomb
D
24 hpf
Pros
Mes
Rhomb
GCL
Lens
E
Frontal
F
G
72 hpf
Frontal
H
72 hpf

Figure 9 Zebrafish *Cacng2a* expression between 12 and 72 hpf. A, B) *In situ* hybridizations (*IS*H) showing ubiquitous expression of *Cacng2a* at 12 hpf, with increased expression at the eye and otic vesicle. C, D) *IS*H showing expression of *Cacng2a* imaged with bright field (BF)(C) and differential interference contrast (DIC)(D) at 24 hpf. Expression is strong in in the eye, particularly the lens and the ganglion cell layer (GCL); and in the tissue of the developing brain - the prosencephalon (pros), mesencephalon (mes), and rhombencephalon (rhomb). E, F) *IS*H showing expression of *Cacng2a* at 48 hpf, imaged with BF microscopy. Frontal sections (E) and dorsal sections (F) show strong expression of *Cacng2a* throughout the eyes and brain. G, H) *IS*H showing expression of *Cacng2a* at 72 hpf using BF microscopy. Frontal sections (G) and dorsal sections (H) show strong expression of *Cacng2a* throughout the eyes and brain. A – lateral view, dorsal up, anterior left; B, C, D, F, H – dorsal views, anterior to the left; E, G – frontal view, dorsal up. n=3 experiments for each age group, ≈50 embryos viewed across all samples, images are representative of staining seen in ≥75% of their age group.

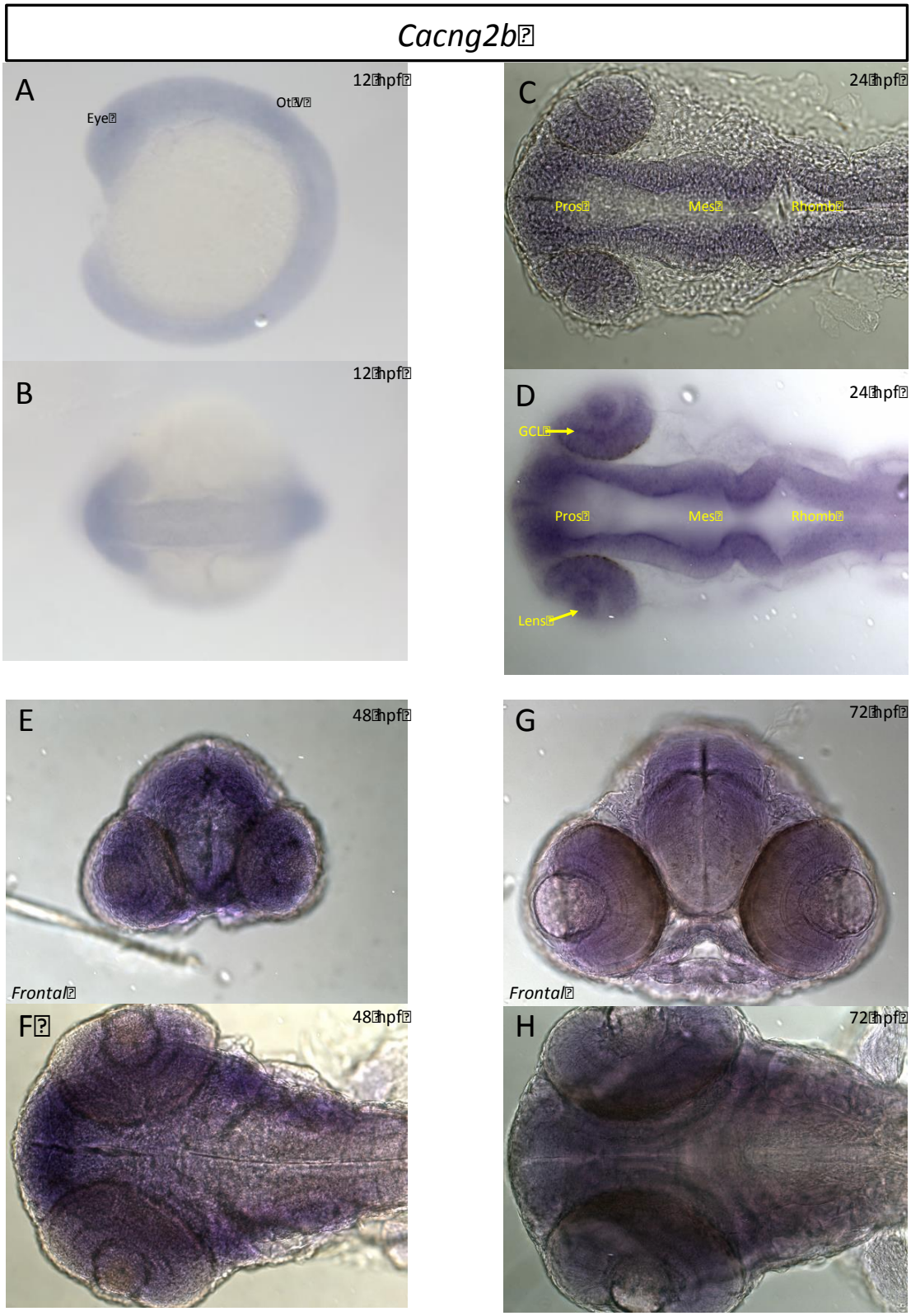
Cacng2b
A
12 hpf
Eye
Otic V
B
12 hpf
C
24 hpf
Pros
Mes
Rhomb
D
24 hpf
GCL
Pros
Mes
Rhomb
Lens
E
48 hpf
Frontal
F
48 hpf
G
72 hpf
Frontal
H
72 hpf

Figure 10 Zebrafish *Cacng2b* expression between 12 and 72 hpf. A, B) *In situ* hybridizations (*IS*H) showing ubiquitous expression of *Cacng2b* at 12 hpf, with increased expression at the eye and otic vesicle. C, D) *IS*H showing expression of *Cacng2b* imaged with bright field (BF)(C) and differential interference contrast (DIC)(D) at 24 hpf. Expression is strong in in the eye, particularly the lens and the ganglion cell layer (GCL); and in the tissue of the developing brain - the prosencephalon (pros), mesencephalon (mes), and rhombencephalon (rhomb). E, F) *IS*H showing expression of *Cacng2b* at 48 hpf, imaged with BF microscopy. Frontal sections (E) and dorsal sections (F) show strong expression of *Cacng2b* throughout the eyes and brain. G, H) *IS*H showing expression of *Cacng2b* at 72 hpf using BF microscopy. Frontal sections (G) and dorsal sections (H) show strong expression of *Cacng2b* throughout the eyes and brain. A – lateral view, dorsal up, anterior left; B, C, D, F, H – dorsal views, anterior to the left; E, G – frontal view, dorsal up. n=3 experiments for each age group, ≈50 embryos viewed across all samples at each age, images are representative of staining seen in ≥75% of each age group.

3.3.2 Developmental Expression of Cacng4

The expression pattern of *Cacng4a* and *Cacng4b* is indistinguishable from the expression pattern of *Cacng2a* and *Cacng2b.* The transcripts are expressed ubiquitously at 12 hpf (Figures 11 and 12, A and B), with small islands of expression at the eye and the otic vesicle. This expression is refined by 24 hpf to clearly mark neural tissue, particularly that of the neural tube and the eye (Figures 11 and12, C and D). As with *Cacng2a/b*, the ventricles of the developing brain are nicely highlighted by staining throughout the tissue of the prosencephalon, mesencephalon, and rhombencephalon. The eyes are stained throughout, but there is darker staining in the region around the lens where the ganglion cell layer is located. 48 hpf larvae show a pattern of ubiquitous staining throughout the nervous tissue of the head (Figures 11 and 12, E and F), particularly in the eyes, forebrain, and midbrain, with a more selective staining pattern in the hindbrain. By 48 hpf, the expression of the *Cacng* genes we have examined has begun to noticeably decrease along the body axis and is becoming exclusive to the nervous tissue of the head. As development continues, at 72 hpf *Cacng4a/b* are expressed exclusively in the head, still particularly in the forebrain, midbrain, and eyes (Figures 11 and 12, G and H).

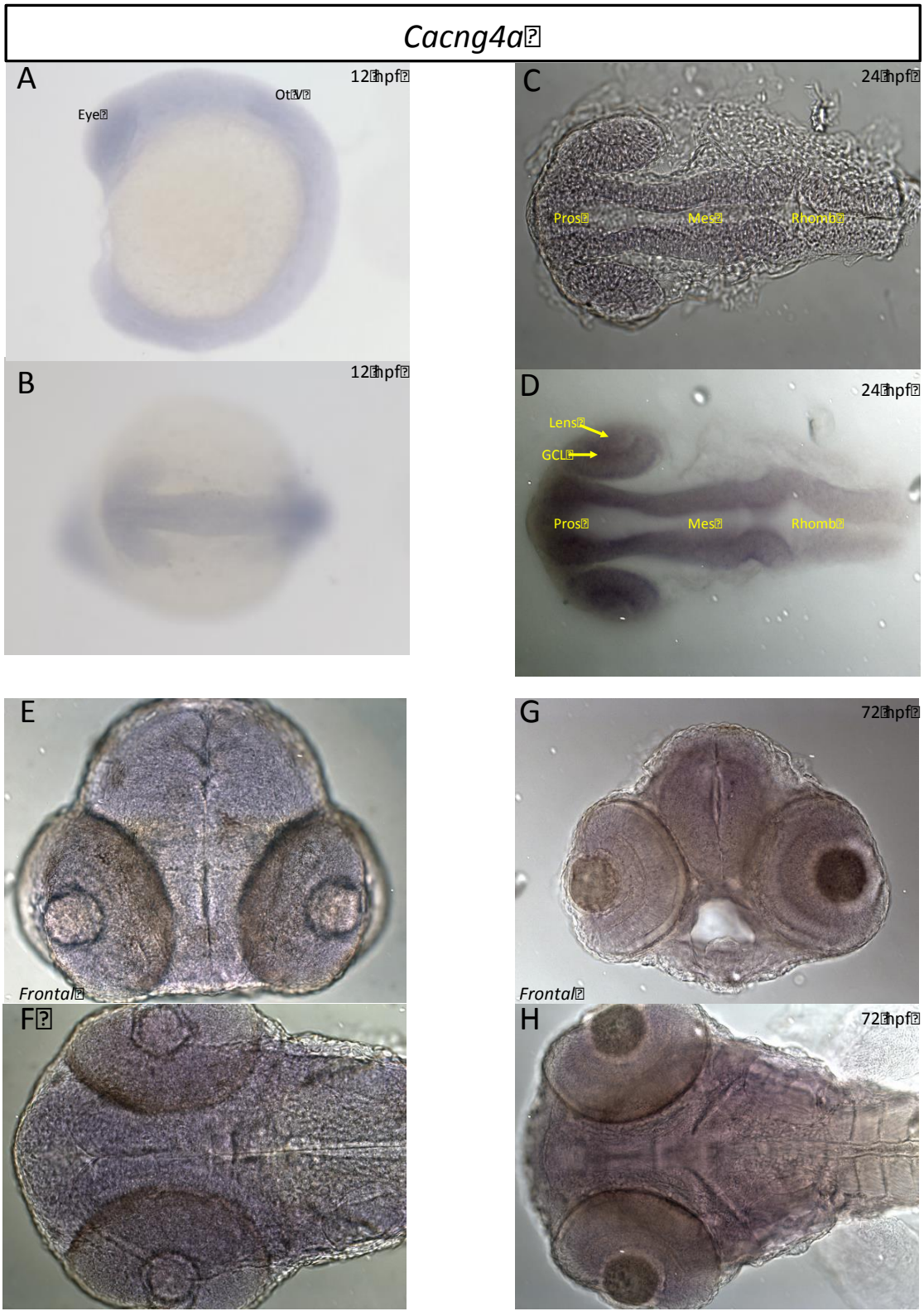
Cacng4a
A
12 hpf
Otic V
Eye
B
12 hpf
C
24 hpf
Pros
Mes
Rhomb
D
24 hpf
Lens
GCL
Pros
Mes
Rhomb
E
Frontal
F
G
72 hpf
Frontal
H
72 hpf

Figure 11 Zebrafish *Cacng4a* expression between 12 and 72 hpf. A, B) *In situ* hybridizations (*IS*H) showing ubiquitous expression of *Cacng4a* at 12 hpf, with increased expression at the eye and otic vesicle. C, D) *IS*H showing expression of *Cacng4a* imaged with bright field (BF)(C) and differential interference contrast (DIC)(D) at 24 hpf. Expression is strong in in the eye, particularly the lens and the ganglion cell layer (GCL); and in the tissue of the developing brain - the prosencephalon (pros), mesencephalon (mes), and rhombencephalon (rhomb). E, F) *IS*H showing expression of *Cacng4a* at 48 hpf, imaged with BF microscopy. Frontal sections (E) and dorsal sections (F) show strong expression of *Cacng4a* throughout the eyes and brain. G, H) *IS*H showing expression of *Cacng4a* at 72 hpf using BF microscopy. Frontal sections (G) and dorsal sections (H) show strong expression of *Cacng4a* throughout the eyes and brain. A – lateral view, dorsal up, anterior left; B, C, D, F, H – dorsal views, anterior to the left; E, G – frontal view, dorsal up. n=3 experiments for each age group, ≈50 embryos viewed across all samples, images are representative of staining seen in ≥75% of their age group.

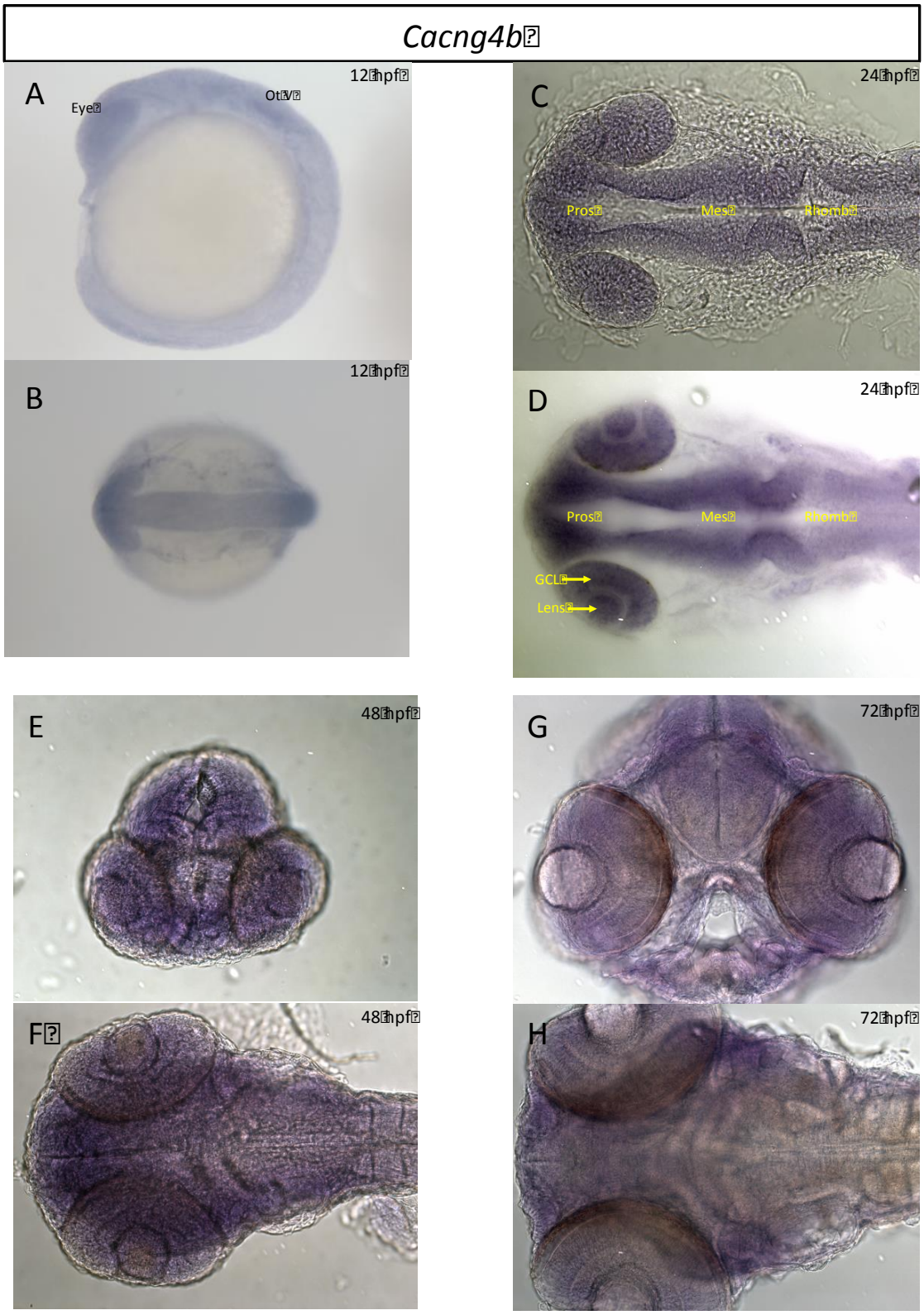
Cacng4b
A
12 hpf
Eye
OtV
B
12 hpf
C
24 hpf
Pros
Mes
Rhomb
D
24 hpf
Pros
Mes
Rhomb
GCL
Lens
E
48 hpf
F
48 hpf
G
72 hpf
H
72 hpf

Figure 12 Zebrafish *Cacng4b* expression between 12 and 72 hpf. A, B) *In situ* hybridizations (*IS*H) showing ubiquitous expression of *Cacng4b* at 12 hpf, with increased expression at the eye and otic vesicle. C, D) *IS*H showing expression of *Cacng4b* imaged with bright field (BF)(C) and differential interference contrast (DIC)(D) at 24 hpf. Expression is strong in in the eye, particularly the lens and the ganglion cell layer (GCL); and in the tissue of the developing brain - the prosencephalon (pros), mesencephalon (mes), and rhombencephalon (rhomb). E, F) *IS*H showing expression of *Cacng4b* at 48 hpf, imaged with BF microscopy. Frontal sections (E) and dorsal sections (F) show strong expression of *Cacng4b* throughout the eyes and brain. G, H) *IS*H showing expression of *Cacng4b* at 72 hpf using BF microscopy. Frontal sections (G) and dorsal sections (H) show strong expression of *Cacng4b* throughout the eyes and brain. A – lateral view, dorsal up, anterior left; B, C, D, F, H – dorsal views, anterior to the left; E, G – frontal view, dorsal up. n=3 experiments for each age group, ≈50 embryos viewed across all samples, images are representative of staining seen in ≥75% of each age group.

3.4 Knockdown with Morpholino Oligonucleotides

My previous experiments suggested that the Type I and II TARPs *are* expressed differentially throughout development; however my experiments in zebrafish failed to show the differential spatial expression pattern that has been demonstrated for TARP genes in post-natal and mature rats (Tomita et al., 2003). My next objective was to observe whether any phenotypic changes to the fish occur when those genes were knocked down using Morpholino antisense oligonucleotides (MOs).

3.4.1 Knockdown Assessment at 48hpf

Splice-blocking MOs were chosen over translation-blocking MOs because they allow for knockdown assessment using RT-PCR and *IS*H, whereas translation-blocking MOs require knockdown confirmation through antibody-mediated techniques such as Western blotting or immunohistochemistry. I designed my PCR primers for knockdown confirmation to bind to the exons on either side of the splice site that the MO was designed against in order to show a weakening of the desired band as confirmation of the knockdown; however this was not evident in most of the PCR reactions that were run. Instead, Figure 13 shows that with the exception of *Cacng2a*, none of the TARP genes I injected MOs for were consistently knocked down with the concentrations of MO I was using. *Cacng2a* does appear to have been knocked down with the 4 ng MO treatment, though I cannot be conclusive with this small sample size. For the most part, the level of *Cacng* expression in the injected fish was equivalent to either the uninjected positive control or the mock-injected positive control. This negative

result could have been due to a flaw in the experimental design or a bad reagent, so I moved forward using the 4 ng concentration and attempted to confirm my transcripts were knocked down using *IS*H experiments for *Cacng2a* and *Cacng4a* at 48 hpf.

*IS*H of MO-injected *Cacng2a/4a* failed to show a noticeable knockdown of expression in the brain (Figures 14 and 15). The MO-injected fish are largely indistinguishable from their uninjected counterparts, with strong staining in the brain and eyes in the same pattern as the controls and my previous *IS*H efforts. In fact, the most noticeable difference between the MO-injected fish and their controls is slightly darker non-specific staining along the tail of the MO-injected fish (Figures 14 and 15, E and F).

According to both of these methods of knockdown assessment, the knockdown of the *Cacng* genes was either very minor or unsuccessful. In order to fully confirm this result, we turned to behavioural assessment of MO-injected 48 hpf larvae, as any deficits in escape response could be indirectly linked to the levels of the TARP proteins: either showing a knockdown phenotype or confirming my previous negative knockdown assessments – or, unfortunately, demonstrating a non-specific effect due to the MO itself, rather than its sequence.

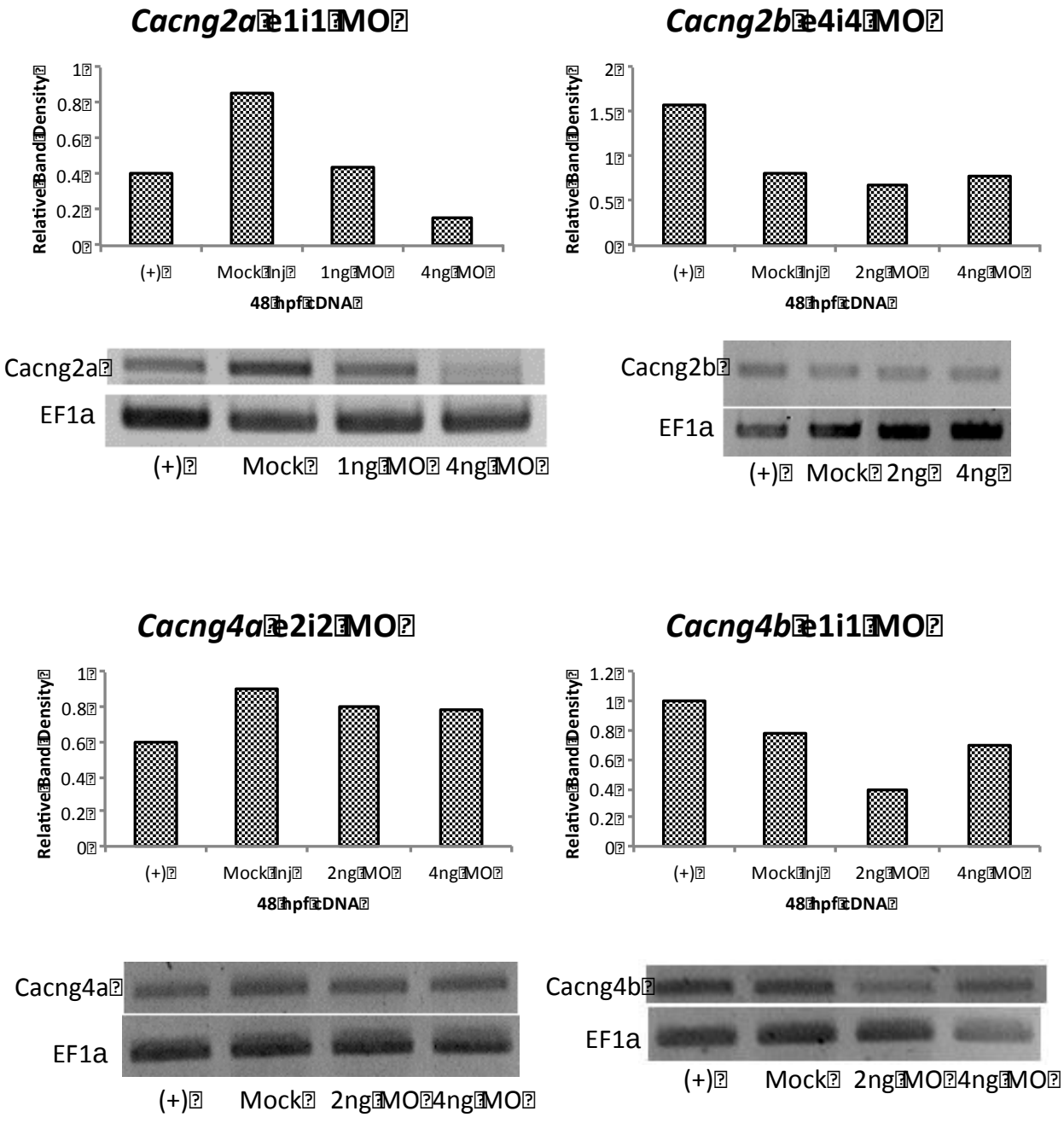
Cacng2a e1i1 MO
Relative Band Density
1
0.8
0.6
0.4
0.2
0
(+)
Mock Inj
1ng MO
4ng MO
48 hpf cDNA
Cacng2a
EF1a
(+) Mock 1ng MO 4ng MO
Cacng2b e4i4 MO
Relative Band Density
2
1.5
1
0.5
0
(+)
Mock Inj
2ng MO
4ng MO
48 hpf cDNA
Cacng2b
EF1a
(+) Mock 2ng 4ng
Cacng4a e2i2 MO
Relative Band Density
1
0.8
0.6
0.4
0.2
0
(+)
Mock Inj
2ng MO
4ng MO
48 hpf cDNA
Cacng4a
EF1a
(+) Mock 2ng MO 4ng MO
Cacng4b e1i1 MO
Relative Band Density
1.2
1
0.8
0.6
0.4
0.2
0
(+)
Mock Inj
2ng MO
4ng MO
48 hpf cDNA
Cacng4b
EF1a
(+) Mock 2ng MO 4ng MO

Figure 13 RT-PCR assay to assess morpholino knockdown of *Cacng* genes. Each splice-blocking morpholino oligonucleotide (MO) was injected into a cohort of ~30 embryos in the 1-4 cell stage at 1-4 ng/nL concentration. RNA was isolated from injected embryos at 48 hpf using TRIzol reagent, and cDNA for each injected concentration was synthesized with 1μg of isolated RNA. (+) indicates an uninjected wild-type cDNA sample. RT-PCR results were inconclusive, with no detectable splice variants at larger size ranges and no clear knockdown for any MO aside from *Cacng2a* e1i1 at 4 ng. Band densities for the *Cacng* genes and EF1α were calculated using ImageJ (NIH). Data are expressed as a ratio of density of *Cacng* to the density of the EF1α housekeeping gene (n=1).

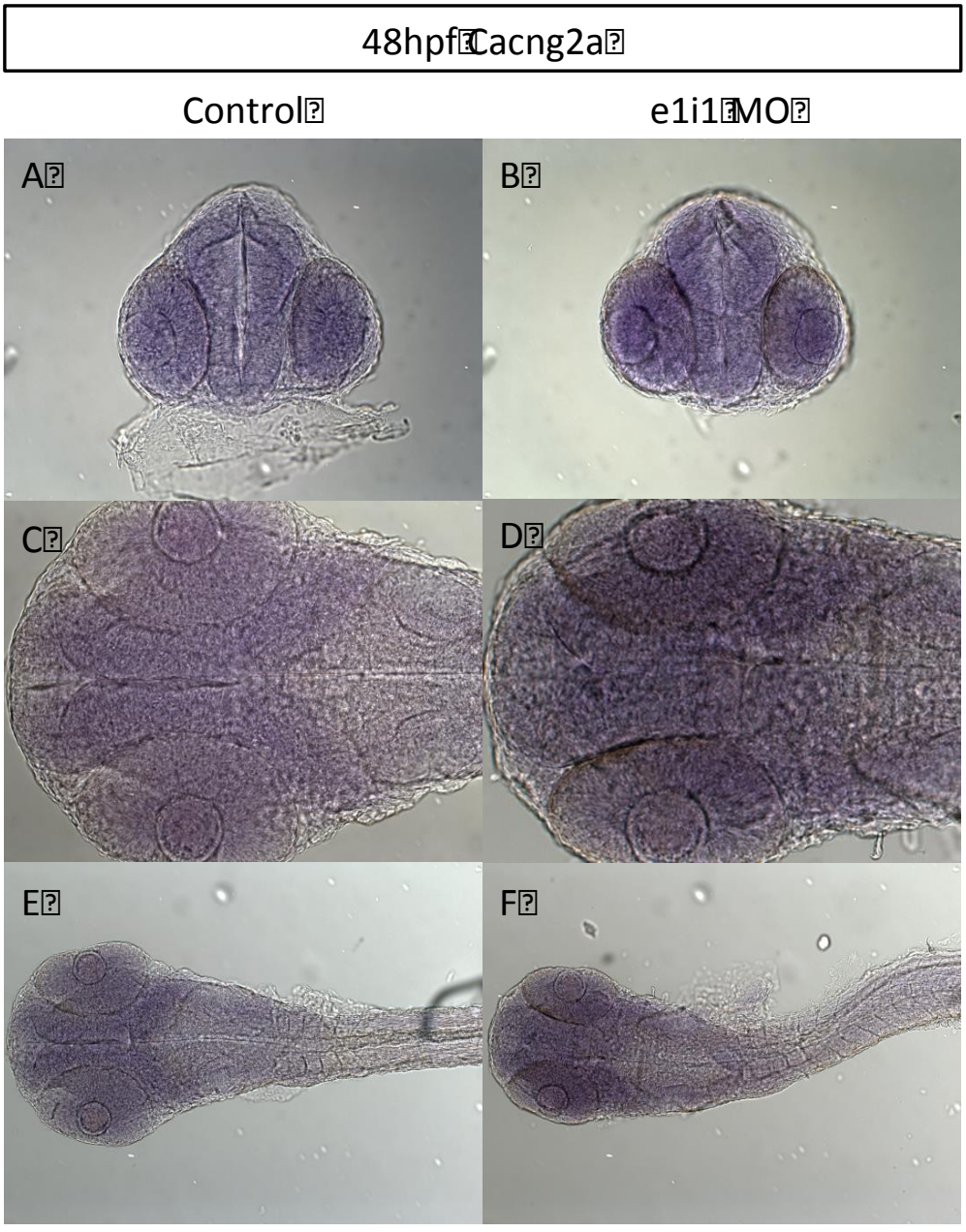
48hpf Cacng2a
Control
e1i1 MO
A
B
C
D
E
F

Figure 14 *In Situ* Hybridization assay to assess morpholino oligonucleotide (MO) knockdown of *Cacng2a* in 48hpf zebrafish larvae. *IS*H was carried out on 48hpf larvae using a probe for the mRNA sequence of *Cacng2a*, and larvae were either untreated controls or were treated with 4ng of *Cacng2a* e1i1 MO during their 1-4 cell stage. A,B) Frontal views at 200X magnification show no change in expression pattern between control and MO-injected fish. C,D) Dorsal views at 200X no change in expression pattern between control and MO-injected fish. E,F) Dorsal views at 100X show a slight increase in the staining of the tail in MO-injected fish, but no further changes. n=2.

48hpf Cacng4a

Control e2i2 MO

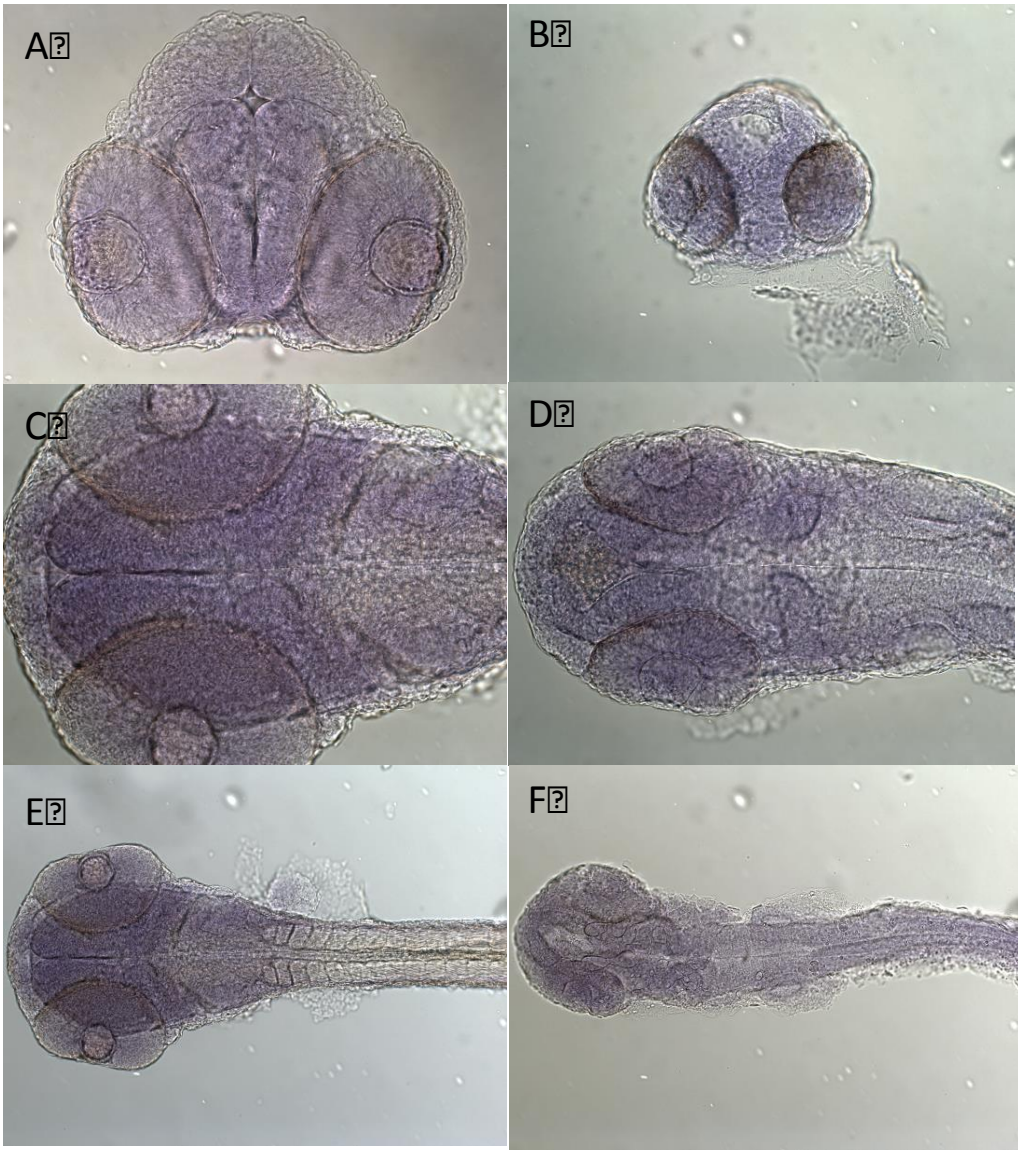

Figure 15 *In Situ* Hybridization assay to assess morpholino oligonucleotide (MO) knockdown of *Cacng4a* in 48hpf zebrafish larvae. *IS*H was carried out on 48hpf larvae using a probe for the mRNA sequence of *Cacng2a*, and larvae were either untreated controls or were treated with 4ng of *Cacng4a* e2i2 MO during their 1-4 cell stage. A,B) Frontal views at 200X magnification show no change in expression pattern between control and MO-injected fish. C,D) Dorsal views at 200X no change in expression pattern between control and MO-injected fish. E,F) Dorsal views at 100X show a slight increase in the staining of the tail in MO-injected fish, but no further changes. n=2.

3.4.2 Behavioural Assessment at 48hpf

Having established the developmental and spatial expression patterns of the *Cacng* genes in zebrafish, my next objective was to examine the result of knocking down some of the *Cacng* genes to observe any phenotypic consequences and begin to determine the role of redundancy among the members of the family. Since the MOs did not detectably knock down their targets at the mRNA level, my continued pursuit of behavioural data was an attempt to indirectly assay protein levels and further confirm my previous results.

1-4 cell embryos were injected with either 4ng of MO, an equivalent volume of isosmotic saline, or left uninjected. At 48hpf, the embryos were placed in small bubbles of embryo medium in a dish and stimulated on the tail with a pulse of coloured isosmotic saline. This free-swimming escape response was captured on high-speed video and analyzed for its latency – the time between stimulus contact and response. Figure 16A shows that there was no significant difference in response latency between any of the treatments ($p>0.05$, unpaired t-tests); however a small number of larvae in each of the MO-injected treatments exhibited abnormal morphology and/or abnormal escape and swimming behaviour (Figure 16B, Figures 17 and 18). The average response latency was between 12 and 20ms, with most fish responding in close to 12ms. A minority of slow responding fish – notably, the same fish possessing abnormal morphology – were responsible for increasing the variance of the MO-injected treatments (particularly the *Cacng4a* treatment) with responses as slow as 68ms; however these abnormal morphologies were rare, and therefore had less of an impact on

the overall average latency of the escape responses. Harder to quantify (and not accounted for in Figure 16A) are the fish that simply failed to respond to our stimulus. I chose to exclude these fish from my quantitative analysis of response latency because I cannot be confident that their lack of response was not due to some error in the experimenters' technique. Of the fish that were video recorded, those that failed to respond were always also abnormal in morphology, so they *are* included in the numbers shown in Figure 16B. The range of morphological abnormalities is shown in figure 16C: severe phenotypes of both MOs showed pericardial edema, small or no eyes, and stunted tails.

The responses of fish with abnormal morphology were often slower, asymmetric and inefficient for creating distance from the stimulus (Figures 17 and 18). A representative sequential image of a mock-injected control fish shows the fish is able to complete a full stroke of the tail in approximately 24 ms (Figure 17); whereas a fish with a moderate abnormal phenotype takes approximately 112 ms for the same full stroke, in spite of an asymmetrically weak contraction of the musculature on the same side as the stimulus (Figure 18).

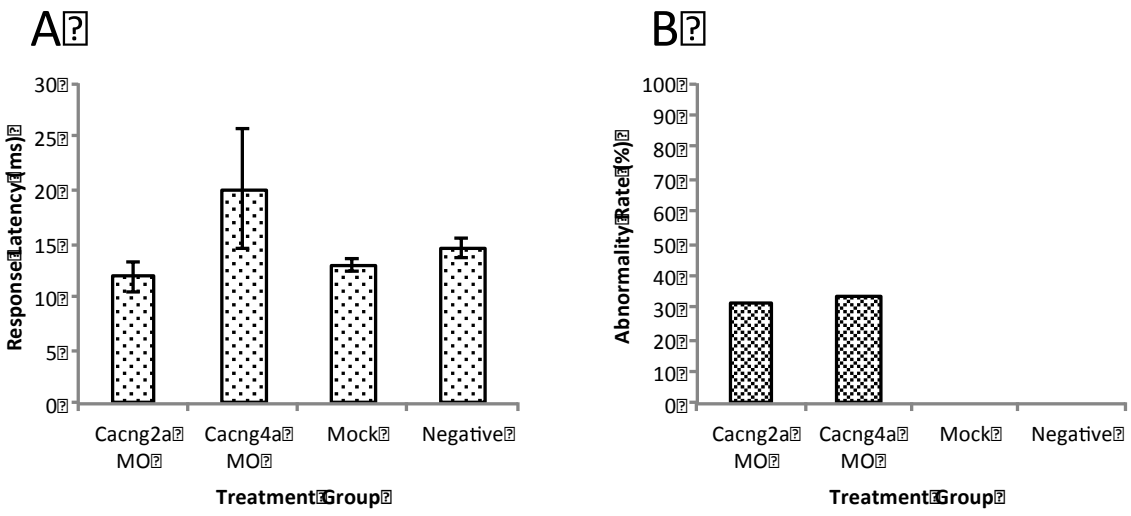
A
Response Latency (ms)
30
25
20
15
10
5
0
Cacng2a MO
Cacng4a MO
Mock
Negative
Treatment Group
B
Abnormality Rate (%)
100
90
80
70
60
50
40
30
20
10
0
Cacng2a MO
Cacng4a MO
Mock
Negative
Treatment Group

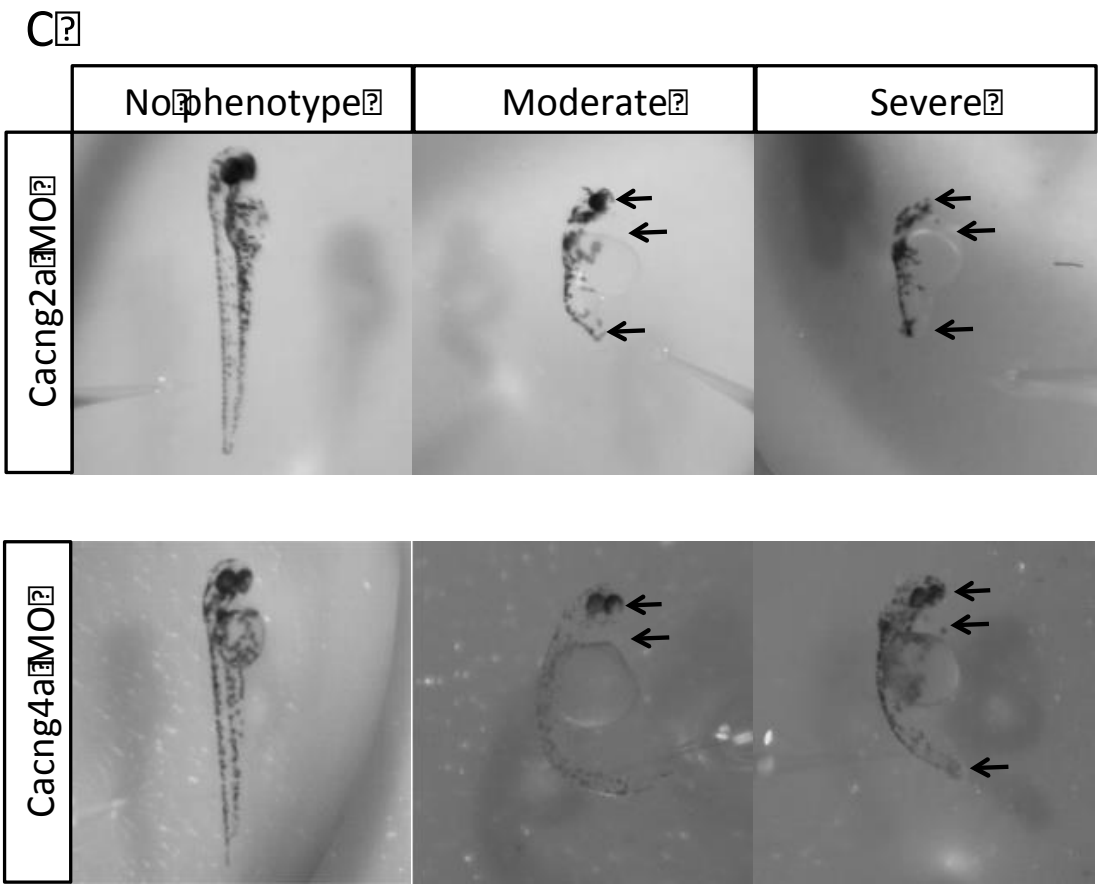
C
No phenotype
Moderate
Severe
Cacng2a MO
Cacng4a MO

Figure 16 Phenotypic and behavioural outcomes of *Cacng* MO injection in zebrafish larvae at 48hpf. A) MO-injected larvae do not experience a slowing of their escape response latency. Larvae were exposed to a 20ms pulse of water at 50psi and their responses were recorded on video at 1000fps. Latency was judged from the first frame of water jet contact to the first frame of response, judged by muscle contraction. Three trials were averaged per fish, and the average of those averages is presented here (n=12-20). There are no significant differences between the response latencies of the different treatments (unpaired t-test, $p>0.05$) B) The percentage rate of morphological or behavioural abnormalities among the video recorded fish are presented. No abnormalities were noted among the mock injected or negative control fish (n=12-20). C) A range of representative phenotypes among the behavioural recordings for the *Cacng2a* and *Cacng4a* MO injections is shown. Arrows indicate smaller eyes, pericardial edema or stunting of the tail.

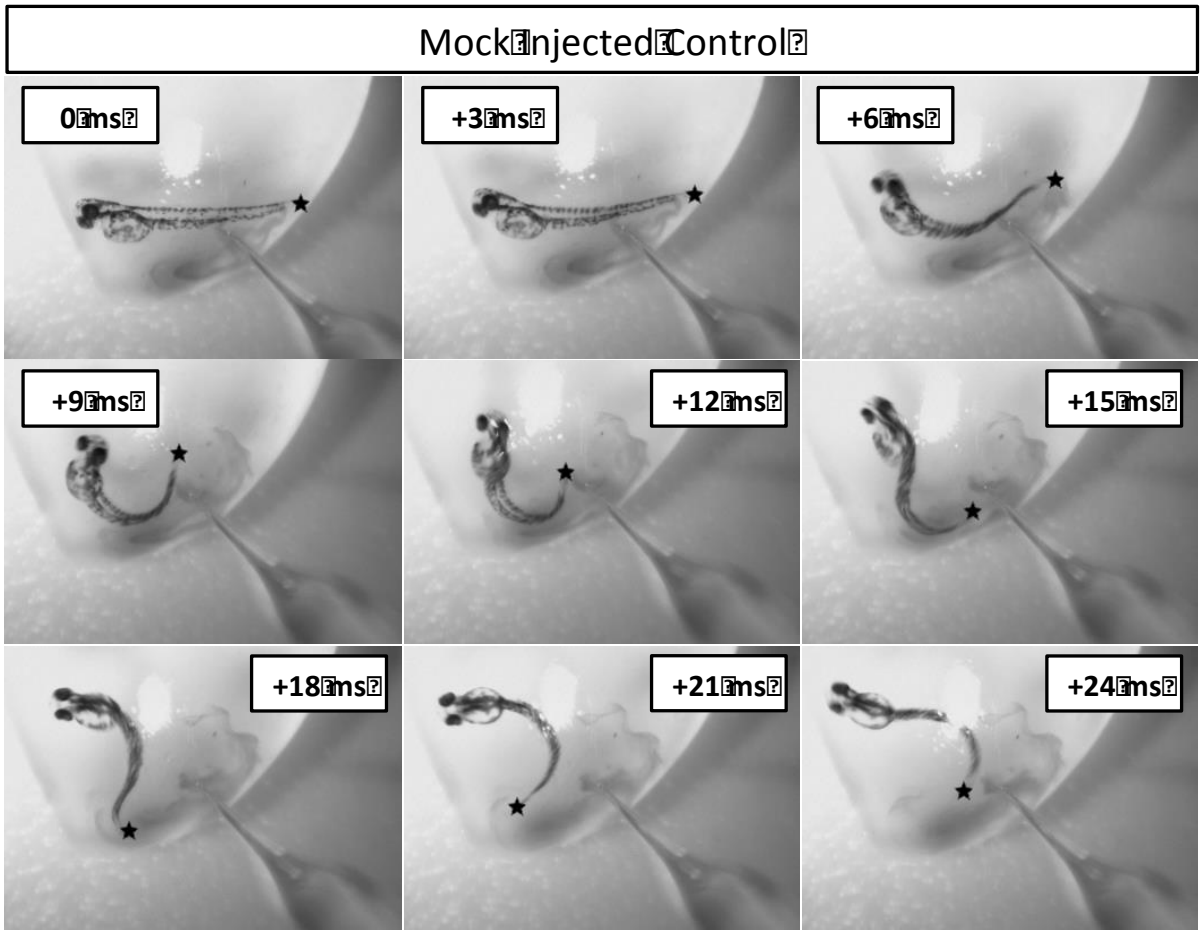
Mock Injected Control
0 ms
+3 ms
+6 ms
+9 ms
+12 ms
+15 ms
+18 ms
+21 ms
+24 ms

Figure 17 Representative post-stimulus escape and swimming response of 48 hpf mock-injected control zebrafish larva. Larvae were stimulated on the tail with a 20 ms pulse of solution at 50 psi and the resulting escape responses were recorded on video at 1000 frames per second. The response was taken from the start of the first detectable contraction of the axial musculature (0 ms), and images were chosen at 3 ms intervals until the tail had completed one full stroke (as judged by the return of the tail to the midline of the fish). The star symbol indicates the tip of the tail.

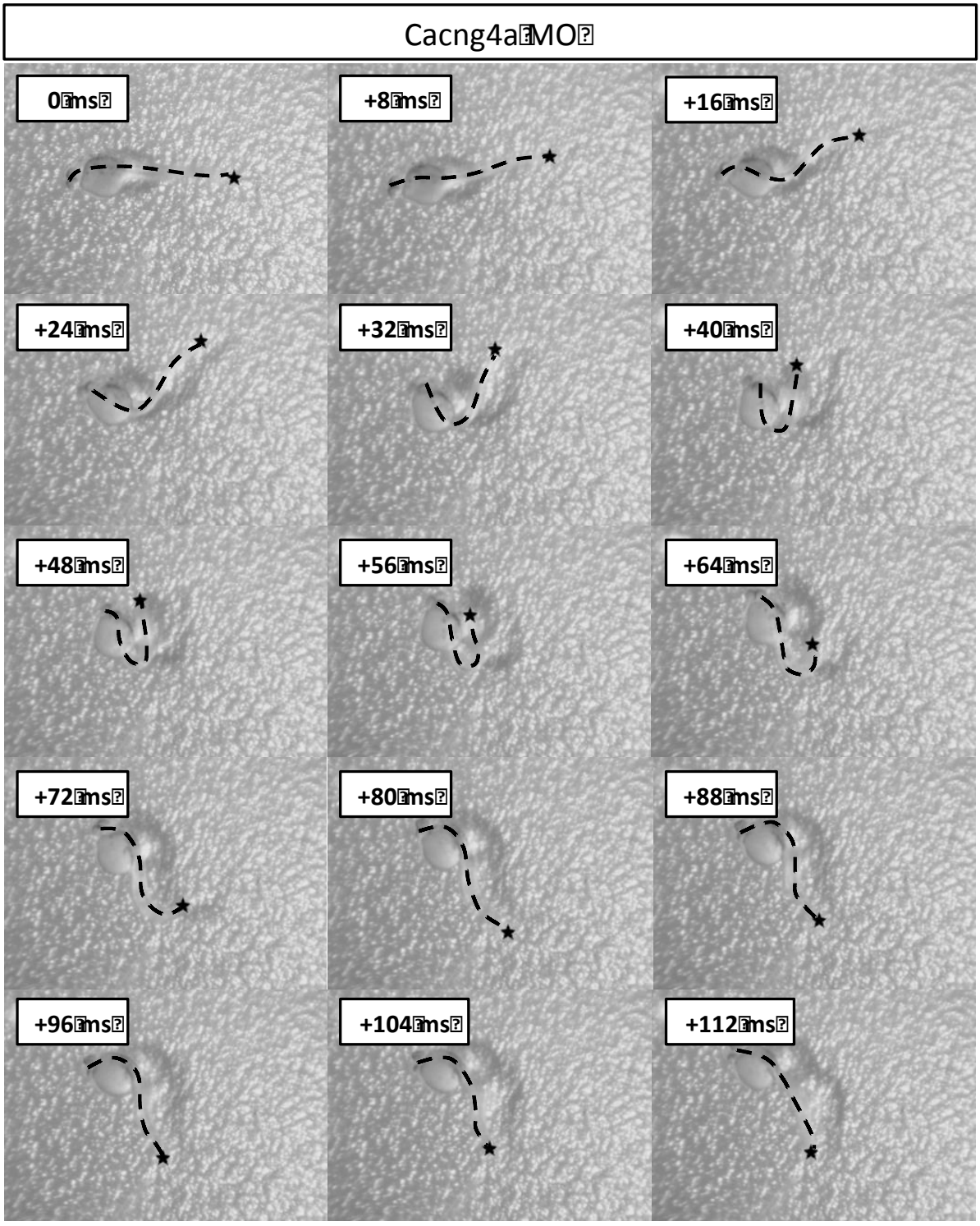
Cacng4a MO
0 ms
+8 ms
+16 ms
+24 ms
+32 ms
+40 ms
+48 ms
+56 ms
+64 ms
+72 ms
+80 ms
+88 ms
+96 ms
+104 ms
+112 ms

Figure 18 Representative post-stimulus escape and swimming response of 48 hpf Cacng4a e2i2 MO-injected zebrafish larva with abnormal morphology. The escape response is asymmetrical and ineffective. Larvae were stimulated on the tail with a 20 ms pulse of solution at 50 psi and the resulting escape responses were recorded on video at 1000 frames per second. The response was taken from the start of the first detectable contraction of the axial musculature (0 ms), and images were chosen at 8 ms intervals until the tail had completed one full stroke (as judged by the return of the tail to the midline of the fish). The star symbol indicates the tip of the tail, and the body axis has been highlighted with a black dotted line to aid visualization of the tail movements.

4. Discussion

The goal of this thesis was to examine the gene expression pattern and possible functional role of a family of auxiliary AMPAR subunits, the TARPs, in the developing zebrafish. There are two subfamilies of TARPs: Type I (typical) and Type II (atypical); however my study focused on the expression of the Type I TARPs in zebrafish, γ2, γ3, γ4, and γ8 because of their well-defined role in the AMPAR trafficking and modulation. Type I TARPs function as chaperones during AMPAR trafficking to the PSD (Chen et al., 2000, Cuadra et al., 2004, Vandenberghe et al., 2005a), but also differentially modulate the glutamate sensitivity, conductance, gating, kinetics and pharmacology of the AMPARs they associate with (Priel et al., 2005, Tomita et al., 2005a, Turetsky et al., 2005, Milstein et al., 2007, Jackson et al., 2011). The TARP-AMPAR interaction is both modular and dynamic: modular in the sense that a variety of AMPAR:TARP subunit stoichiometries are permissible (Hastie et al., 2013), and different stoichiometries or combinations of a given TARP with different subunits of AMPARs can have a variety of effects (Cho et al., 2007, Kott et al., 2007); and dynamic in the sense that these interactions between TARPs and AMPARs can be physiologically disengaged in order to cycle the AMPAR back into the endosomal system (Tomita et al., 2004). In mammals, γ2 and γ3 cause less dramatic increases to the conductance and mean open time of AMPARs than do γ4 and γ8 (Jackson et al., 2011), and these different TARP isoforms are also differentially expressed throughout the adult mammalian brain (Klugbauer et al., 2000, Tomita et al., 2003) – suggesting a physiological preference for the properties of certain TARPs in

certain areas. In spite of this apparent distinction between the different TARPs, they have also been found to be significantly redundant with each other (Menuz et al., 2008, Menuz et al., 2009), as γ2 is the only single knockout among the TARPs that results in a phenotype in mice. The γ2 knockout mouse is known as *Stargazer* for its ataxic epileptic phenotype (Letts et al., 1998). Recent research has shown that differential dysregulation of TARPs in humans is associated with schizophrenia (Drummond et al., 2013), with schizophrenic patients exhibiting increased levels of γ3 and γ5, but decreased γ4, γ7, and γ8 in their anterior cingulate cortices. Clearly, the appropriate differential expression of TARPs is important not only for basic neuronal functioning, but also for prevention of emergent pathophysiological disease states such as schizophrenia and epilepsy.

Previous research has examined the role of TARP proteins in the development of the mammalian nervous system, particularly from the perspectives of protein expression via immunoblotting and Western blotting (Tomita et al., 2003) or the consequences of multigene knockout on development and AMPAR function (Menuz et al., 2009). Immunoblots showed strong CNS-specific expression of γ4 in postnatal day 6 rats, weaker CNS-specific expression of γ2 and γ8 – in that order – and even less expression of γ3; results that were also supported by Western blot analysis (Tomita et al., 2003). These results in neonatal rats are in contrast with other findings from the same study, showing strong expression and highly specific, differential localization of TARPs γ2, γ3, and γ8 in adult rat brain, with extremely confined and generally low expression of γ4 in adults (Tomita et al., 2003). This demonstrates a developmental change in the

expression patterns of the different TARPs, and implies a functional shift in the number and properties of the AMPARs at mature synapses, as compared to immature synapses (Cho et al., 2007, Milstein et al., 2007, Jackson et al., 2011). This study shows that γ4 is particularly strongly expressed throughout the CNS in neonates but hardly expressed at all in adults, while γ3 is primarily expressed in adult cortex and hardly expressed in neonates. This implies that TARPs are specialized both spatially and temporally, suggesting that association with specific TARPs at specific times and places finely tunes the function of AMPARs and helps to produce the excitability of the nervous system.

In probing the phenotypic consequences of multi-TARP knockout mice, the most important TARP for survival past birth appears to be γ2: single knockouts produce ataxic/epileptic *Stargazer* mice; γ2,3, γ2,8 or γ2,4 double KOs survive poorly; and γ2,3,4 or γ2,3,8 triple knockouts do not survive past birth (Letts et al., 2005, Rouach et al., 2005, Menuz et al., 2009). In comparison, both γ3,4 double KO and γ3,4,8 triple KOs produce viable offspring with decreased AMPAR function only in the triple KO (Menuz et al., 2009). Based on these results, γ2 is likely the most important TARP during development, followed by γ4 and γ8. These results show that though the organism can compensate for the loss of one or two TARP isoforms due to their functional redundancy, the loss of certain combinations of TARPs results in severe or lethal phenotypes – suggesting that the presence of TARPs, and presumably their interaction with AMPARs, is critical for proper neural function during development. The addition of paralogs for each TARP gene in zebrafish creates an opportunity for significantly more

redundancy among the TARP isoforms, which may make zebrafish quite resilient against developing phenotypes normally associated with TARP knockout. Moreover, the function of AMPARs and excitability of the nervous system could possibly be tuned even more finely in a system with twice as many TARP genes – provided that those TARPs possess the same functionality as their murine counterparts.

I found that the amino acid sequences of the *Cacng* gene family, which encode the TARP proteins as well as the voltage-gated calcium channel γ subunits for which the *Cacng* genes are named, are generally well-conserved between mice and zebrafish – with 75% overall AA identity on average. Interestingly, we found that the two significant functional domains of the TARP proteins, ECL1 (Figure 3) and the C-terminus (Figure 2), are differentially conserved. The C-terminus, which governs the trafficking and anchoring of the TARP-AMPAR complex to the PSD, is significantly less conserved than the overall sequence in zebrafish; however the nine known functional serine residues of the TARP C-terminus *were* found to be highly conserved. Conversely, in ECL1, where the only conserved motif is a portion of the claudin domain, located at the 3' end of the loop and continuing mostly in the second transmembrane domain, I found that the level of sequence conservation was generally equal to that of the overall sequence. Interestingly, I found that the level of conservation of the charged residues of ECL1 between zebrafish and mice was significantly better than the level of overall conservation – with more than 90% identity on average. These data provide a jumping off point for further research examining the functional aspects

of ECL1 and the C-terminus. Specifically, though some previous work has demonstrated that TARPs have some cell-adhesive character *in vitro* (Price et al., 2005), what if any, role does the claudin motif – partially found in ECL1 – have on function *in vivo*? Claudins are separated functionally based on their charge preference, which gives the tight junctions they form some permeability and allows for paracellular transport of ions (Anderson and Van Itallie, 2009) – what role do the charged residues in the claudin domain of the ECL1 of TARP proteins have in regulating the permeability of AMPARs? At this time, no studies have investigated these properties of TARPs.

My phylogenetic analyses showed that the duplicated *Cacng* genes of zebrafish are indeed paralogous to each other and orthologous to the sequences in mice. After creating a phylogenetic tree with several other members of the vertebrate family as well as mice and zebrafish, little uncertainty remains about the relationships between the TARP proteins of the vertebrates. My results strongly confirm the previous phylogenetic analyses of the TARP proteins done in mammals (Chu et al., 2001), and extend them by suggesting that those relationships are conserved as far back as teleost fish.

In my RT-PCR studies, I found that there were roughly two waves of developmental *Cacng* gene expression – one group reaching a plateau of expression at 36 hpf or earlier, and one group reaching an expression plateau by 72 hpf. The early expressed genes (γ2b, γ4a, γ4b, and γ8b) and the late expressed genes (γ2a, γ3a, γ3b, γ5a, γ7b, and γ8a) were divided along similar lines to the

developmental expression pattern already established in mice (γ4 early, γ3 later) (Tomita et al., 2003). Unlike in mice, the presence of duplicate pairs of genes for γ2 and γ8 where one paralog of each seems to act earlier than the other is new and unexpected in the field of TARP research. This suggests that the paralogs of γ2 and γ8 may be functionally split across developmental time. Functional splitting is one hypothesized way for duplicated genes to be preserved: where once a single gene carried out two functions, now two duplicated genes will specialize in either of the functions of the parent gene (Sidow, 1996). qPCR would allow me to make statements about the expression levels of the *Cacng* genes compared to each other, rather than being restricted to making statements about the changes made to single genes over time.

My *IS*H experiments showed a ubiquitous staining pattern with slightly darker patches at the eye and otic vesicle at 12 hpf that sharpened and clarified by 48 hpf to be exclusively found in the brain and eyes, but not the spinal cord. This staining pattern was identical for each of the four TARP genes studied: *Cacng2a, Cacng2b, Cacng4a* and *Cacng4b.* This lack of differential expression was somewhat unexpected given previous results in neonatal mammals showing primarily expression of γ4 and very little else (Tomita et al., 2003). Likewise, given my PCR results I would have expected *Cacng2a* at least to perhaps be expressed strongly later than the other genes assayed. A previous high throughput study performed *IS*H on a wide variety of zebrafish genes, including *Cacng2a* at 24, 36 and 48 hpf, and found a similar (but markedly more refined) staining pattern the brain, and no staining in the eyes or elsewhere (Thisse, 2004). The

difference between my result and this previous result is that mine shows darker and less distinct staining, which may be an indicator of non-specific binding of the probe. This appears especially likely, as the MO-injected negative controls for my *IS*H showed essentially the same staining pattern as my *IS*H treatments; therefore, the parameters of the *IS*H assay itself should likely be re-evaluated to ensure maximum specificity of the staining.

Finally, I injected embryos with splice-blocking MOs for *Cacng2a* and *Cacng4a* to characterize the knockdown phenotype of these genes and to examine the escape response. In order to determine the optimal dosage of MO, I injected embryos at multiple concentrations, generated cDNA and assayed the knockdown via RT-PCR. This method of knockdown confirmation suggested that the transcripts were not knocked down by the splice-blocking MO, a finding that is also consistent with the negative results from my *IS*H of MO-injected larvae. The latencies of the escape responses of the MO-injected larvae were identical to both mock-injected and uninjected negative controls; however a minority (~30%) of the MO-injected larvae had morphological abnormalities and significantly altered swimming after their escape responses. Not shown or quantified were the larvae that failed to respond to the stimulus, as this was a common occurrence among all treatment and control groups. It has been suggested to us (M.E.C. and D.W.A.) anecdotally in personal communication with Dr. Waskiewicz that the manufacturer's claimed half-lives of their MOs are not realistic, and that certain MOs have been found to degrade within six months of purchase, regardless of storage conditions, which is supported by at least one other group's unpublished

observations (Bill et al., 2009) (Waskiewicz, 2012). I did not get a chance to begin injecting my MOs until around six months after we received them, so it is possible that they had already degraded by the time they were used for injections. At this point, the best way to determine the level of knockdown would be to directly assay the protein using Western blot; however the lack of zebrafish-specific TARP antibodies means that we would have to use commercial antibodies designed against the C-terminus of the different TARPs in mice (which I have already determined are not well-conserved in zebrafish).

4.1 Phylogenetic Differences Between Teleosts and Mammals

The significant lack of conservation of the C-terminal trafficking domains in TARPs between mice and zebrafish was unexpected. Given the amount of previous research that has gone into the characterization of the function of this domain and the emphasis of that research on the importance of a properly functional C-terminus for TARP function, it was strange to me that the sequences would be so different; however it is actually not unusual for duplicated genes to diverge in this way. Immediately after a duplication event, the selective pressure on each paralog is significantly decreased because of the ability of its duplicate to act redundantly, which allows either gene to mutate more freely and eventually either be lost or develop new functional characteristics (Sidow, 1996). Most duplicated genes are degraded into pseudogenes and are lost before they develop a useful mutation; however just one new functional distinction between the original gene and the duplicated gene can be enough to protect the duplicate from degradation (Sidow, 1996). For

example, in the case of the *Gria2* genes (which code for the GluA2 AMPAR subunit) basal vertebrates genomically encode the arginine residue that confers charge specificity to the channel, a feature that otherwise relies on RNA editing in more derived species such as mammals and teleosts (Kung et al., 2001). Thanks to the genome duplication in zebrafish, we can see an intermediate between the basal and derived (mammalian) genotypes: the ancestral paralog of *Gria2* genomically encodes R; and the derived paralog, genomically encoding Q, is subject to RNA editing. This may be similar to the evolutionary mechanism we are seeing with respect to the C-termini of the *Cacng* family: an evolutionarily recent (18 million years ago) duplication event (Jaillon et al., 2004) further decreasing the selective pressure on an already thrice-duplicated gene family (Chu et al., 2001), allowing for mutations to accumulate in the sequences of certain members of the family.

It is important to note that though the C-termini of zebrafish TARPs are significantly different from their murine orthologs in *overall* sequences, many of the *functional* aspects of the amino acid sequence – phosphorylated serine and threonine residues, the terminal PDZ-binding domain – were preserved. The preservation of these particular sequence elements, especially in spite of a significant lack of identity for the rest of the nearby sequence, makes an even stronger case for the functional importance and selective value of those previously identified sequence elements than strong overall identity would. The levels of sequence identity I have reported between mice and zebrafish only reflect sites where the *a* and *b* zebrafish paralogs are identical to each other as

well as the murine sequence – positions where one zebrafish paralog differs from the other but is still identical to the murine sequence were not counted. This means that a high level of identity in one paralog could be "muted" in the analysis by a low level of identity in the other. Given that the 8 ancestral TARPs were already paralogous and somewhat redundant, it is possible that further redundancy – as seen in zebrafish – is not necessary, at least not for every TARP, and some of the *Cacng* genes of zebrafish may already be in the process of being lost.

The high level of conservation between the sequences of the first extracellular loops of the TARP proteins is interesting, especially given the significantly lower overall conservation of the C-terminus, which has been exhaustively established as a critical functional domain for AMPAR trafficking and synaptic plasticity (Chen et al., 2000, Choi et al., 2002, Tomita et al., 2005a, Tomita et al., 2005b). Though the functional importance of ECL1 in modifying the gating, pharmacology and kinetics of AMPARs is known (Tomita et al., 2004, Tomita et al., 2005a, Milstein et al., 2007), no studies have examined the specific functional components of the extracellular loop sequences of TARPs, so it was not possible to pinpoint specific important residues for controlling the kinetics and pharmacology of the AMPAR. As an extracellular loop that interacts with the inside of the pore of a receptor channel, ECL1 is an unlikely target for phosphorylation as compared to the C-terminus; however the biophysical properties of the AA sequence – the total charge and/or physical bulk of the chain, for instance – are probably significantly more important. In

the case of the *Cacng* family's closest relatives, the Claudins, certain specific charged residues in ECL1 have been identified as critical determinants of the charge selectivity of their channel pores (Krug et al., 2012); but these particular residues are not well-conserved in the *Cacng* family. Instead, the *Cacng* genes possess a conserved motif containing two cysteine residues that is known to create a disulfide bridge, which contributes to pore formation in Claudin-2 (Li et al., 2013). In Claudins, presence of a charged residue in either of the two positions after the second conserved cysteine is crucial for determining the ion selectivity of the pore (see Figure 3, for comparison). Claudins have two other similarly charged positions, approximately 10 residues up and downstream from that second C, that help to determine the charge-selectivity of ECL1 (Krug et al., 2012); however the charge at these positions has completely been lost in the *Cacng* family (Figure 3). In spite of these differences, the general rule likely remains true: even a small amount of charge in the right location in the chain can attract oppositely-charged ions to the pore. Carrying a net negative charge of -1 or -2, with condensed areas of negative charge such as the 5 to 6 consecutive negatively charged residues in the sequence leading up to TM2, TARPs may represent a strong attractive force that draws cations to the pore of the AMPAR. This is a particularly attractive hypothesis, given previous studies showing the increased single-unit conductance of AMPARs in association with TARPs (Shelley et al., 2012).

My phylogenetic results broadly confirm previous analyses of TARP sequences (Burgess et al., 1999, Burgess et al., 2001, Chu et al., 2001), and

extend them using several non-mammalian vertebrate species whose TARPs have not previously been examined (chicken, zebrafish, frog). Previous studies using mammalian sequences provided the relationships ((((γ2, γ3),(γ4, γ8)), (γ5, γ7)), (γ1, γ6)), which have been confirmed by my analysis. The clarity of the familial relationships in my phylogeny could be further analyzed using mRNA sequences rather than AA sequences. AA sequences were used in my phylogenies because I was looking at several relatively distant species and I wanted to maximize the similarity of my input data.

4.2 Developmental Changes to TARP Expression

Interestingly, my results suggest that the *Cacng* genes of zebrafish are not simultaneously expressed during neurodevelopment; rather, there may be multiple waves of TARP expression as each gene turns on according to its own program. γ2a, γ3a, γ3b, γ5a, γ7b and γ8a reach their peak between 48 and 72 hpf, while γ2b, γ4a, γ4b, and γ8b are turned on at different points prior to 48 hpf. Previous studies have demonstrated developmental differences in expression (Klugbauer et al., 2000, Tomita et al., 2003, Menuz et al., 2009), and in those studies the early expression pattern was a combination of strong expression of γ4 and light but increasing expression in γ2 and γ8. Here the pattern is similar to what has previously been observed in mammals, but the presence of additional later-acting paralogs for γ2 and γ8 is unfamiliar. γ3 is one of the more maturely expressed members of the family in both mice and zebrafish, but in zebrafish γ2a and γ8a are also expressed later. This implied functional splitting of paralogs across development –γ2/8b early, γ2/8a later – suggests the sort of useful mutation that

may protect duplicated genes from degrading over evolutionary time (Sidow, 1996). The bigger question is why certain TARPs should be expressed earlier than others? Given previous studies showing that γ4 and γ8 increase channel conductance and significantly alter kinetics to increase the activation of the AMPAR in comparison to γ2 and γ3 (Milstein et al., 2007, Jackson et al., 2011), and studies showing the slower deposition of AMPARs to the developing PSD (Washbourne et al., 2002), perhaps the association of AMPARs with a strongly activating TARP such as γ4 or γ8 is important for ensuring sufficient depolarization to result an action potential and signal transmission. As the neural network is consolidated and more AMPARs are trafficked to the surface, strongly activating TARPs may be replaced across the brain with more moderate activators such as γ2 and γ3 which allow for more finely tuned responses, except in areas where strong depolarization is important for plasticity – hence the presence of γ8 in the hippocampus.

4.3 **Expression Pattern of γ2a, γ2b, γ4a, and γ4b**

My *in situ* hybridization results were somewhat unexpected, showing no discernible difference between the expression patterns of any of the genes that I probed for. This was unexpected because previous research comparing developing mammalian brains for their expression pattern with either γ2 or γ4 showed extremely strong staining with γ4 and weak staining with γ2 at postnatal day 6 (Tomita et al., 2003). In that study, developmental levels of TARP protein expression were compared using whole neonatal rat pups and adult brain slices. Those authors found that γ4 was strongly expressed throughout the CNS during

development, but was localized to only a few small brain areas in the adult; likewise, though γ2 and γ8 were initially expressed at a much lower level than γ4, they appear to be ubiquitous in the CNS during development and much more specifically and strongly expressed in adulthood. My study uses a functionally similar developmental period in zebrafish, focusing on recently hatched larvae as they are developing their locomotory skills, but lacks the adult brain slice images in the previous study. Using fish between 12 and 72 hpf only allows me to see the changes in expression during that short window of time; further experiments using slices from adult zebrafish brain would allow me to make correlations between the expression patterns in adult mice and zebrafish, as well as draw clearer conclusions about the roles of zebrafish TARPs in neurodevelopment.

My results do begin to support the general finding from that previous study (Tomita et al., 2003) that TARP expression goes from ubiquitous to specific – in examining the *IS*H images between 12 or 24 hpf and 48 or 72 hpf, there is a clear drop in the expression of the *Cacng* genes in the tails of the older fish (Figs 9-12, 14 and 15), suggesting that the expression patterns may become more specific and defined over time; however there is no clear explanation for *why* this should happen. One possibility for the early and apparently ubiquitous expression of *Cacng* genes in the embryo has been suggested to be maternal gene expression; however this seems unlikely as maternally expressed genes begin to be outnumbered by embryonic genes just after the midblastula transition (~3 hpf) in zebrafish (Kane and Kimmel, 1993) – long before our first *IS*H treatment group at

12 hpf. Moreover, there is still staining in the spinal cord at 24 hpf – a result that cannot be accounted for by maternal gene expression.

AMPARs occur throughout the CNS, including the spinal cord, and yet previous studies have mostly neglected to examine the role of TARPs in the spinal cord. A recent study has examined the expression of TARP proteins in rat spinal cord using immunofluorescence and immunogold labeling of spinal sections, and showed that the Type I and II TARPs (not including γ5) are all differentially expressed in the spinal cord (Larsson et al., 2013). This suggests that a certain amount of *Cacng* staining would not be out of place in the spinal cord, even in adults, which adds another layer of complexity to the interpretation of my data. No studies aside from mine have yet examined the expression (or changes to expression) of TARPs in the spinal cord during development; however AMPARs have been shown to be expressed in the spinal cord during development (Hoppmann et al., 2008), and given the finding that TARPs are in fact found in the adult spinal cord, the presence of TARPs in association with the AMPARs of the developing spinal cord does not seem far-fetched. If my staining pattern is real, it suggests that the interaction between the TARPs I have studied and AMPARs in the spinal cord could be developmentally regulated. As the expression of γ2 and γ4 in the tail wanes between 24 and 48 hpf, other members of the TARP family (γ3, γ5, γ7, γ8) may replace them in their association with the AMPARs of the spinal cord. This speculation of an early switch to less-activating members of the TARP family in the spinal cord of zebrafish is attractive because gap junctions in the developing muscle cells cause uncoordinated spontaneous coiling movements

in response to motoneuron activation in embryos younger than 27 hpf (Saint-Amant and Drapeau, 1998). A switch to a TARP isoform that mediates a more refined response may help to improve the accuracy and precision of motoneuron firing, which is of critical importance to the coordination of the escape response and swimming.

Another limitation of my study was the decision to only look at the paralogs of γ2 and γ4: only looking at four of the twelve *Cacng* genes in zebrafish that correspond to Type I or II TARPs in mice. Given some of the differences in developmental expression that I saw in my RT-PCR study, investigating the expression of exclusively later-expressed genes such as γ3a/b as compared to the earlier-expressed γ4a/b paralogs might have been more informative about the developmental role of different members of the TARP family. Similarly, investigating the expression patterns of the split early/late pairs, γ2b/γ8b and γ2a/γ8a respectively, might help to suggest functional differences within the genes of some of the paralogous branches. The clearest take-home message for me is that being able to do *IS*H of all the members of the *Cacng* family would be ideal.

Owing to the uncertainty of such similarly and widely expressed genes, further experiments and controls should be run to ensure the accuracy of these initial results. Using qPCR rather than RT-PCR in the initial expression study could have provided me with trustworthy quantitative data about the relative expression levels of each *Cacng* gene, which may have made choosing my targets for *IS*H easier. Isolating separate RNA fractions from the heads and tails of 48 hpf

larvae and using that RNA for cDNA synthesis and RT-PCR could provide some confirmation of the expression of TARPs in the spinal cord after 24 hpf. There are also several protocol changes that may still be able to improve the clarity and specificity of my staining. I am confident about the specificity of my probes to their targets because of the rigorous synthesis protocol I used, which included sequencing the specific PCR product being used as template, as well as running the products out on gels at numerous steps, including the final step after probe synthesis was complete. Instead, I think changes to the hybridization step may be the most beneficial: increasing the hybridization temperature to 70°C and/or decreasing the hybridization time from 40 hours to a more standard 12-16 hours may significantly improve my staining (both of these changes are currently being tested in the lab). My *IS*H experiments also lack reliable negative and positive controls. Many labs use *IS*H probes designed against the sense strand for a particular gene: probes that should theoretically not be able to bind to any mRNAs and therefore provide no signal. In our experience with sense probes, this has not been the case, and I chose to exclude sense probes from my experimental design based on my early experience with them and on the advice of Dr. Andrew Waskiewicz – our lab's advisor on matters relating to *IS*H. Instead, I chose to use MO-injected fish for *IS*H to confirm the specificity of my probes. Unfortunately this method did not work.

4.4 **Role of TARPs in Escape Behaviour**

There were no observable changes to the escape response latency of MO-injected fish, as compared to mock-injected controls: both groups were able to

engage their contralateral musculature to turn their bodies away from the stimulus and begin swimming away in between 10 and 20 ms. The swimming behaviour observed from each group was not identical: MO-injected fish were sometimes spasmodic and uncoordinated, with an asymmetric tail beat pattern that made their swimming less efficient. By 48 hpf, wild-type zebrafish are capable of fast and efficient swimming, and none of the control fish exhibited these behavioural abnormalities. This subset of the MO-injected fish also had morphological abnormalities that were not found in our uninjected or mock-injected controls, further suggesting that some aspect of the MO injection was having an effect. We tested the level of knockdown with RT-PCR, using primers that bound to the exonic sequence on either side of the targeted splice site. These primers would normally produce products between 238 and 918 bp, depending on the primer pair; however MO-induced splice variant mRNAs should have been between 900 and 20 000 bp longer than wild-type. Though my PCR elongation step was not changed to account for up to a 21 kb product, it still picked up the wild-type products easily. PCR relies on a geometric duplication of templates, such that the starting material is doubled in every cycle, and relative differences in quantity of starting material are maintained throughout the cycles (ie, if sample A starts with 1 transcript and sample B starts with 5, even after 30 cycles of doubling, sample B should still have 5 times as much product as sample A). This means that as long as my reagents do not run out from doing too many cycles or from having too much template initially, I should be able to at least qualitatively discern between the levels of expression in a control and knocked-down cDNA sample. Only

Cacng2a showed any evidence of knocked-down wild-type mRNA, while the levels of the other TARP transcripts were equivalent to their controls. The sample size of these PCR assays is problematic – with an n of 1 I cannot make definitive claims, but I am confident with my proficiency at all the techniques involved and believe the chance of human error being the cause of this negative result to be minimal. We are in the process of confirming these PCR results with further experiments in order to increase the sample size to a satisfactory level (likely n=3).

I attempted to further characterize our MO knockdowns using *IS*H, but this technique gave me similar staining patterns for both controls and MO-injected larvae. If I was confident with the outcome of my *IS*H protocol, I could also confidently say whether the knockdown was occurring; likewise, if I was confident that the knockdown was occurring, these *IS*H results could confirm the specificity of my probes and my staining pattern. The uncertainty of both my *IS*H results *and* the knockdown using MOs made this attempted control frustratingly useless. The only indication of difference between the controls and MO-injected fish is an increase in staining in the tails of the MO-injected fish. This may be indicative of the nonspecific staining that I have been suspicious of in all of my *in situ* hybridization results. In order to clarify the results of these MO-injected *IS*H experiments, I should first increase the stringency of my hybridization step as discussed previously and see what effect this has on my staining.

In spite of these uncertainties, there *are* phenotypic differences between the MO-injected and mock-injected controls, which suggest that something about the

MO is having an effect on the physiology of the developing larvae. Since my PCR experiments for *Cacng2b, Cacng4a,* and *Cacng4b* failed to show a knockdown of the normal transcript, it is likely that the Morpholino oligonucleotides themselves are causing the effect, rather than inducing a targeted change in the composition of specific mRNAs and decreasing the translation of the resultant proteins. Off-target effects of MO-injection in zebrafish have been well characterized, and typically consist of shortened tails, small eyes, and widespread apoptosis (detected using TUNEL staining) (Oates et al., 2000, Eisen and Smith, 2008, Bill et al., 2009). The best method to control for these off-target effects (for genes that are not involved in an apoptotic pathway) is co-injection of a translation-blocking p53 MO at 1-1.5x the dose of the treatment MO. Given the relatively high dosage required to elicit a drop in expression of *Cacng2a*, an effective dosage of a p53 MO would be between 4 and 6 ng – a total of 8-10 ng of MO. Injection of this much MO would normally induce off-target effects, and previous studies have shown off-target effects outside of the apoptotic pathway that is inhibited by the p53 MO (Oates et al., 2000); however the majority of the off-target effects could likely be curbed through this co-injection. Future experiments should utilize a co-injection of *Cacng* MO with a translation-blocking p53 MO, in order to minimize the off-target effects seen in my *Cacng2a* and *Cacng4a* treatments.

4.5 **Future Directions**

Semi-Q RT-PCR should be performed on *Cacng5b* and *Cacng7a,* as these are the only TARP genes that I have not yet characterized the developmental expression patterns for. Our *IS*H protocol should be adjusted according to my

specifications in order to (hopefully) clarify the staining patterns of the *Cacng* genes I have examined thus far. Furthermore, *IS*H probes should be generated for the remaining *Cacng* isoforms to create a thorough developmental expression profile for all of the genes in the *Cacng* family in zebrafish. The functional characterization of the MO knockdowns remains incomplete: MOs should be co-injected with a translation-blocking p53 MO and modified RT-PCR with fewer cycles to confirm the effectiveness of the single knockdown. Future MO experiments should track of any mortality associated with the injection (and compare to control mock-injections and p53 injections), changes to hatch rate, anatomical changes and the effect of the knockdown on escape response as I have already established. Future experiments should also take advantage of video analysis software to quantify the observed changes to the swimming behaviour of the abnormal MO-injected fish.

Once the functional characterization is complete with all morpholinos, double knockdown morphants lacking γ2a and γ2b (or γ4a and γ4b) should be generated and the characterization repeated in order to test the role of redundancy in the TARP gene paralogs. Changes to AMPAR activity could be assayed by performing whole-cell patch clamp experiments examining miniature excitatory post-synaptic currents (mEPSCs) in the Mauthner cells of single and double morphants. These recordings on a developmental scale as well as in comparison to wild-type/sham-injected control fish could provide us with information regarding the number of AMPARs trafficked to the PSD, the opening and closing kinetics of

those AMPARs and their single channel conductance. Together this data could provide a good picture of the function of γ2a and γ2b in neural development.

Cacng knock-out zebrafish lines could potentially be generated using TALENs in order to examine the effect of TARPs across a longer developmental scale, as well as allow for a deeper examination of TARP redundancy in zebrafish. Once synthesized, the TALEN would be injected into the yolk of 1-8 cell stage zebrafish embryos, as with a MO. Unlike MO injections, TALENs can produce permanent heritable knockout lines of fish, which would allow multiple knockouts of TARP genes or combinations of KOs with MO KDs in order to deeply probe their redundancy. These manipulations would allow a clear determination of the functional roles of the TARPs (and their paralogs) in AMPAR function during development. Due to the extreme challenge of generating even a single TALEN KO lineage, this line of experimentation would most likely require an extensive collaboration or a co-supervised student with the Waskiewicz lab.

Adult TARPs are already known to be phosphorylated by PKA and CamKII (Chetkovich et al., 2002, Choi et al., 2002, Tomita et al., 2005b), so it is likely that similar activity occurs developmentally. We are particularly interested in the possibility that PKCγ may phosphorylate TARPs in order to affect the AMPAR subunit switch that has been observed developmentally (Patten and Ali, 2007, Patten et al., 2010). These relationships could be probed with whole-cell patch clamp electrophysiology of Mauthner neurons by using activating extracellular solutions, and inhibiting calcium-dependent kinase activity. This should indicate

whether activity-dependent changes to AMPAR currents in wild-type Mauthner cells are dependent on Ca^{2+} and therefore likely to be mediated by a calcium dependent protein kinase (conventional PKC/CaMKII). Repeating these experiments using TARP KD fish at 24 and 48 hpf could determine the dependence of Ca^{2+}-mediated synaptic strengthening on the presence of TARP proteins. PKC or CaMKII activation could be discerned using pharmacological tools. There may be no Ca^{2+} dependence in the activity-dependent increases in AMPAR activity in wild-type or TARP KD fish – in this case, cPKCs and CaMKII could be ruled out as being the modulators of these responses. There are two other families of PKCs (novel and atypical) as well as a wide variety of other protein kinases that could be responsible.

4.6 **Conclusion**

In this thesis I set out to probe the developmental expression of the *Cacng* genes of zebrafish, particularly γ2 and γ4, which have been previously shown to be important for and strongly expressed during development. I confirmed that the *Cacng* genes of zebrafish have been duplicated relative to mice, and showed that the relevant AA sequences of the functional ECL1 and C-terminal domains have been conserved between zebrafish and mice. I found that the Type I TARPs of zebrafish are expressed in two waves: an early wave comprising of TARPs that have been previously shown to be strongly activating; and a later wave, coincident with the development of locomotion, consisting of TARPs that have been shown

to be more moderately activating and associated with adult brain tissue. My *IS*H experiments suggest identical expression patterns in the CNS for *Cacng2a, Cacng2b, Cacng4a* and *Cacng4b* in developing zebrafish; however these experiments should be revisited using a slightly modified protocol to attempt to improve the specificity of the staining. My MO knockdown and behavioural experiments were inconclusive because I was unable to confirm the efficacy of my MOs on their target genes through PCR or *IS*H. Overall, my findings show important differential expression patterns of the different TARP genes, and provide sequence analysis that can be used for future research examining the function of these proteins in modulating the excitability of the developing nervous system.

5. Literature Cited

Adesnik H, Li G, During MJ, Pleasure SJ, Nicoll RA (2008) NMDA receptors inhibit synapse unsilencing during brain development. Proceedings of the National Academy of Sciences of the United States of America 105:5597-5602.

Altschul SF, Madden TL, Schaffer AA, Zhang J, Zhang Z, Miller W, Lipman DJ (1997) Gapped BLAST and PSI-BLAST: a new generation of protein database search programs. Nucleic acids research 25:3389-3402.

Altschul SF, Wootton JC, Gertz EM, Agarwala R, Morgulis A, Schaffer AA, Yu YK (2005) Protein database searches using compositionally adjusted substitution matrices. The FEBS journal 272:5101-5109.

Anderson JM, Van Itallie CM (2009) Physiology and function of the tight junction. Cold Spring Harbor perspectives in biology 1:a002584.

Armougom F, Moretti S, Poirot O, Audic S, Dumas P, Schaeli B, Keduas V, Notredame C (2006) Expresso: automatic incorporation of structural information in multiple sequence alignments using 3D-Coffee. Nucleic acids research 34:W604-608.

Armstrong N, Gouaux E (2000) Mechanisms for activation and antagonism of an AMPA-sensitive glutamate receptor: crystal structures of the GluR2 ligand binding core. Neuron 28:165-181.

Armstrong N, Sun Y, Chen GQ, Gouaux E (1998) Structure of a glutamate-receptor ligand-binding core in complex with kainate. Nature 395:913-917.

Ayalon G, Stern-Bach Y (2001) Functional assembly of AMPA and kainate receptors is mediated by several discrete protein-protein interactions. Neuron 31:103-113.

Azevedo FA, Carvalho LR, Grinberg LT, Farfel JM, Ferretti RE, Leite RE, Jacob Filho W, Lent R, Herculano-Houzel S (2009) Equal numbers of neuronal and nonneuronal cells make the human brain an isometrically scaled-up primate brain. The Journal of comparative neurology 513:532-541.

Barria A, Derkach V, Soderling T (1997a) Identification of the Ca2+/calmodulin-dependent protein kinase II regulatory phosphorylation site in the alpha-amino-3-hydroxyl-5-methyl-4-isoxazole-propionate-type glutamate receptor. The Journal of biological chemistry 272:32727-32730.

Barria A, Muller D, Derkach V, Griffith LC, Soderling TR (1997b) Regulatory phosphorylation of AMPA-type glutamate receptors by CaM-KII during long-term potentiation. Science 276:2042-2045.

Bedoukian MA, Weeks AM, Partin KM (2006) Different domains of the AMPA receptor direct stargazin-mediated trafficking and stargazin-mediated modulation of kinetics. The Journal of biological chemistry 281:23908-23921.

Bedoukian MA, Whitesell JD, Peterson EJ, Clay CM, Partin KM (2008) The stargazin C terminus encodes an intrinsic and transferable membrane sorting signal. The Journal of biological chemistry 283:1597-1600.

Bettler B, Boulter J, Hermans-Borgmeyer I, O'Shea-Greenfield A, Deneris ES, Moll C, Borgmeyer U, Hollmann M, Heinemann S (1990) Cloning of a novel glutamate receptor subunit, GluR5: expression in the nervous system during development. Neuron 5:583-595.

Biederer T, Sara Y, Mozhayeva M, Atasoy D, Liu X, Kavalali ET, Sudhof TC (2002) SynCAM, a synaptic adhesion molecule that drives synapse assembly. Science 297:1525-1531.

Bill BR, Petzold AM, Clark KJ, Schimmenti LA, Ekker SC (2009) A primer for morpholino use in zebrafish. Zebrafish 6:69-77.

Boulter J, Hollmann M, O'Shea-Greenfield A, Hartley M, Deneris E, Maron C, Heinemann S (1990) Molecular cloning and functional expression of glutamate receptor subunit genes. Science 249:1033-1037.

Bowie D, Mayer ML (1995) Inward rectification of both AMPA and kainate subtype glutamate receptors generated by polyamine-mediated ion channel block. Neuron 15:453-462.

Brorson JR, Li D, Suzuki T (2004) Selective expression of heteromeric AMPA receptors driven by flip-flop differences. The Journal of neuroscience : the official journal of the Society for Neuroscience 24:3461-3470.

Burgess DL, Davis CF, Gefrides LA, Noebels JL (1999) Identification of three novel Ca(2+) channel gamma subunit genes reveals molecular diversification by tandem and chromosome duplication. Genome research 9:1204-1213.

Burgess DL, Gefrides LA, Foreman PJ, Noebels JL (2001) A cluster of three novel Ca2+ channel gamma subunit genes on chromosome 19q13.4: evolution and expression profile of the gamma subunit gene family. Genomics 71:339-350.

Byrne JH, Kandel ER (1996) Presynaptic facilitation revisited: state and time dependence. The Journal of neuroscience : the official journal of the Society for Neuroscience 16:425-435.

Chang JM, Di Tommaso P, Taly JF, Notredame C (2012) Accurate multiple sequence alignment of transmembrane proteins with PSI-Coffee. BMC bioinformatics 13 Suppl 4:S1.

Chen L, Chetkovich DM, Petralia RS, Sweeney NT, Kawasaki Y, Wenthold RJ, Bredt DS, Nicoll RA (2000) Stargazin regulates synaptic targeting of AMPA receptors by two distinct mechanisms. Nature 408:936-943.

Chetkovich DM, Chen L, Stocker TJ, Nicoll RA, Bredt DS (2002) Phosphorylation of the postsynaptic density-95 (PSD-95)/discs large/zona occludens-1 binding site of stargazin regulates binding to PSD-95 and synaptic targeting of AMPA receptors. The Journal of neuroscience : the official journal of the Society for Neuroscience 22:5791-5796.

Cho CH, St-Gelais F, Zhang W, Tomita S, Howe JR (2007) Two families of TARP isoforms that have distinct effects on the kinetic properties of AMPA receptors and synaptic currents. Neuron 55:890-904.

Choi J, Ko J, Park E, Lee JR, Yoon J, Lim S, Kim E (2002) Phosphorylation of stargazin by protein kinase A regulates its interaction with PSD-95. The Journal of biological chemistry 277:12359-12363.

Chu PJ, Robertson HM, Best PM (2001) Calcium channel gamma subunits provide insights into the evolution of this gene family. Gene 280:37-48.

Colledge M, Dean RA, Scott GK, Langeberg LK, Huganir RL, Scott JD (2000) Targeting of PKA to glutamate receptors through a MAGUK-AKAP complex. Neuron 27:107-119.

Collingridge GL, Olsen RW, Peters J, Spedding M (2009) A nomenclature for ligand-gated ion channels. Neuropharmacology 56:2-5.

Cuadra AE, Kuo SH, Kawasaki Y, Bredt DS, Chetkovich DM (2004) AMPA receptor synaptic targeting regulated by stargazin interactions with the Golgi-resident PDZ protein nPIST. The Journal of neuroscience : the official journal of the Society for Neuroscience 24:7491-7502.

Dong H, O'Brien RJ, Fung ET, Lanahan AA, Worley PF, Huganir RL (1997) GRIP: a synaptic PDZ domain-containing protein that interacts with AMPA receptors. Nature 386:279-284.

Dong H, Zhang P, Liao D, Huganir RL (1999) Characterization, expression, and distribution of GRIP protein. Annals of the New York Academy of Sciences 868:535-540.

Drummond JB, Tucholski J, Haroutunian V, Meador-Woodruff JH (2013) Transmembrane AMPA receptor regulatory protein (TARP) dysregulation in anterior cingulate cortex in schizophrenia. Schizophrenia research.

Durand GM, Kovalchuk Y, Konnerth A (1996) Long-term potentiation and functional synapse induction in developing hippocampus. Nature 381:71-75.

Eisen JS, Smith JC (2008) Controlling morpholino experiments: don't stop making antisense. Development 135:1735-1743.

Gerrow K, Romorini S, Nabi SM, Colicos MA, Sala C, El-Husseini A (2006) A preformed complex of postsynaptic proteins is involved in excitatory synapse development. Neuron 49:547-562.

Glossmann H, Striessnig J, Ferry DR, Goll A, Moosburger K, Schirmer M (1987) Interaction between calcium channel ligands and calcium channels. Circ Res 61:I30-36.

Greger IH, Khatri L, Kong X, Ziff EB (2003) AMPA receptor tetramerization is mediated by Q/R editing. Neuron 40:763-774.

Greger IH, Khatri L, Ziff EB (2002) RNA editing at arg607 controls AMPA receptor exit from the endoplasmic reticulum. Neuron 34:759-772.

Greger IH, Ziff EB, Penn AC (2007) Molecular determinants of AMPA receptor subunit assembly. Trends in neurosciences 30:407-416.

Harris EW, Ganong AH, Cotman CW (1984) Long-term potentiation in the hippocampus involves activation of N-methyl-D-aspartate receptors. Brain research 323:132-137.

Hastie P, Ulbrich MH, Wang HL, Arant RJ, Lau AG, Zhang Z, Isacoff EY, Chen L (2013) AMPA receptor/TARP stoichiometry visualized by single-

molecule subunit counting. Proceedings of the National Academy of Sciences of the United States of America 110:5163-5168.

Hebb DO (1949) The Organization of Behavior: A Neuropsychological Theory. New York: Wiley and Sons.

Higuchi M, Single FN, Kohler M, Sommer B, Sprengel R, Seeburg PH (1993) RNA editing of AMPA receptor subunit GluR-B: a base-paired intron-exon structure determines position and efficiency. Cell 75:1361-1370.

Hofmann KS, W. (1993) TMBASE - A database of membrane spanning protein segments. In: Biological Chemistry Hoppe-Seyler, vol. 374, p 166: De Gruyter.

Hollmann M, Maron C, Heinemann S (1994) N-glycosylation site tagging suggests a three transmembrane domain topology for the glutamate receptor GluR1. Neuron 13:1331-1343.

Honore T, Lauridsen J, Krogsgaard-Larsen P (1982) The binding of [3H]AMPA, a structural analogue of glutamic acid, to rat brain membranes. J Neurochem 38:173-178.

Hoppmann V, Wu JJ, Soviknes AM, Helvik JV, Becker TS (2008) Expression of the eight AMPA receptor subunit genes in the developing central nervous system and sensory organs of zebrafish. Developmental dynamics : an official publication of the American Association of Anatomists 237:788-799.

Hsia AY, Malenka RC, Nicoll RA (1998) Development of excitatory circuitry in the hippocampus. Journal of neurophysiology 79:2013-2024.

Isaac JT, Crair MC, Nicoll RA, Malenka RC (1997) Silent synapses during development of thalamocortical inputs. Neuron 18:269-280.

Isaac JT, Nicoll RA, Malenka RC (1995) Evidence for silent synapses: implications for the expression of LTP. Neuron 15:427-434.

Ives JH, Fung S, Tiwari P, Payne HL, Thompson CL (2004) Microtubule-associated protein light chain 2 is a stargazin-AMPA receptor complex-interacting protein in vivo. The Journal of biological chemistry 279:31002-31009.

Jackson AC, Milstein AD, Soto D, Farrant M, Cull-Candy SG, Nicoll RA (2011) Probing TARP modulation of AMPA receptor conductance with polyamine toxins. The Journal of neuroscience : the official journal of the Society for Neuroscience 31:7511-7520.

Jaillon O, Aury JM, Brunet F, Petit JL, Stange-Thomann N, Mauceli E, Bouneau L, Fischer C, Ozouf-Costaz C, Bernot A, Nicaud S, Jaffe D, Fisher S, Lutfalla G, Dossat C, Segurens B, Dasilva C, Salanoubat M, Levy M, Boudet N, Castellano S, Anthouard V, Jubin C, Castelli V, Katinka M, Vacherie B, Biemont C, Skalli Z, Cattolico L, Poulain J, De Berardinis V, Cruaud C, Duprat S, Brottier P, Coutanceau JP, Gouzy J, Parra G, Lardier G, Chapple C, McKernan KJ, McEwan P, Bosak S, Kellis M, Volff JN, Guigo R, Zody MC, Mesirov J, Lindblad-Toh K, Birren B, Nusbaum C, Kahn D, Robinson-Rechavi M, Laudet V, Schachter V, Quetier F, Saurin W, Scarpelli C, Wincker P, Lander ES, Weissenbach J, Roest Crollius H (2004) Genome duplication in the teleost fish Tetraodon nigroviridis reveals the early vertebrate proto-karyotype. Nature 431:946-957.

Jay SD, Ellis SB, McCue AF, Williams ME, Vedvick TS, Harpold MM, Campbell KP (1990) Primary structure of the gamma subunit of the DHP-sensitive calcium channel from skeletal muscle. Science 248:490-492.

Kamboj SK, Swanson GT, Cull-Candy SG (1995) Intracellular spermine confers rectification on rat calcium-permeable AMPA and kainate receptors. The Journal of physiology 486 (Pt 2):297-303.

Kane DA, Kimmel CB (1993) The zebrafish midblastula transition. Development 119:447-456.

Kato AS, Siuda ER, Nisenbaum ES, Bredt DS (2008) AMPA receptor subunit-specific regulation by a distinct family of type II TARPs. Neuron 59:986-996.

Kato AS, Zhou W, Milstein AD, Knierman MD, Siuda ER, Dotzlaf JE, Yu H, Hale JE, Nisenbaum ES, Nicoll RA, Bredt DS (2007) New transmembrane AMPA receptor regulatory protein isoform, gamma-7, differentially regulates AMPA receptors. The Journal of neuroscience : the official journal of the Society for Neuroscience 27:4969-4977.

Kauer JA, Malenka RC, Nicoll RA (1988) A persistent postsynaptic modification mediates long-term potentiation in the hippocampus. Neuron 1:911-917.

Kerchner GA, Nicoll RA (2008) Silent synapses and the emergence of a postsynaptic mechanism for LTP. Nature reviews Neuroscience 9:813-825.

Kim KS, Yan D, Tomita S (2010) Assembly and stoichiometry of the AMPA receptor and transmembrane AMPA receptor regulatory protein complex. The Journal of neuroscience : the official journal of the Society for Neuroscience 30:1064-1072.

Kimmel CB, Ballard WW, Kimmel SR, Ullmann B, Schilling TF (1995) Stages of embryonic development of the zebrafish. Developmental dynamics : an

official publication of the American Association of Anatomists 203:253-310.

Klugbauer N, Dai S, Specht V, Lacinova L, Marais E, Bohn G, Hofmann F (2000) A family of gamma-like calcium channel subunits. FEBS Lett 470:189-197.

Koh DS, Burnashev N, Jonas P (1995) Block of native Ca(2+)-permeable AMPA receptors in rat brain by intracellular polyamines generates double rectification. The Journal of physiology 486 (Pt 2):305-312.

Kott S, Sager C, Tapken D, Werner M, Hollmann M (2009) Comparative analysis of the pharmacology of GluR1 in complex with transmembrane AMPA receptor regulatory proteins gamma2, gamma3, gamma4, and gamma8. Neuroscience 158:78-88.

Kott S, Werner M, Korber C, Hollmann M (2007) Electrophysiological properties of AMPA receptors are differentially modulated depending on the associated member of the TARP family. The Journal of neuroscience : the official journal of the Society for Neuroscience 27:3780-3789.

Kromann H, Krikstolaityte S, Andersen AJ, Andersen K, Krogsgaard-Larsen P, Jaroszewski JW, Egebjerg J, Stromgaard K (2002) Solid-phase synthesis of polyamine toxin analogues: potent and selective antagonists of Ca2+-permeable AMPA receptors. Journal of medicinal chemistry 45:5745-5754.

Krug SM, Gunzel D, Conrad MP, Lee IF, Amasheh S, Fromm M, Yu AS (2012) Charge-selective claudin channels. Annals of the New York Academy of Sciences 1257:20-28.

Kung SS, Chen YC, Lin WH, Chen CC, Chow WY (2001) Q/R RNA editing of the AMPA receptor subunit 2 (GRIA2) transcript evolves no later than the appearance of cartilaginous fishes. FEBS letters 509:277-281.

Larsson M, Agalave N, Watanabe M, Svensson CI (2013) Distribution of transmembrane AMPA receptor regulatory protein (TARP) isoforms in the rat spinal cord. Neuroscience.

Lee HK, Barbarosie M, Kameyama K, Bear MF, Huganir RL (2000) Regulation of distinct AMPA receptor phosphorylation sites during bidirectional synaptic plasticity. Nature 405:955-959.

Lee HK, Takamiya K, He K, Song L, Huganir RL (2010) Specific roles of AMPA receptor subunit GluR1 (GluA1) phosphorylation sites in regulating synaptic plasticity in the CA1 region of hippocampus. Journal of neurophysiology 103:479-489.

Leonard AS, Davare MA, Horne MC, Garner CC, Hell JW (1998) SAP97 is associated with the alpha-amino-3-hydroxy-5-methylisoxazole-4-propionic acid receptor GluR1 subunit. The Journal of biological chemistry 273:19518-19524.

Letts VA, Felix R, Biddlecome GH, Arikkath J, Mahaffey CL, Valenzuela A, Bartlett FS, 2nd, Mori Y, Campbell KP, Frankel WN (1998) The mouse stargazer gene encodes a neuronal Ca2+-channel gamma subunit. Nat Genet 19:340-347.

Letts VA, Mahaffey CL, Beyer B, Frankel WN (2005) A targeted mutation in Cacng4 exacerbates spike-wave seizures in stargazer (Cacng2) mice. Proc Natl Acad Sci U S A 102:2123-2128.

Li J, Angelow S, Linge A, Zhuo M, Yu AS (2013) Claudin-2 Pore Function Requires an Intramolecular Disulfide Bond Between Two Conserved Extracellular Cysteines. American journal of physiology Cell physiology.

Liao D, Hessler NA, Malinow R (1995) Activation of postsynaptically silent synapses during pairing-induced LTP in CA1 region of hippocampal slice. Nature 375:400-404.

Lin WH, Wu CH, Chen YC, Chow WY (2006) Embryonic expression of zebrafish AMPA receptor genes: zygotic gria2alpha expression initiates at the midblastula transition. Brain research 1110:46-54.

Lomeli H, Mosbacher J, Melcher T, Hoger T, Geiger JR, Kuner T, Monyer H, Higuchi M, Bach A, Seeburg PH (1994) Control of kinetic properties of AMPA receptor channels by nuclear RNA editing. Science 266:1709-1713.

Low SE, Woods IG, Lachance M, Ryan J, Schier AF, Saint-Amant L (2012) Touch responsiveness in zebrafish requires voltage-gated calcium channel 2.1b. Journal of neurophysiology 108:148-159.

Luscher C, Xia H, Beattie EC, Carroll RC, von Zastrow M, Malenka RC, Nicoll RA (1999) Role of AMPA receptor cycling in synaptic transmission and plasticity. Neuron 24:649-658.

Lynch G, Larson J, Kelso S, Barrionuevo G, Schottler F (1983) Intracellular injections of EGTA block induction of hippocampal long-term potentiation. Nature 305:719-721.

Maccaferri G, Dingledine R (2002) Complex effects of CNQX on CA1 interneurons of the developing rat hippocampus. Neuropharmacology 43:523-529.

Malenka RC, Kauer JA, Zucker RS, Nicoll RA (1988) Postsynaptic calcium is sufficient for potentiation of hippocampal synaptic transmission. Science 242:81-84.

Mansour M, Nagarajan N, Nehring RB, Clements JD, Rosenmund C (2001) Heteromeric AMPA receptors assemble with a preferred subunit stoichiometry and spatial arrangement. Neuron 32:841-853.

Mayer ML, Westbrook GL, Guthrie PB (1984) Voltage-dependent block by Mg2+ of NMDA responses in spinal cord neurones. Nature 309:261-263.

McCurley AT, Callard GV (2008) Characterization of housekeeping genes in zebrafish: male-female differences and effects of tissue type, developmental stage and chemical treatment. BMC molecular biology 9:102.

Menuz K, Kerchner GA, O'Brien JL, Nicoll RA (2009) Critical role for TARPs in early development despite broad functional redundancy. Neuropharmacology 56:22-29.

Menuz K, O'Brien JL, Karmizadegan S, Bredt DS, Nicoll RA (2008) TARP redundancy is critical for maintaining AMPA receptor function. The Journal of neuroscience : the official journal of the Society for Neuroscience 28:8740-8746.

Menuz K, Stroud RM, Nicoll RA, Hays FA (2007) TARP auxiliary subunits switch AMPA receptor antagonists into partial agonists. Science 318:815-817.

Meyer MP, Smith SJ (2006) Evidence from in vivo imaging that synaptogenesis guides the growth and branching of axonal arbors by two distinct mechanisms. The Journal of neuroscience : the official journal of the Society for Neuroscience 26:3604-3614.

Milstein AD, Zhou W, Karimzadegan S, Bredt DS, Nicoll RA (2007) TARP subtypes differentially and dose-dependently control synaptic AMPA receptor gating. Neuron 55:905-918.

Monyer H, Seeburg PH, Wisden W (1991) Glutamate-operated channels: developmentally early and mature forms arise by alternative splicing. Neuron 6:799-810.

Moretti S, Armougom F, Wallace IM, Higgins DG, Jongeneel CV, Notredame C (2007) The M-Coffee web server: a meta-method for computing multiple sequence alignments by combining alternative alignment methods. Nucleic acids research 35:W645-648.

Morita K, Furuse M, Fujimoto K, Tsukita S (1999) Claudin multigene family encoding four-transmembrane domain protein components of tight junction strands. Proceedings of the National Academy of Sciences of the United States of America 96:511-516.

Mosbacher J, Schoepfer R, Monyer H, Burnashev N, Seeburg PH, Ruppersberg JP (1994) A molecular determinant for submillisecond desensitization in glutamate receptors. Science 266:1059-1062.

Muller D, Joly M, Lynch G (1988) Contributions of quisqualate and NMDA receptors to the induction and expression of LTP. Science 242:1694-1697.

Nakagawa T, Cheng Y, Ramm E, Sheng M, Walz T (2005) Structure and different conformational states of native AMPA receptor complexes. Nature 433:545-549.

Nakagawa T, Cheng Y, Sheng M, Walz T (2006) Three-dimensional structure of an AMPA receptor without associated stargazin/TARP proteins. Biological chemistry 387:179-187.

Nilsen A, England PM (2007) A subtype-selective, use-dependent inhibitor of native AMPA receptors. Journal of the American Chemical Society 129:4902-4903.

Notredame C, Higgins DG, Heringa J (2000) T-Coffee: A novel method for fast and accurate multiple sequence alignment. Journal of molecular biology 302:205-217.

Nowak L, Bregestovski P, Ascher P, Herbet A, Prochiantz A (1984) Magnesium gates glutamate-activated channels in mouse central neurones. Nature 307:462-465.

Oates AC, Bruce AE, Ho RK (2000) Too much interference: injection of double-stranded RNA has nonspecific effects in the zebrafish embryo. Developmental biology 224:20-28.

Olsen O, Bredt DS (2003) Functional analysis of the nucleotide binding domain of membrane-associated guanylate kinases. The Journal of biological chemistry 278:6873-6878.

Patten SA, Ali DW (2007) AMPA receptors associated with zebrafish Mauthner cells switch subunits during development. The Journal of physiology 581:1043-1056.

Patten SA, Ali DW (2009) PKCgamma-induced trafficking of AMPA receptors in embryonic zebrafish depends on NSF and PICK1. Proceedings of the

National Academy of Sciences of the United States of America 106:6796-6801.

Patten SA, Roy B, Cunningham ME, Stafford JL, Ali DW (2010) Protein kinase Cgamma is a signaling molecule required for the developmental speeding of alpha-amino-3-hydroxyl-5-methyl-4-isoxazole-propionate receptor kinetics. The European journal of neuroscience 31:1561-1573.

Payne HL (2008) The role of transmembrane AMPA receptor regulatory proteins (TARPs) in neurotransmission and receptor trafficking (Review). Molecular membrane biology 25:353-362.

Petralia RS, Esteban JA, Wang YX, Partridge JG, Zhao HM, Wenthold RJ, Malinow R (1999) Selective acquisition of AMPA receptors over postnatal development suggests a molecular basis for silent synapses. Nature neuroscience 2:31-36.

Price MG, Davis CF, Deng F, Burgess DL (2005) The alpha-amino-3-hydroxyl-5-methyl-4-isoxazolepropionate receptor trafficking regulator "stargazin" is related to the claudin family of proteins by Its ability to mediate cell-cell adhesion. The Journal of biological chemistry 280:19711-19720.

Priel A, Kolleker A, Ayalon G, Gillor M, Osten P, Stern-Bach Y (2005) Stargazin reduces desensitization and slows deactivation of the AMPA-type glutamate receptors. The Journal of neuroscience : the official journal of the Society for Neuroscience 25:2682-2686.

Reymann KG, Matthies HK, Schulzeck K, Matthies H (1989) N-methyl-D-aspartate receptor activation is required for the induction of both early and late phases of long-term potentiation in rat hippocampal slices. Neuroscience letters 96:96-101.

Rosenmund C, Stern-Bach Y, Stevens CF (1998) The tetrameric structure of a glutamate receptor channel. Science 280:1596-1599.

Rouach N, Byrd K, Petralia RS, Elias GM, Adesnik H, Tomita S, Karimzadegan S, Kealey C, Bredt DS, Nicoll RA (2005) TARP gamma-8 controls hippocampal AMPA receptor number, distribution and synaptic plasticity. Nature neuroscience 8:1525-1533.

Sabo SL, Gomes RA, McAllister AK (2006) Formation of presynaptic terminals at predefined sites along axons. The Journal of neuroscience : the official journal of the Society for Neuroscience 26:10813-10825.

Saint-Amant L, Drapeau P (1998) Time course of the development of motor behaviors in the zebrafish embryo. J Neurobiol 37:622-632.

Schneider CA, Rasband WS, Eliceiri KW (2012) NIH Image to ImageJ: 25 years of image analysis. Nature methods 9:671-675.

Shelley C, Farrant M, Cull-Candy SG (2012) TARP-associated AMPA receptors display an increased maximum channel conductance and multiple kinetically distinct open states. The Journal of physiology 590:5723-5738.

Shi S, Hayashi Y, Esteban JA, Malinow R (2001) Subunit-specific rules governing AMPA receptor trafficking to synapses in hippocampal pyramidal neurons. Cell 105:331-343.

Shi SH, Hayashi Y, Petralia RS, Zaman SH, Wenthold RJ, Svoboda K, Malinow R (1999) Rapid spine delivery and redistribution of AMPA receptors after synaptic NMDA receptor activation. Science 284:1811-1816.

Shi Y, Lu W, Milstein AD, Nicoll RA (2009) The stoichiometry of AMPA receptors and TARPs varies by neuronal cell type. Neuron 62:633-640.

Sidow A (1996) Gen(om)e duplications in the evolution of early vertebrates. Current opinion in genetics & development 6:715-722.

Sommer B, Keinanen K, Verdoorn TA, Wisden W, Burnashev N, Herb A, Kohler M, Takagi T, Sakmann B, Seeburg PH (1990) Flip and flop: a cell-specific functional switch in glutamate-operated channels of the CNS. Science 249:1580-1585.

Sommer B, Kohler M, Sprengel R, Seeburg PH (1991) RNA editing in brain controls a determinant of ion flow in glutamate-gated channels. Cell 67:11-19.

Soto D, Coombs ID, Kelly L, Farrant M, Cull-Candy SG (2007) Stargazin attenuates intracellular polyamine block of calcium-permeable AMPA receptors. Nature neuroscience 10:1260-1267.

Srivastava S, Osten P, Vilim FS, Khatri L, Inman G, States B, Daly C, DeSouza S, Abagyan R, Valtschanoff JG, Weinberg RJ, Ziff EB (1998) Novel anchorage of GluR2/3 to the postsynaptic density by the AMPA receptor-binding protein ABP. Neuron 21:581-591.

Srivastava S, Ziff EB (1999) ABP: a novel AMPA receptor binding protein. Annals of the New York Academy of Sciences 868:561-564.

Stamatakis A, Hoover P, Rougemont J (2008) A rapid bootstrap algorithm for the RAxML Web servers. Systematic biology 57:758-771.

Stromgaard K, Jensen LS, Vogensen SB (2005) Polyamine toxins: development of selective ligands for ionotropic receptors. Toxicon : official journal of the International Society on Toxinology 45:249-254.

Sun Q, Turrigiano GG (2011) PSD-95 and PSD-93 play critical but distinct roles in synaptic scaling up and down. J Neurosci 31:6800-6808.

Thisse B (2004) Fast Release Clones: A High Throughput Expression Analysis. In: ZFIN Direct Data Submission http://zfin.org.

Thisse C, Thisse B (2008) High-resolution in situ hybridization to whole-mount zebrafish embryos. Nature protocols 3:59-69.

Tomita S, Adesnik H, Sekiguchi M, Zhang W, Wada K, Howe JR, Nicoll RA, Bredt DS (2005a) Stargazin modulates AMPA receptor gating and trafficking by distinct domains. Nature 435:1052-1058.

Tomita S, Chen L, Kawasaki Y, Petralia RS, Wenthold RJ, Nicoll RA, Bredt DS (2003) Functional studies and distribution define a family of transmembrane AMPA receptor regulatory proteins. The Journal of cell biology 161:805-816.

Tomita S, Fukata M, Nicoll RA, Bredt DS (2004) Dynamic interaction of stargazin-like TARPs with cycling AMPA receptors at synapses. Science 303:1508-1511.

Tomita S, Stein V, Stocker TJ, Nicoll RA, Bredt DS (2005b) Bidirectional synaptic plasticity regulated by phosphorylation of stargazin-like TARPs. Neuron 45:269-277.

Turetsky D, Garringer E, Patneau DK (2005) Stargazin modulates native AMPA receptor functional properties by two distinct mechanisms. The Journal of neuroscience : the official journal of the Society for Neuroscience 25:7438-7448.

Vandenberghe W, Nicoll RA, Bredt DS (2005a) Interaction with the unfolded protein response reveals a role for stargazin in biosynthetic AMPA receptor transport. J Neurosci 25:1095-1102.

Vandenberghe W, Nicoll RA, Bredt DS (2005b) Stargazin is an AMPA receptor auxiliary subunit. Proc Natl Acad Sci U S A 102:485-490.

Verpelli C, Schmeisser MJ, Sala C, Boeckers TM (2012) Scaffold proteins at the postsynaptic density. Advances in experimental medicine and biology 970:29-61.

Walker CS, Brockie PJ, Madsen DM, Francis MM, Zheng Y, Koduri S, Mellem JE, Strutz-Seebohm N, Maricq AV (2006) Reconstitution of invertebrate glutamate receptor function depends on stargazin-like proteins. Proceedings of the National Academy of Sciences of the United States of America 103:10781-10786.

Wallace IM, O'Sullivan O, Higgins DG, Notredame C (2006) M-Coffee: combining multiple sequence alignment methods with T-Coffee. Nucleic acids research 34:1692-1699.

Washbourne P, Bennett JE, McAllister AK (2002) Rapid recruitment of NMDA receptor transport packets to nascent synapses. Nature neuroscience 5:751-759.

Waskiewicz AJ (2012) Morpholinos have inconsistent half-lives, regardless of storage temperature. (Cunningham, M. E., Ali, D.W., ed).

Watkins JC (1981) Pharmacology of excitatory amino acid transmitters. Advances in biochemical psychopharmacology 29:205-212.

Wenthold RJ, Petralia RS, Blahos J, II, Niedzielski AS (1996) Evidence for multiple AMPA receptor complexes in hippocampal CA1/CA2 neurons. The Journal of neuroscience : the official journal of the Society for Neuroscience 16:1982-1989.

Westerfield M (2007) The Zebrafish Book: A guide for the laboratory use of zebrafish (Danio rerio). Eugene, OR: University of Oregon Press.

Wyszynski M, Valtschanoff JG, Naisbitt S, Dunah AW, Kim E, Standaert DG, Weinberg R, Sheng M (1999) Association of AMPA receptors with a subset of glutamate receptor-interacting protein in vivo. The Journal of neuroscience : the official journal of the Society for Neuroscience 19:6528-6537.

Xia J, Zhang X, Staudinger J, Huganir RL (1999) Clustering of AMPA receptors by the synaptic PDZ domain-containing protein PICK1. Neuron 22:179-187.